Doctorate Program in Molecular Oncology
and Endocrinology
Doctorate School in Molecular Medicine

XXI cycle - 2005–2008
Coordinator: Prof. Giancarlo Vecchio

"RET-mediated CD44 proteolysis promotes autonomous proliferation of thyroid cells"

Anna Tamburrino

University of Naples Federico II
Dipartimento di Biologia e Patologia Cellulare e Molecolare
"L. Califano"

Administrative Location

Dipartimento di Biologia e Patologia Cellulare e Molecolare "L. Califano"
Università degli Studi di Napoli Federico II

Partner Institutions

Italian Institutions
Università di Napoli "Federico II", Naples, Italy
Istituto di Endocrinologia ed Oncologia Sperimentale "G. Salvatore", CNR, Naples, Italy
Seconda Università di Napoli, Naples, Italy
Università del Sannio, Benevento, Italy
Università di Genova, Genoa, Italy
Università di Padova, Padua, Italy

Foreign Institutions
Johns Hopkins School of Medicine, Baltimore, MD, USA
Johns Hopkins Krieger School of Arts and Sciences, Baltimore, MD, USA
National Institutes of Health, Bethesda, MD, USA
Ohio State University, Columbus, OH, USA
Université Paris Sud XI, Paris, France
Universidad Autonoma de Madrid, Spain
Centro de Investigaciones Oncologicas (CNIO), Spain
Universidade Federal de Sao Paulo, Brazil
Albert Einstein College of Medicine of Yeshiwa University, USA

Supporting Institutions
Università di Napoli "Federico II", Naples, Italy
Ministero dell'Istruzione, dell'Università e della Ricerca
Istituto Superiore di Oncologia (ISO)
Terry Fox Foundation, Canada
Istituto di Endocrinologia ed Oncologia Sperimentale "G. Salvatore", CNR, Naples, Italy
Centro Regionale di Competenza in Genomica (GEAR)

FACULTY

ITALIAN FACULTY

Giancarlo Vecchio, MD, Co-ordinator
Salvatore Maria Aloj, MD
Francesco Beguinot, MD
Maria Teresa Berlingieri, PhD
Angelo Raffaele Bianco, MD
Bernadette Biondi, MD
Francesca Carlomagno, MD
Gabriella Castoria, MD
Angela Celetti, MD
Annamaria Cirafici, PhD
Mario Chiariello, MD
Vincenzo Ciminale, MD
Annamaria Colao, MD
Alma Contegiacomo, MD
Sabino De Placido, MD
Monica Fedele, PhD
Pietro Formisano, MD
Alfredo Fusco, MD
Fabrizio Gentile, MD, PhD
Massimo Imbriaco, MD
Paolo Laccetti, PhD
Antonio Leonardi, MD
Barbara Majello, PhD
Rosa Marina Melillo, MD
Claudia Miele, PhD
Roberto Pacelli, MD
Giuseppe Palumbo, PhD
Angelo Paradiso MD, PhD
Silvio Parodi, MD
Giuseppe Portella, MD
Giorgio Punzo, MD
Antonio Rosato, MD
Massimo Santoro, MD
Giampaolo Tortora, MD
Donatella Tramontano, PhD
Giancarlo Troncone, MD
Bianca Maria Veneziani, MD
Giuseppe Viglietto, MD
Roberta Visconti, MD

FOREIGN FACULTY

Université Libre de Bruxelles (Belgium)
Gilbert Vassart

Universidade Federal de Sao Paulo (Brazil)
Janete Maria Cerutti
Rui Maciel

University of Turku (Finland)
Mikko O. Laukkanen

Université Paris Sud XI (France)
Martin Schlumberger, MD

University of Madras (India)
A.K: Munirajan

Pavol Jozef Šafàrik University (Slovakia)
Peter Fedorocko

Universidad Autonoma de Madrid (Spain)
Juan Bernal, MD, PhD
Pilar Santisteban

Centro de Investigaciones Oncologicas (Spain)
Mariano Barbacid, MD

Albert Einstein College of Medicine of Yeshiwa University (USA)
Luciano D'Adamio, MD
Nancy Carrasco

Johns Hopkins School of Medicine (USA)
Vincenzo Casolaro, MD
Pierre Coulombe, PhD
James G. Herman MD
Robert Schleimer, PhD

Johns Hopkins Krieger School of Arts and Sciences (USA)
Eaton E. Lattman, MD

National Institutes of Health (USA)
Michael M. Gottesman, MD
Silvio Gutkind, PhD
Stephen Marx, MD
Ira Pastan, MD
Phil Gorden, MD

Ohio State University, Columbus (USA)
Carlo M. Croce, MD

ANNA TAMBURRINO

RET-mediated CD44 proteolysis promotes autonomous proliferation of thyroid cells

Doctoral dissertation

LIST OF MANUSCRIPTS

This dissertation is based on the following manuscripts. The first one covers the main body of the dissertation. The others are appended at the end.

I) De Falco V, **Tamburrino A**, Castellone MD, Basolo F, Maniè S, Santoro M. RET signaling-mediated CD44 proteolysis promotes autonomous proliferation of thyroid cells. Manuscript in preparation (main body of the dissertation).

II) De Falco V, Giannini R, **Tamburrino A**, Ugolini C, Lupi C, Puxeddu E, Santoro M, Basolo F. Functional Characterization of the Novel T599I-VKSRdel BRAF Mutation in a Follicular Variant Papillary Thyroid Carcinoma. J Clin Endocrinol Metab. 2008 Nov;93(11):4398-402 (appended at the end of the dissertation).

III) Salerno P, De Falco V, **Tamburrino A**, Nappi TC, Vecchio G, Bollag GE, Santoro M, Salvatore G. Cytostatic activity of PLX4032 and PLX4720 BRAF ATP-competitive inhibitors in BRAF mutant thyroid carcinoma cells. Manuscript submitted (appended at the end of the dissertation).

IV) Vitagliano D, De Falco V, **Tamburrino A**, Coluzzi S, Troncone G, Ciardiello F, Tortora G, Wells SA Jr, Ryan AJ, Carlomagno F, Santoro M. The tyrosine kinase inhibitor ZD6474 blocks the growth and tumorigenicity of RET mutation-positive medullary thyroid carcinoma cells. Manuscript submitted (appended at the end of the dissertation).

TABLE OF CONTENTS

ABBREVIATIONS

Aβ	amyloid β-peptide
AC	adenylate cyclase
AP-1	activator protein 1
APP	amyloid precursor protein
ATC	anaplastic thyroid carcinoma
cAMP	3',5'-cyclic adenosine monophosphate
CD44st	standard CD44
CREB	cAMP response element -CRE- binding protein
CREM	cAMP response element modulator
CTF	C-terminal fragment
DMEM	Dulbecco's modified Eagle's medium
ECM	extracellular matrix
EMCs	extracellular matrix components
ERK	extracellular signal-regulated kinase
ERM	ezrin, radixin and moesin
FAP	familial adenomatous polyposis
FBS	fetal bovine serum
FMTC	familial medullary thyroid carcinoma
FNMTC	familial non medullary thyroid carcinoma
FTC	follicular thyroid carcinoma
GAG	glycosaminoglycan
GDNF	glial cell line-derived neurotrophic factor
GLI	Glioma-associated oncogene homologue
GST	glutathione S-transferase
HA	hyaluronic acid
ICD	intracellular domain
KID	kinase-inducible domain

MAPK	mitogen-activated protein kinase
MEK	mitogen-activated protein kinase kinase
MEN2	multiple endocrine neoplasia type 2 syndrome
MMP	matrix metalloprotease
MTC	medullary thyroid carcinoma
NFKB	nuclear factor kappa-B
NGF	nerve growth factor
OPN	osteopontin
PDC	poorly differentiated carcinoma
PKC	protein kinase C
PI3K	phosphatidylinositol 3-kinase
PS	presenilin
PTC	papillary thyroid carcinoma
PTK	protein tyrosine kinase
RET	REarranged during Transfection
RFG	RET fused gene
RIP	regulated intramembrane proteolysis
SF/HGF	scatter factor/hepatocyte growth factor
siRNA	small interfering RNA
SRF	serum response factor
TG	thyroglobulin
TPA	2-0-tetradecanoylphorbol 13-acetate
TPO	thyroperoxidase
TRE	TPA-responsive element
TRH	thyrotropin releasing hormone
TSH	thyroid stimulating hormone
TSHR	thyroid stimulating hormone receptor
WDC	well-differentiated carcinoma

1. ABSTRACT

This dissertation addresses signaling mechanisms involved in thyroid carcinoma formation, with a view of identifying novel levels for therapeutic intervention. In this frame, appended manuscripts **II**, **III** and **IV** focus on the functional characterization of a novel BRAF mutation and on molecular targeting of RET or BRAF pathways in thyroid cancer. The main body of the dissertation describes a novel signaling mechanism that we have identified in thyroid carcinomas harboring BRAF or RET/PTC oncogenes and that involves CD44. CD44, a cell surface adhesion molecule overexpressed in a wide range of cancer types, undergoes sequential proteolytic cleavage at the extracellular and intramembrane domains. This results in the shedding of the ectodomain (ectoCD44) and in the intracellular release of an intracellular fragment (CD44-ICD). CD44-ICD is translocated to the nucleus and activates gene transcription. Our group has previously demonstrated that CD44 is overexpressed in papillary thyroid carcinoma (PTC) tissue samples and in cell lines harboring RET/PTC or BRAF oncogenes. Here, we show that RET/PTC signaling induces γ-secretase-dependent CD44 proteolysis through the ERK pathway. Chemical blockade of either RET/PTC or MEK abrogates CD44 cleavage. Adoptive overexpression of CD44-ICD stimulates TSH-independent proliferation of thyroid follicular PC cells. CD44-ICD binds to CREB and stimulates CREB-mediated transcription in PC cells by potentiating CREB S133 phosphorylation. Through this mechanism, CD44-ICD up-regulates cyclin D1 expression and proliferation of thyroid cells. Taken together, these findings suggest that ERK kinase pathway-mediated CD44 cleavage sustains proliferation of thyrocytes harboring RET/PTC, RAS or BRAF oncogenes. This novel pathway may provide new molecular targets for therapeutic intervention in thyroid carcinoma.

2. BACKGROUND

2.1 THYROID CANCER

2.1.1 Thyroid function

The thyroid is an endocrine organ that regulates a wide range of functions: ranging from development to metabolism. The thyroid gland is formed by two separated lobes connected by the isthmus and resides on the anterior surface of the trachea at the base of the neck. It is comprised of aggregates or lobules of spherical follicles ranging between 50-500 μm in size, surrounded by a network of blood vessels (Larsen *et al*., 2003). Thyroid follicles include two distinct hormone-producing cell types, follicular and parafollicular (or C-) cells (**Fig. 1,** right). Follicular epithelial cells are responsible for thyroid hormone synthesis. The follicle lumen contains the colloid, where the precursor of thyroid hormones, thyroglobulin (TG), is stored. Parafollicular C-cells are interspersed within the follicles or lie in a parafollicular location. They contain granules of the peptide hormone calcitonin (Larsen *et al*., 2003). The main functions of the thyroid gland is the synthesis, storage and secretion of thyroid hormones tri- (T3) and tetra- (T4) iodothyronine. After protein synthesis glycosidic group and Iodine are added to TG, thereby stored into the lumen of the follicles. Upon stimulation, follicular cells release T3 and T4 from TG through proteolytic activity (Kondo *et al*. 2006). The synthesis and release of thyroid hormones is regulated by the hypothalamic-pituitary axis. Thyrotropin releasing hormone (TRH), secreted by hypothalamus, stimulates the release of thyroid stimulating hormone (TSH) from the anterior pituitary gland. TSH, in turn, stimulates the follicular cells to synthesize and release thyroid hormones. Pituitary is under the control of a negative feedback loop by thyroid hormones (**Fig. 1,** left). Calcitonin secretion by parafollicular cells is regulated as well. Serum calcium levels regulate hormone secretion from C-cell (Lin *et al*. 1991).

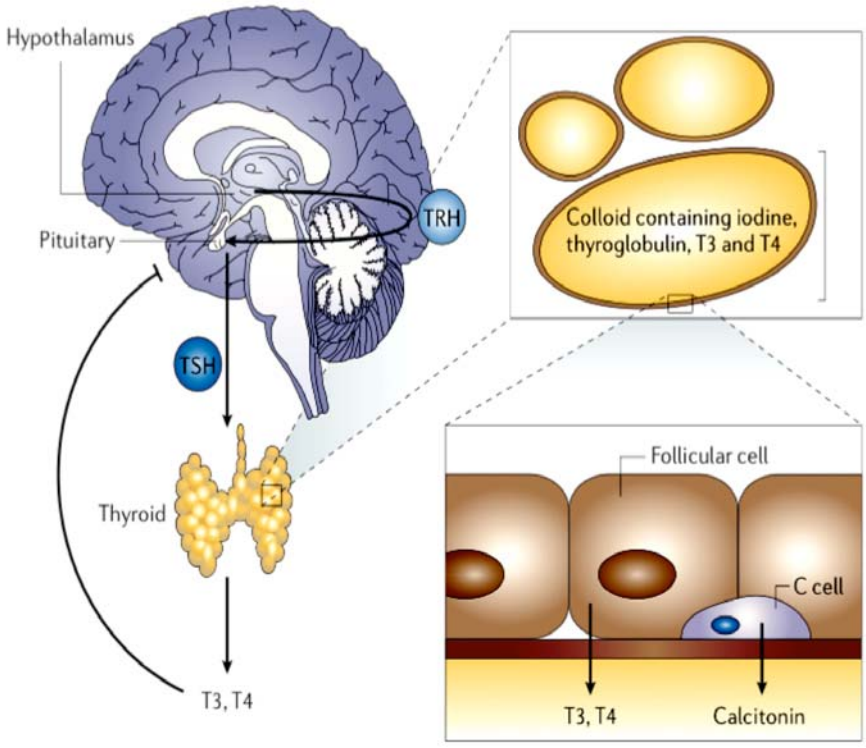

Figure 1 - Thyroid follicle organization and regulation of thyroid hormones synthesis.

Thyroid gland is composed of aggregates of follicles. The follicles range between 50-500 μm in size and contain colloid. Here TG, the precursor of thyroid hormones, is stored. Cells surrounding the lumen are cuboidal-to-flat in shape and produce thyroid hormones T3 and T4. C-cells are interspersed within the follicles and synthesize calcitonin (right). Thyroid hormone production is positively regulated by hypothalamic-pituitary axis. TRH from hypothalamus stimulates secretion of TSH from anterior pituitary gland, which in turn stimulates thyroid hormones synthesis and secretion. A negative feedback is exerted by T3 and T4 on pituitary secretion of TSH (left). (Image adapted from Kondo *et al.* 2006)

.

2.1.2 Thyroid pathology

Diseases of the thyroid gland mainly consist in alterations in hormone secretion, enlargement of the gland (goiter) or both. Inadequate secretion of thyroid hormones causes hypothyroidism or myxedema while an excess causes hyperthyroidism (Larsen *et al.*, 2003). Goiter may be associated with

increased, normal or decreased hormone secretion. Focal enlargement of the gland usually reflects a neoplastic process, a nodule. Thyroid nodules are broadly subdivided in benign and malignant lesions (Mazzaferri, 1993). Thyroid adenomas are benign tumors and are typically solitary neoplasms, arising from a genetic alteration in a single precursor cell (Kondo *et al*. 2006). They may be clinically silent or functional, producing increased levels of thyroid hormones, which results in symptomatic hyperthyroidism (referred to as a toxic thyroid adenoma). The most common genetic lesion in functional thyroid adenomas is somatic activating mutation in TSH receptor (TSHR) gene (~80%) (Parma *et al*. 1995). Mutations in Gsα gene coding for TSHR-coupled G protein have been also found in toxic adenomas (~25%). Malignant thyroid lesions comprise a heterogeneous group of neoplasm with distinctive clinical and pathological features and are discussed below.

.

2.1.3 Classification of thyroid carcinomas

Thyroid carcinomas are the most common malignancies of endocrine organs and comprise approximately 1% of newly diagnosed cancer cases (Hundahl *et al*. 1998; Gimm, 2001), and incidence rates have increased over the past few decades (Kondo *et al*. 2006; Jemal *et al*. 2008). More than 95% of thyroid cancers derive from follicular cells whereas only 3-5% derive from C-cells. According to histological parameters, follicular-cell-derived carcinomas are divided into different classes: 1) well-differentiated carcinoma (WDC) including papillary thyroid carcinoma (PTC, 85%) and follicular thyroid carcinoma (FTC, 5-10%) (Pacini *et al*. 2006); 2) undifferentiated or anaplastic thyroid carcinoma (ATC, 2%) and 3) poorly differentiated carcinoma (PDC, 5%) (DeLellis and Williams, 2004; DeLellis, 2006; Kondo *et al*. 2006). Thyroid carcinomas vary considerably in aggressiveness, with tumor growth rate as well as mortality progressively increasing from WDC to PDC and to

ATC. C-cell derived carcinomas comprise both sporadic and hereditary medullary thyroid carcinoma (MTC).

1) WDC

PTC is currently defined as a malignant epithelial tumor arising from follicular cells with characteristic nuclear alterations and retaining a differentiated phenotype. PTC is classically characterized by a branching (papillary) architecture, but several morphological variants are known (DeLellis, 2006). PTC occurrence has a female to male ratio of 4.5:1 and patients are between 20 and 50 years of age. PTC may occur in childhood as consequence of accidental or therapeutic radiation exposure. PTC usually has an indolent behavior, tendency to form metastasis to local lymph nodes and an overall good prognosis (Schlumberger, 1998; Sherman 2003; DeLellis, 2006). However, despite being usually curable with surgery and adjuvant radioiodine treatment, in some patients the disease may show an aggressive behavior and lose the ability to concentrate radioiodine. Moreover, some PTC subtypes like the tall-cell variant, display aggressive features (Sherman, 2003; Leboulleux *et al*. 2005; Adeniran *et al*. 2006; Elisei *et al*. 2008a; Romei *et al*. 2008).

FTC is a malignant epithelial tumor with evidence of follicular cell differentiation in the absence of the diagnostic nuclear features of PTC. Its incidence peaks during the 5th decade of life with a female to male ratio of 3-4:1 (DeLellis 2006). Despite a higher frequency of distant haematogenous metastasis compared to PTC, most FTC patients can also be cured, with good long-term survival rates (Schlumberger, 1998; Sherman, 2003; Durante *et al*. 2006).

2) ATC

ATC is morphologically defined as a malignant tumor composed entirely or partially of undifferentiated cells exhibiting evidence of epithelial

differentiation by immunohistochemistry or electron microscopy (DeLellis, 2006). ATC occurs between the 6th to 7th decades of life. At least in some cases, ATC may derive from a pre-existing well-differentiated carcinoma as suggested by the coincidental detection of WDC tissue in more than 25% of ATC patients (Pasieka, 2003; Ordonez *et al.* 2004; Ain, 1999). ATC disseminates both to regional lymph nodes and to distant sites (Pasieka, 2003; Ordonez *et al.* 2004; Ain, 1999). At present the treatment of ATC has in most cases only palliative purposes, therefore there is an urgent need of novel therapeutic approaches for this rare tumor type.

3) PDC

Both morphologically and clinically, PDC occupies an intermediate position between WDC and ATC. PDC is defined as neoplasm of follicular origin with limited evidence of follicular cell differentiation; similar to ATC, PDC may arise *de novo* or in association with pre-existing WDC (DeLellis, 2006; Pulcrano *et al.* 2007; Volante *et al.* 2007).

4) MTC

Medullary thyroid carcinoma (MTC) is a rare malignant tumor that arises from C-cells (Elisei *et al.* 2007; Elisei *et al.* 2008b; Miccoli *et al.* 2008; Schlumberger *et al.* 2008). The majority of cases are sporadic, while roughly 25% of cases are autosomal dominantly inherited (Marx, 2005). Familial MTC can present as single disease as in isolated familial MTC (FMTC), or associated to pheochromocytoma, parathyroid adenoma and other tumors in the context of MEN2 (multiple endocrine neoplasia type 2) syndromes A and B (MEN2A, MEN2B) (Leboulleux *et al.* 2004; DeLellis, 2006).

2.1.4 Mechanisms of thyroid tumorigenesis

The aetiology of most thyroid cancers is unknown. Familial occurrence of WDC has been described (FNMTC: familial non medullary thyroid carcinoma) (Malchoff and Malchoff, 2006; Sturgeon *et al.* 2005; Nosè, 2008; Capezzone *et al.* 2008). Moreover, WDC has been reported to occur in association with hereditary cancer syndromes, such as FAP (Familial Adenomatous Polyposis), Cowden disease, Carney complex and Werner syndrome. However, such familial clustering accounts only for a small fraction of WDC cases (Malchoff and Malchoff 2006; Sturgeon *et al.* 2005; Nosè, 2008; Capezzone *et al.* 2008).

Radiation exposure is the only exogenous risk factor that has clearly been identified as being able to cause thyroid carcinoma. An increase in PTC prevalence has been clearly documented in subjects exposed to ionizing radiations. In particular, after the Chernobyl nuclear accident, PTC frequency markedly increased in children exposed to radiations (Williams, 2002; Ciampi and Nikiforov, 2007). Nikiforov and co-workers proposed an intriguing mechanism to explain how ionizing radiation can cause RET/PTC rearrangements (see below) and why this occurs preferentially in thyrocytes. In the interphase chromatin of thyroid cells, spatial contiguity between RET gene and H4 loci may provide the structural basis for radiation-induced illegitimate nonhomologous recombination between the two genes, giving rise to RET/PTC1 (Nikiforova *et al.* 2000). Propensity of thyrocytes to increase DNA end joining activity upon radiation-induced DNA damage may allow chromosomal rearrangements (Yang *et al.* 1997) and the high sensitivity of the RET gene to radiation-induced dsDNA break may favor in particular the occurrence of RET rearrangements (Volpato *et al.* 2008). In addition, iodine excess and deficiency, as well as immunological and hormone influences are also debated as risk factors (Kondo *et al.* 2006).

A variety of genetic lesions have been disclosed over the past two decades to be associated to thyroid cancer. The genetic lesions can affect either proto-

oncogenes (gain-of-function mutations) or tumor suppressor genes (loss-of-function mutations). A summary of prevalent genetic lesions in each of the different thyroid tumor subtypes is shown in **Table 1**.

Tumor	Cell type	Risk factor	Genetic lesion	
			Gain	Loss
PTC	Follicular cell	Ionizing radiation	**RET (r)** **NTRK1 (r)** **BRAF (pm)**	**PTEN (deletion)**
FTC	Follicular cell	Iodine deficiency	**PAX8/PPARγ (r)** **RAS (pm)**	**PTEN (deletion)**
ATC	Follicular cell	Unknown (tumor progression)	**RAS (pm)** **BRAF (pm)** **PIK3CA (pm)**	**PTEN (deletion)** **TP53 (various)**
MTC	C-cell	Familial	**RET(pm)**	**CDKN2C (pm)**
	C-cell	Sporadic	**RET (pm)**	**CDKN2C (pm)**

NTRK1, neurotrophic tyrosine receptor kinase type 1; PPARγ, peroxisome proliferator activated receptor γ; PTEN, phosphatase, tensin homologue, deleted on chromosome 10; CDKN2C, p18INK4C; pm, point mutation; r, rearrangement.

Table 1 – Structural genetic alterations in thyroid cancer.
(Table modified from Santoro and Carlomagno 2006).

Genetic alterations in PTC

Genetic alterations associated with PTC include chromosomal rearrangements targeting the RET (REarranged during Transfection) or NTRK1 (neurotrophic receptor-tyrosine kinase 1) genes, and point mutations in the BRAF and RAS genes. The most common lesions are those affecting RET and BRAF. All these genes encode proteins that signal along the ERK (extracellular signal-regulated kinase) pathway, and the genetic alterations targeting them result in constitutive ERK1/2 pathway activation. Overall, genetic events involving RET, NTRK1, BRAF or RAS are found in the vast majority of PTC cases and rarely overlap in the same tumor (Kimura *et al.* 2003; Soares *et al.* 2003; Nikiforova *et al.* 2003a; Nikiforova *et al.* 2003b; Frattini *et al.* 2004; Elisei *et al.* 2008a), underlining the relevance of ERK

signaling pathway abnormalities in the pathogenesis of PTC. A schematic representation of components of ERK pathway is presented in **Figure 2**.

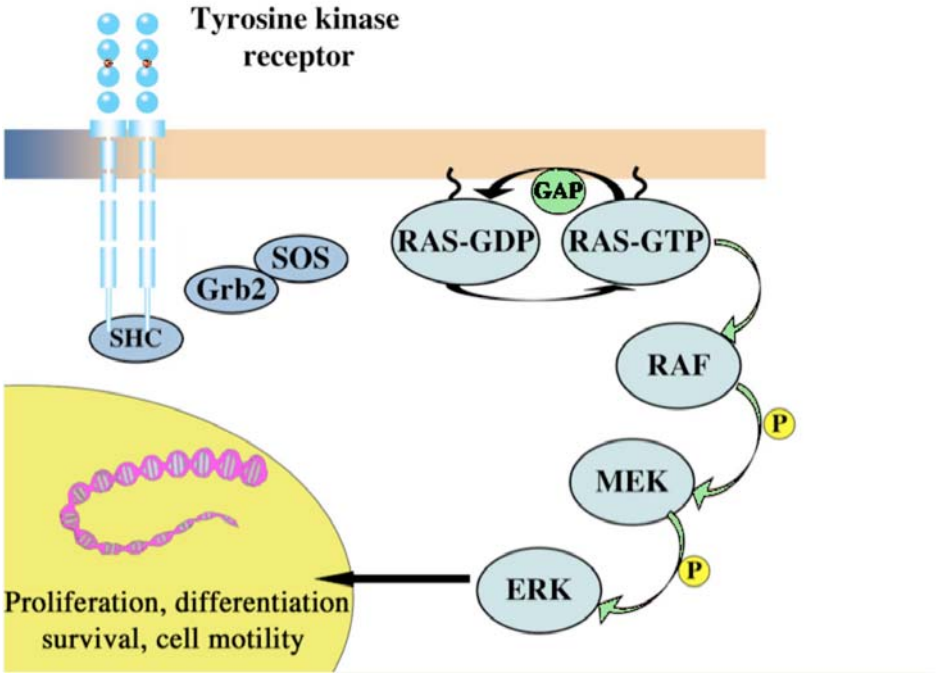

Figure 2 - ERK signaling pathway.

- *RET*

The RET proto-oncogene is located on chromosome 10q11.2 and codes for a membrane receptor tyrosine kinase (RTK). RET RTK is able to bind growth factors of the GDNF (Glial cell line-derived neurotrophic factor) family (Takahashi *et al.* 1985; Manié *et al.* 2001; Ciampi and Nikiforov 2007). Ligand binding, in presence of co-receptors of the GFRα (GDNF family receptor α) family, causes RET dimerization and activation. Once activated, RET autophosphorylates tyrosine residues within its intracellular domain. Phosphorylated tyrosines function as binding sites for signaling molecules containing phosphotyrosine-binding motifs (SH2 or PTB), thereby activating several signaling pathways (Santoro *et al.* 2004; Santoro *et al.*, 2006). Through phosphorylated Y1062, RET binds SHC and FRS2, which recruit Grb2-SOS

complexes leading to the activation of the RAS-RAF-ERK cascade (Asai *et al.* 1996; Melillo *et al.* 2001). Through Y1062, RET is also able to activate the phosphatidylinositol 3-kinase (PI3K)/AKT pathway (Segouffin-Cariou and Billaud, 2000; Pelicci *et al.* 2002; Frêche *et al.* 2005).

In PTC, chromosomal inversions or translocations disrupt the RET gene between the transmembrane and the tyrosine kinase domain and mediate the recombination of the tyrosine kinase domain to the N-terminus encoded by heterologous genes, thus generating chimeric RET/PTC oncogenes (Fusco *et al.* 1987). So far, many RET/PTC variants have been identified, formed by the RET fusion to different partners. RET/PTC1 and RET/PTC3, resulting from fusion with the H4 (D10S170) (Grieco *et al.* 1990) or the RFG (NCOA4, ELE1 or ARA70) (Santoro *et al.* 1994; Borganzone *et al.* 1994) genes, are the most prevalent variants (Ciampi and Nikiforov, 2007) (**Fig. 3**). RET rearrangements are found in 20-40% of PTC, but the prevalence is significantly higher in patients with a history of accidental or therapeutic radiation exposure. In the thyroid gland, RET is normally expressed at high levels in C-cells, but not in follicular cells. By providing an active promoter, RET/PTC rearrangements enable thyroid expression of the chimeric RET/PTC oncoproteins (Fusco *et al.* 1987; Grieco *et al.* 1990). Moreover, fusion with partner genes coding for proteins possessing protein-protein interaction motifs results in RET/PTC ligand-independent dimerization and autophosphorylation. Breakpoints in the RET gene leave intact the kinase domain, and most of the autophosphorylation sites thereby allowing downstream signaling (Ciampi and Nikiforov, 2007). RET/PTC1 is more frequently associated with classic PTCs and with the diffuse sclerosing variant; conversely, RET/PTC3 is more common in the solid variant and in PTC associated to ionizing radiation (Thomas *et al.* 1999). RET rearrangements have a lower prevalence in the follicular variant PTC compared to classic PTC (DeLellis 2006). Moreover, at a variance from BRAF (see below), RET/PTC it is not a negative prognostic factor (Elisei *et al.* 2008a). RET/PTC induces transformation and dedifferentiation of cultured thyroid cells

(Santoro *et al.* 1993; De Vita *et al.* 1998), and thyroid-specific RET/PTC-transgenic mice develop PTC, showing that RET/PTC oncogenes are able to initiate thyroid carcinogenesis (Santoro *et al.* 1996; Powell *et al.* 1998). Moreover, RET/PTC is frequently detected in clinically silent papillary microcarcinomas, proving it can be an early event in thyroid tumorigenesis (Fusco *et al.* 2002). Recent findings support the idea that RET/PTC signals along the MAPK (ERK) pathway (Knauf *et al.* 2003; Melillo *et al.* 2005, Mitsutake *et al.* 2005). However, other pathways downstream RET/PTC, particularly the PI3K/AKT one, may contribute to its biological effects as well (Pelicci *et al.* 2002; Miyagi *et al.* 2004; Jung *et al.* 2005, De Falco *et al.* 2005).

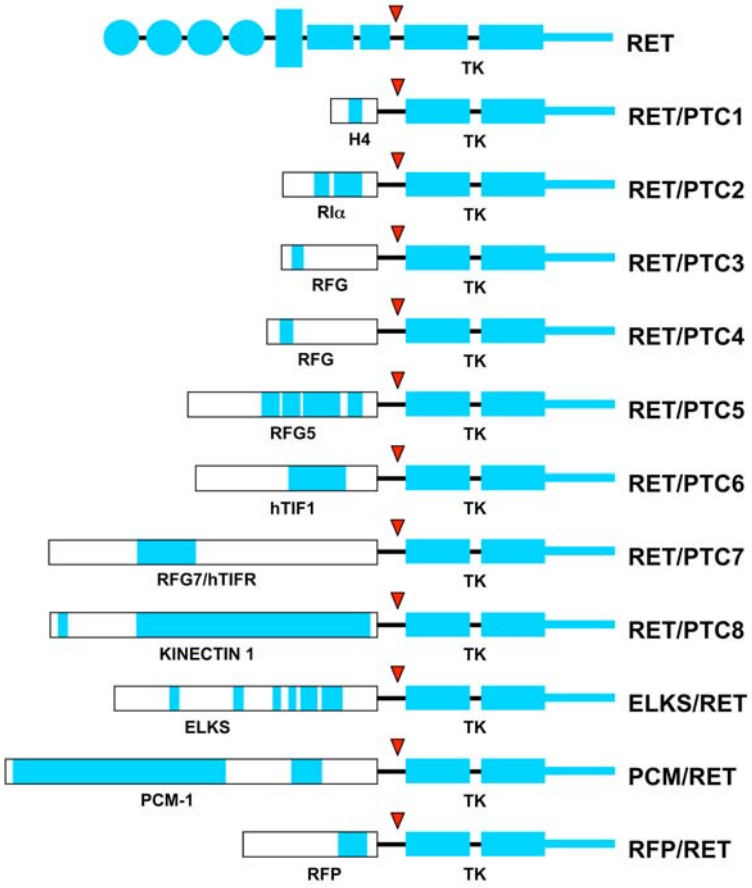

Figure 3 – RET/PTC rearrangements in papillary thyroid cancer.

- *NTRK1*

Similar to RET, the NGF (Nerve Growth Factor) high affinity receptor NTRK1 gene undergoes oncogenic conversion by chromosomal rearrangements in PTC (Greco *et al*. 2004). At least three partner genes are involved in these rearrangements (Greco *et al*. 1993; Greco *et al*. 1995; Greco *et al*. 1997). NTRK1 rearrangements appear however less prevalent than RET ones.

- *BRAF*

BRAF is a serine-threonine kinase belonging to the RAF family (ARAF, BRAF, CRAF) of intracellular effectors of the MAPK (ERK) pathway. Recruitment to the cell membrane and binding to RAS, in its GTP-bound state, triggers RAF activation. Active RAF phosphorylates and activates MEK (MAPK/ERK Kinase), which in turn activates ERK, causing sequential activation of downstream effectors of the ERK cascade. Among the RAF family members, BRAF has the highest basal kinase activity and is the most potent activator of the MAPK pathway (Wellbrock *et al*. 2004).

Activating point mutations within the kinase domain of the BRAF gene have been found in several tumor types, including melanoma and colorectal cancer. A thymine to adenine transversion at nucleotide 1799 (T1799A), resulting in a substitution of glutamic acid for a valine at residue 600 (V600E) of the protein, is the most common event. V600E and most other mutations within the BRAF kinase domain target either the activation loop or the ATP binding site (P loop). By disrupting the interactions between the activation loop and the P loop that hold the kinase in an inactive conformation, these mutations cause BRAF constitutive activation (Wan *et al*. 2004).

BRAF mutation represents the most common genetic event in PTC, occurring approximately in 45% of all cases (Ciampi and Nikiforov, 2007; Xing, 2007; Elisei *et al*. 2008a). V600E is by far the most common oncogenic

mutation. Other rare mutations, like point mutation K601E, insertion V599Ins, mutation and the inversion of chromosome 7q fusing the kinase domain encoding-region of the BRAF gene with the AKAP9 gene, have been described (Trovisco *et al*. 2004; Carta *et al*. 2006; Ciampi *et al*. 2005; Lupi *et al*. 2007). We have recently identified and functionally described the novel T599I-VKSR(600-603)del in PTC patients affected by a follicular variant thyroid carcinoma (**Manuscript II**).

BRAF mutation has been found in very early stages of PTC (Ugolini *et al*. 2007), supporting its role in the initiation of these tumors. BRAF mutations are highly prevalent in classic and tall-cell variant PTCs, but similar to RET rearrangements, they are rarely found in the follicular variant, where sometimes variant BRAF (rather than the classic V600E) mutations are found (Xing, 2007). BRAF mutations correlate with aggressive tumor behavior, tumor recurrence, decreased radioiodine concentration ability, and decreased survival (Namba *et al*. 2003; Nikiforova *et al*. 2003a; Xing *et al*. 2005; Riesco-Eizaguirre *et al*. 2006; Lupi *et al*. 2007; Elisei *et al*. 2008a). Importantly (see below), BRAF mutations are also found in ATC. Thyroid-specific BRAFV600E-transgenic mice develop PTCs that closely recapitulate the features of human PTC. These transgenic PTCs show characteristics of aggressive behavior and tendency towards progression to PDC (Knauf *et al*. 2005). This suggests the involvement of BRAF mutation not only in PTC initiation but also progression to PDC. Accordingly, BRAF and the downstream MEK kinase have emerged as promising molecular targets for thyroid cancer treatment, in particular aggressive PTC variants as well as ATC (**Manuscript III**).

- *RAS*

Activating point mutations in RAS small GTPases are quite uncommon in PTC, with an overall frequency of less than 10%, and appear to be confined to

the follicular variant PTC (Zhu *et al.* 2003; De Lellis, 2006, Kondo *et al.* 2006).

Genetic alterations in FTC

FTC may develop through at least two different pathways, involving either RAS or PPARγ (peroxisome proliferator-activated receptor γ) genes (Nikiforova *et al.* 2003a). RAS point mutations are detected in about 50% of follicular adenomas and carcinomas (Nikiforova *et al.* 2003a). Another subset of FTC (~30%) harbors the t(2;3)(q12-13;p24-25) chromosomal translocation, which causes the fusion of the region encoding the DNA binding domains of the thyroid transcription factor PAX8 to the region encoding domains A-F of PPARγ steroid-hormone receptor; the resulting fusion oncoprotein contributes to malignant transformation through a dominant-negative effect on transcriptional activity of wild-type PPARγ (Kroll *et al.* 2000; Castro *et al.* 2006). Other more rare PPARγ rearrangements have been found (Lui *et al.*, 2008). As in PTC, point mutations or gene amplification of PI3KCA have been reported in few FTC cases (García-Rostán *et al.* 2005; Wu *et al.* 200; Liu *et al.* 2008). Moreover, increased incidence of FTC has been observed in the context of Cowden disease, determined by PTEN hemizygous deletion (Liaw *et al.* 1997).

Genetic alterations in PDC and ATC

Overall ATC as well as PDC share genetic lesions with WDC, consistent with the possibility that at least some cases may derive from pre-existing WDC (Nikiforov, 2004; Smallridge *et al.* 2008). Indeed, while RET/PTC and PAX8-PPARγ rearrangements are rarely found, point mutations are instead frequently detected. RAS point mutations are quite prevalent in PDC and ATC (García-Rostán *et al.* 2003). Roughly 30% of ATC and PDC harbor the V600E BRAF mutation, particularly those samples with morphological evidence of pre-

existing PTC (Nikiforova *et al.* 2003a; Soares *et al.* 2004; Begum *et al.* 2004). Both BRAF and RAS mutation appear to confer a predisposition to the development of both PDC and ATC. Finally, amplification or point mutation in PIK3CA that is rarely associated to WDC is instead frequently found in ATC (García-Rostán *et al.* 2005; Wu *et al.* 2005; Liu *et al.* 2008).

However, in particular mutations in TP53 and CTNNB1 have been selectively associated to ATC (Nikiforov, 2004; Smallridge *et al.* 2008).

- *TP53*

The TP53 gene encodes the nuclear transcription tumor suppressor factor p53 that plays a central role in the regulation of cell cycle, DNA repair, and apoptosis. P53 exerts this functions largely by its ability to transactivate expression of genes coding for proteins such as p21(CIP/WAF1) that induce cell cycle arrest by inhibiting cyclin-dependent kinase (CDK) complexes (Weinberg, 2007). p53 is overexpressed immediately after the exposure to DNA-damaging agents and causes transient cell cycle arrest, presumably to allow DNA repair to progress. However, if the DNA damage is severe, p53 initiates apoptosis to prevent clonal expansion of the damaged cell (Weinberg, 2007). Alteration of p53 function in various cancer cells, by inactivating point mutation or by deletion, results in progressive genome destabilization, accumulation of mutations, and evolution of more malignant clones.

In thyroid tumors, point mutations of TP53 occur in approximately 70% of ATC and in a significant fraction of PDC, but only in rare cases of PTC and FTC (Nikiforov, 2004; Kondo *et al.* 2006). Furthermore, besides mutation affecting TP53 itself, several other mechanisms can prevent p53 function in thyroid cancer, including up-regulation of negative p53 regulators or of proteins fostering p53 degradation. Consistent with a common loss-of-function of p53, ATC samples exert a gene expression signature that includes the up-regulation of many cell cycle-related genes normally under a negative control

exerted by p53 (Salvatore *et al.* 2007).

- *CTNNB1*

Another gene whose mutation is associated to thyroid tumor dedifferentiation is β-catenin. This cytoplasmic protein, encoded by the CTNNB1 gene, plays an important role in E-cadherin-mediated cell-cell adhesion and is also an important intermediate in the wingless (Wnt) signaling pathway. In thyroid tumors, point mutations in exon 3 of CTNNB1 have been reported in PDC and more frequently in ATC, but not in WDC (García-Rostán *et al.* 2001; Miyake *et al.* 2001), suggesting that they might play a direct role in the dedifferentiation and progression to ATC.

Genetic alterations in MTC

RET point mutation is so far virtually the only genetic lesion consistenly associated to MTC formation (Elisei *et al.* 2007; Elisei *et al.* 2008; Schlumberger *et al.* 2008). As previously mentioned, MTC can occur either sporadically or in the context of autosomal dominant MEN 2 syndromes (MEN 2A, MEN 2B and FMTC) (Manié *et al.* 2001; Marx, 2005). MEN 2 is caused by germline point mutations that convert RET into a dominant oncogene (Santoro *et al.* 1995). In all MEN 2A cases, mutations target extracellular cysteine residues in RET. In more than 80% of the cases, MEN 2B is caused by the Met918Thr intracellular substitution in the P+1 loop of the kinase. FMTC is caused by mutations in the RET extracellular or kinase domains. Sporadic MTC presents with somatic RET mutation, up to 50% of the cases harbor point mutations in RET similar to those in MEN2B (Cote and Gagel, 2003; Leboulleux *et al.* 2004). Accordingly, RET kinase has emerged as a promising molecular target for treatment of MTC (**Manuscript IV**).

2.2 TSH/PKA/CREB PATHWAY IN THYROID FOLLICULAR CELLS

The pituitary hormone TSH binds TSHR, a seven-transmembrane G-protein coupled receptor expressed in thyroid cells (Larsen *et al*. 2003; Kimura *et al*. 2001; Ledent *et al*. 1991; Dremier *et al*. 2002). The end result of TSH stimulation of thyrocytes is growth and differentiation. Stimulation of TSHR activates the membrane bound enzyme adenylate cyclase (AC). In turn, the increase in intracellular levels of 3',5'-cyclic adenosine monophosphate (cAMP) stimulates protein kinase A (PKA). In the basal state, PKA resides in the cytoplasm as an inactive heterotetramer of paired regulatory (R) and catalytic (C) subunits. Induction of cAMP liberates the C subunits, which passively diffuse into the nucleus and induce cellular gene expression. Transcription factors that are substrate of PKA-mediated phosphorylation include the cAMP response element (CRE) binding protein (CREB) and the cAMP response element modulator (CREM) (Johannessen *et al*. 2004). PKA-mediated phosphorylation of CREB at serine residue 133 ultimately leads to transcriptional upregulation of CREB-binding promoters, featuring the conserved cAMP-responsive element (CRE) "TGACGTCA" (Mayr and Montminy, 2001) (**Fig. 4**).

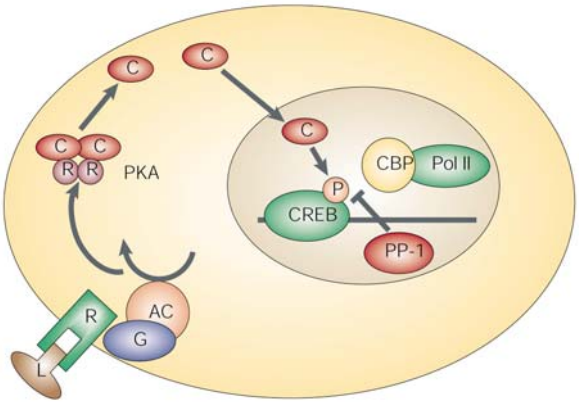

Figure 4 - The TSH-PKA-CREB cascade.
(Image modified from Mayr and Montminy, 2001).

The TSH-PKA-CREB pathway represents the dominant regulatory cascade in the proliferation and differentiation of thyroid follicular cells (Kimura *et al.* 2001; Ledent *et al.* 1991; Dremier *et al.* 2002). Accordingly, a dominant negative CREB mutant triggered apoptosis of cultured thyrocytes and inhibited cell number increase, due to delayed cell cycle transit (Dworet *et al.* 2006). *In vivo*, in transgenic mice, a dominant negative CREB inhibited growth of the thyroid gland as well as the expression of thyroid differentiated markers, TSHR, thyroperoxidase (TPO), thyroglobulin (TG) (Nguyen *et al.* 2000).

Cyclin D1 is a prototypic CREB target. The D-type cyclins control progression through the G1 phase of the cell cycle as the regulatory component in the cyclin D/cdk4-6 kinase complex. Enhanced cyclin D1 expression is a hallmark of many cancers and several elements in the cyclin D1 gene promoter are implicated in such up-regulation; these include binding sites for the transcription factors AP1, Ets-1, NF- B, SP-1, TCF/LEF, Oct-1, ATF-2, and CREB. The CRE element, located upstream of the mRNA start site, has a key role in both basal and induced cyclin D1 expression and the CRE-binding protein CREB is an essential component in its activity, either alone or in association with ATF-1 or ATF-2 (Albanese *et al.* 1995; Boulon *et al.* 2002).

Moreover, in thyroid cells TSH/CREB cascade regulates expression and/or activity of thyroid-specific transcription factors Pax8, TTF1 and TTF-2

(Rossi *et al*. 1995, Van Renterghem *et al*. 1996, Ortiz *et al*. 1997; Missero *et al*. 1998). Thus, TSH/cAMP targets include the thyroid differentiation specific genes TSHR, thyroperoxidase (TPO), thyroglobulin (TG) (Nagayama *et al*. 1989) and sodium-iodine symporter (NIS) (Ohmori *et al*. 1998). Most of the TSH/cAMP-regulated genes contain CRE elements in their promoters or enhancers.

CREB is a member of the CREB/ATF-1 (activating transcription factor 1)/CREM (CRE modulator) bZIP transcription factors family (Montminy and Bilezitjian, 1987; Mayr and Montminy, 2001; Johannessen *et al*. 2004) (**Fig. 5**).

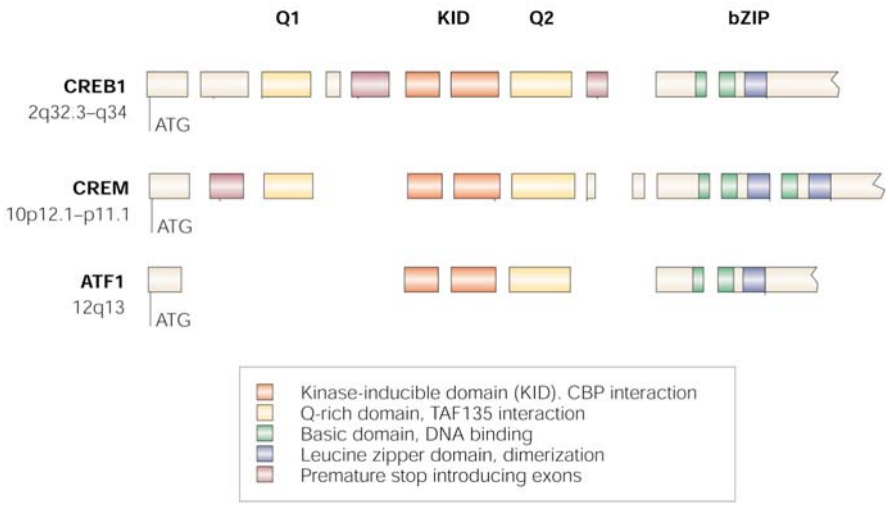

Figure 5 – The CREB, ATF1, CREM factors.
(Image modified from Mayr and Montminy 2001).

The C-terminus contains the basic leucine zipper (bZIP) domain responsible for dimerization and binding to DNA. The N-terminus contains a kinase-inducible domain (KID) and a glutamine-rich domain termed Q2, both necessary for full activation in response to external stimuli. Cyclic AMP transactivates CREs via phosphorylation of CREB at Ser133 in the KID domain by PKA (Gonzáles and Montminy, 1989). However, CREB has been

found to mediate transcriptional responses to a variety of growth factor and stress signals. In fact, the same S133 residue can be phosphorylated in response to multiple kinases, which are activated by different signaling pathways (Shaywitz and Greenberg, 1999; Johannessen *et al.* 2004). Phosphorylated CREB then binds its coactivator CREB binding protein (CBP), which facilitates unwinding of DNA and interaction with the basal transcriptional machinery (Chrivia *et al.* 1993; Arias *et al.* 1994; Mayr *et al.* 2001). Of note, CREB S133 phosphorylation induces expression of only a small fraction (2%) of target genes, reflecting a requirement for additional CREB-regulatory partners in recruiting the transcriptional machinery (Zhang *et al.* 2005; Impey *et al.* 2004). In fact, CREB activity is also regulated by a family of latent cytoplasmic coactivators, called TORCs, which translocate to the nucleus and bind to CREB. Genome-wide studies have identified a high number of putative CREB target genes (up to 5,000) including several cell-cycle and growth-factor genes (Zhang *et al.* 2005; Impey *et al.* 2004).

CREB is involved in cancer formation (Conkright and Montminy, 2005). A potential role for the CREB family in cellular transformation was first appreciated in clear-cell sarcomas of soft tissues (CSSTs), which contain a t(12,22) (q13,q12) translocation that fuses the bZIP domain of ATF1 to the Ewing's sarcoma oncogene product (EWS), generating a EWS–ATF1 chimera able to enhance expression of CREB targets. Moreover, virally encoded oncoproteins such as human T-cell leukemia virus (HTLV-1) tax and hepatitis B virus X enhance CREB target gene expression, by binding to the CREB bZIP domain and increasing the affinity of CREB for binding to cellular promoters. Finally, the CREB gene is amplified in myeloid blast leukemic cells from several patients and the elevated expression of CREB is associated with poor clinical outcome by enhancing S-phase entry and growth-factor-independent proliferation Levels of Bcl-2 were unchanged in CREB-amplified cells, while cyclin A1 was induced (Conkright and Montminy, 2005).

2.3 CD44

2.3.1 Role of CD44

CD44 is a type I transmembrane protein and represents the principal cell surface receptor for hyaluronic acid (HA), a component of the extracellular matrix (ECM) (Ponta *et al*. 2003). CD44 is involved in a variety of physiological processes and its dysfunction is associated to a wide range of diseases. These functions include:

- morphogenesis and organogenesis (Knudson and Knudson, 1993; Ruiz *et al*. 1995; Goshen *et al*. 1996; Kaya *et al*. 1997; Kaya *et al*. 1999; Günthert *et al*. 1998; Sherman *et al*. 1998);
- haematopoiesis (Lewinsohn *et al*. 1990; Long *et al*. 1992; Kinashi and Springer, 1994; Günthert *et al*. 1998; Ghaffari *et al*. 1997; Ghaffari *et al*. 1999);
- lymphocyte homing (Berg *et al*. 1989, Picker *et al*. 1989; Seth *et al*. 1991) and migration (Puré and Cuff, 2001; Isacke and Yarwood, 2002; Yasuda *et al*. 2002);
- leucocyte activation (Dianzani and Malavasi, 1995; Zöller, 1996; Günthert *et al*. 1998), effector functions (Shimizu and Shaw, 1991; Tan *et al*. 1993; Wang 1993; Galandrini *et al*. 1993; Yang and Binns, 1993) and activation-induced cell death (AICD) (Wittig *et al*. 2000; Fujita *et al*. 2002; Guy *et al*. 2002; McKallip *et al*. 2002; Marhaba *et al*. 2003);
- tumor growth and metastasis (Sherman *et al*. 1996; Naor *et al*. 1997; Naor *et al*. 2002; Puré and Cuff, 2001; Yasuda *et al*. 2002; Jothy, 2003).

Although the number of diverse and complex processes to which CD44 takes part may be surprising, this complexity can be explained through a small number of CD44 molecular properties:

- adhesion to extracellular matrix elements: GAGs, enzymes and soluble growth factors;
- cooperation with other transmembrane receptors;
- interaction with cytoskeleton components and signal transduction.

A comprehensive description of the molecular properties of CD44 is provided in recent review articles (Ponta *et al.* 2003; Marhaba and Zöller, 2004).

2.3.2 CD44 protein family

CD44 comprises a family of transmembrane glycoproteins that are encoded by a single gene located on the short arm of chromosome 11 in humans, of 20 exons spanning ~50kb of genomic DNA (Screaton *et al.* 1992) (**Fig. 6**). Overall, human CD44 shows high degree of sequence conservation compared to orthologues protein, in particular in transmembrane and cytoplasmic domains. The size of the protein varies between 80 and 200 kDa. Such a size heterogeneity is due to variable N- and O-linked glycosylation and to alternative splicing. The smallest, so-called standard CD44 (CD44st) or haematopoietic isoform is present on the membrane of most vertebrate cells (Naor *et al.* 1997). It is the most abundant form and consists of an N-terminal signal sequence (exon 1), a link-homology hyaluronan-binding module (exons 2 and 3), a stem region (exons 4, 5, 6, and 7), a single-pass transmembrane domain (exon 8) and a cytoplasmic domain (exon 9 and 10).

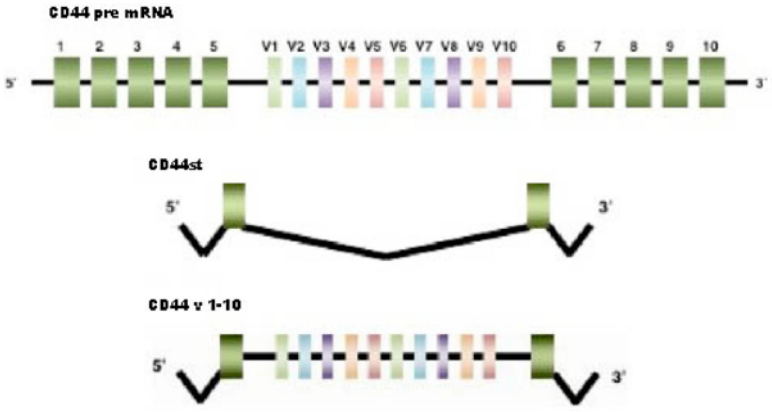

Figure 6 - CD44 isoforms.
Exons in green from 1 to 10 represent the constant region; exons from v1 to v10 are inserted by alternative splicing. CD44st (standard CD44) contains only the constant region and is the most abundant form in vertebrate cells; CD44 V1-10 contains all the variant exons and is predominantly expressed in differentiated ectodermal cells. (Image adapted from Ponta *et al.* 2003).

CD44 domains

- *N-terminal domain and the stem region*

The N-terminal portion of CD44 is folded in a globular structure and is responsible for the binding to extracellular matrix components (EMCs): mainly hyaluronic acid (HA) (Stamenkovic *et al.* 1991; Lesley *et al.* 1998), and with lower affinity other glycosaminoglycans (GAGs), collagen (Wayner *et al.* 1988), laminin, fibronectin (Jalkanen and Jalkanen, 1992) and osteopontin. Between the N-terminal domain and the transmembrane domain of the molecule, there is the stem region, a heavily glycosylated stalk-like stretch of 46 AA (Screaton *et al.* 1992). This region contains putative proteolytic cleavage sites (Okamoto *et al.* 1999a,b). This stretch can be enlarged by the insertion of the variable exons v1-10 through alternative splicing. Tissue-specific factors regulate alternative splicing as mesenchymal cells mostly splice out the variant exons, whereas differentiated ectodermal cells encode CD44 proteins including all variant exon products (CD44 v1-10). Multiple

combinations of variant exons have been described, some combinations being predominantly found on defined tissue or in a particular state of activation of the cells.

- *Transmembrane domain and cytoplasmic tail region*

The transmembrane region consists of 23 hydrophobic AA and a cysteine residue. This domain is responsible for the association of CD44 with lipid raft microdomains (Perschl *et al.* 1995). The cytoplasmic tail is important for anchoring to the cytoskeleton and association with non-receptor tyrosine kinases (PTKs). The CD44 interaction with cytoskeleton is indirect and involves binding to cytosolic proteins like ankyrin and members of the ERM (ezrin, radixin and moesin) family. In lymphocytes, CD44 has a co-stimulatory role on TCR activation through the association of the cytoplasmic tail with lck, fyn and lyn members of the Src family of PTKs (Föger *et al.* 2000).

2.3.3 CD44 in cancer

CD44 has been implicated in cell-cell and cell-matrix interactions and homing of tumor cell metastasis (Ponta *et al.* 2003). There is substantial evidence that CD44 splicing variants are aberrantly expressed in many human tumors, being in some instances correlated to tumor progression and poor prognosis. CD44 lacks intrinsic kinase activity and must therefore associate with other proteins to modulate signaling. As mentioned above, the cytoplasmic tail of CD44 is associated to the c-Src family of PTK. This association facilitates hyaluronan-mediated stimulation of the catalytic activity of c-Src and induces cytoskeleton-regulated tumor cell migration. In certain tumors, CD44, acts as a co-receptor to activate a group of RTKs. For instance, in human colon carcinoma and in rat pancreatic adenocarcinoma, the c-Met receptor undergoes autophosphorylation when the scatter factor

(SF)/hepatocyte growth factor (HGF) binds CD44 variants v3 and v6 (van der Voort *et al.* 1999; Orian-Rousseau *et al.* 2002). Furthermore, CD44 functions as a co-receptor for the EGFR RTK family member ERBB4. In an ovarian carcinoma cell line, CD44v3 is bound to Her2/neu (ERBB2), this association leading to activation of RAS and Rac1 and to cell proliferation and reorganization of the cytoskeleton (Bourguignon *et al.* 1997; 2001). Heparin-binding epidermal growth factor (HBEGF) associates to heparan-sulphate side chains of CD44v3. When associated to CD44v3, HBEGF is cleaved by matrix metalloprotease 7 (MMP7), recruited at cell surface by CD44. In such a way, CD44 acts as a platform for the release of active EGF ligands by MMP7, thus enabling the activation of ERBB4. Moreover, CD44 acts as a signaling receptor able to induce activation of the PI3K/AKT pathway (Kamikura *et al.* 2000; Lin and Yang-Yen 2001) and to associate to ezrin to control cell motility in a protein kinase C (PKC)-regulated manner (Legg *et al.* 2002).

In addition to HA binding, it was demonstrated that CD44 was one of the cell surface receptors for osteopontin (OPN) (Weber *et al.* 1996). OPN (SPP1, secreted phosphoprotein 1) is expressed in many neoplastic tissues, such as colon, breast, prostate and lung carcinomas, being a circulating plasma marker for several neoplasms (Weber, 2001). The presence of v6 exon in CD44 is important for efficient OPN binding, while v3 exon is important for the binding of heparin binding growth factors (Ponta *et al.* 2003). Our group demonstrated that OPN is one of the most strongly induced transcripts in thyroid follicular cells transformed by RET/PTC3 or BRAF (Melillo *et al.* 2005). Interestingly RET/PTC3 transformed cells also feature CD44 transcript upregulation, in particular v3 and v6 containing variants (Castellone *et al.* 2004). Upregulation of both OPN and CD44 was also found in thyroid carcinoma cell lines spontaneously harboring RET/PTC1 oncogene (Castellone *et al.* 2004). Moreover, OPN positivity, detected by immunohistochemistry in human PTC, carrying mutations at the level of the RET-RAS-BRAF-MAPK signaling cascade, correlates with the presence of lymph node metastasis

(Guarino *et al*. 2005). In matrigel invasion assays, RET/PTC3 transformed cells and thyroid carcinoma cells, treated with exogenous OPN show higher migratory response compared to non-treated cells, and invasiveness was decreased by pretreatment with anti-OPN or anti-CD44 blocking antibodies (Castellone *et al*. 2004). CD44 stimulation by OPN caused rapid activation of ERK and AKT pathways (Guarino *et al*. 2005). Ultimately the activation of ERK and AKT pathways promotes cellular migration, as demonstrated by the marked reduction of invasiveness observed after treatment with specific inhibitors of these pathways (Guarino *et al*. 2005).

2.3.4 Modification of CD44 by proteolytic processing

The extracellular domain (ectodomain) of CD44 is subject to regulated proteolytic cleavage (reviewed by Cichy and Puré, 2003) (**Fig. 7**). A soluble form of ectoCD44 (sCD44) has been detected in the blood and other body fluids. Shedding of ectoCD44 has been demonstrated in various cancer cell lines (Okamoto *et al*. 1999a) and in tumor specimens (Okamoto *et al*. 2002). Recent work has revealed that further proteolytic processing occurs within the residual CD44 transmembrane and cytoplasmic domains (see below) (**Fig. 7**).

Matrix metalloprotease cleavage

Extracellular CD44 proteolytic cleavage is mediated by membrane-associated matrix metalloproteases (MMPs), this cleavage being responsible for dynamic regulation of the interaction between CD44 and the ECM during cell migration (Okamoto *et al*. 1999a). Membrane type 1 metalloprotease (MT1-MMP) has been shown to cleave CD44 ectodomain at the cell surface and promote cell migration (Kajita *et al*. 2001) (**Fig. 7**). Multiple signaling pathways regulate CD44 cleavage: the activation of PKC, the influx of extracellular Ca^{2+}, members of the Rho family of GTPases and the RAS oncoprotein (Okamoto *et al*. 1999b; Kawano *et al*. 2000). In particular, RAS

oncoprotein induces CD44 ectodomain cleavage through PI3K and the Rho family of GTPases, allowing cell migration (Kawano *et al*. 2000; Nagano and Saya, 2004).

γ-Secretase cleavage

In addition to the extracellular domain fragment (ectoCD44), secondary to stepwise proteolysis, CD44 cleavage generates two cell associated CD44 species (~ 25 kDa and ~12 kDa) (Murakami *et al*. 2003; Okamoto *et al*. 1999a; Okamoto et al 2001; Okamoto *et al*. 1999b; Nagano and Saya, 2004) (**Fig. 7**). The 25 kDa species correspond to the residual membrane-bound C-terminal fragment of CD44 (CD44-CTF) after MMP cleavage. Instead, the 12 kDa band is a soluble CD44 intracellular domain (ICD) fragment resulting from a cleavage just inside the CD44 transmembrane domain (Okamoto *et al*. 2001). After cleavage, CD44-ICD translocates into the nucleus and enhances transcription that is mediated through the TPA-responsive element. A γ-secretase complex, requiring presenilin-1 as catalytic subunit, was shown to mediate this transmembrane domain cleavage (Lammich *et al*. 2002; Murakami *et al*. 2003). The ICD appears to be derived from the CTF since incubation with membrane-permeable protease inhibitors increased the accumulation of the 25 kDa band (CTF) and prevented the appearance of the 12 kDa band (ICD) (Okamoto *et al*. 2001). Importantly, it has been demonstrated that in RET MEN2A transformed cells CD44st is among the main up-regulated proteins and that MEN2A is able to increase expression of CD44-ICD (Pelletier *et al*. 2006).

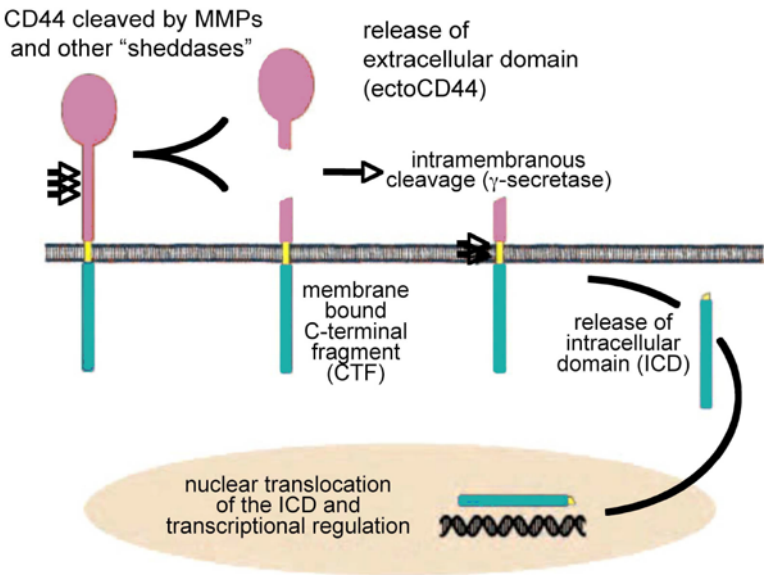

Figure 7 - Proteolytic processing of CD44.
After cleavage by matrix metalloproteases (MMPs), extracellular domain of CD44 (ectoCD44) is released, leaving the membrane bound C-terminal fragment (CTF). A subsequent proteolytic step by γ-secretases in the transmembrane domain releases the intracellular domain (ICD). Image adapted by Thorne *et al.* 2004.

2.3.5 Regulated intramembrane proteolysis

The generation the cytosolic CD44-ICD fragment from CD44, represents a new example of the process termed regulated intramembrane proteolysis (RIP) (Brown *et al.* 2000; Kopan and Ilagan, 2004). The key element in RIP is the γ-secretase complex, in particular presenilin (PS), the catalytic subunit (Sherrington *et al.* 1995). The list of membrane proteins that are targeted by γ-secretase activity is continuously increasing and includes Notch family and the amyloid precursor protein (APP) (Chyung *et al.* 2004), Ephrin B1 (Tomita *et al.* 2006), ERBB4 (Ni *et al.* 2001), and E-cadherin (Marambaud, 2002). Intriguingly in the case of APP and Notch, similarly to CD44, RIP requires a previous step of cleavage, performed at the extracellular level which sheds the bulk of extracellular domain. Then presenilin-1/γ-secretase cleaves within the plasma membrane to generate the ICDs cytoplasmic fragments. The resulting

ICDs can translocate to the nucleus and promote transcription.

The Notch pathway

The Notch pathway is a well-established example of RIP. It is an evolutionarily conserved signaling mechanism that plays a critical role in cell fate decision and pattern formation. A comprehensive description of Notch pathway and its regulation is provided in recent review articles (Bray, 2006; Kovall, 2008). In mammals, the Notch pathway provides key signals during neural, cardiovascular, immune, liver and kidney development. In adult organisms, the Notch pathway has been implicated in tissue regeneration and in stem cells function. Notch is a cell surface receptor that is processed constitutively by a furin-like enzyme in the secretory pathway. The enzyme cleaves the precursor to generate an extracellular and a transmembrane subunit. The two subunits remain associated as a non-covalent heterodimer. At the cell surface, the heterodimer remains intact until it binds the membrane-bound ligand Delta; after binding, Notch is cleaved in the transmembrane domain liberating the Notch-ICD. The latter translocates to the nucleus where leads to activation of several genes, including those that encode a family of bHLH transcription factors. These factors in turn regulate other genes, whose net effect is to influence cell fate during development (Chan and Jan, 1999).

APP

APP (amyloid precursor protein) is a transmembrane protein of unclear function. Abnormal cleavage of APP is involved in the pathogenesis of Alzheimer's disease. Like CD44 and Notch, APP undergoes RIP. The first cleavage takes place in the lumen by a α- or a by β-secretase. After the first cleavage, presenilin1/γ-secretase releases in the lumen the amyloid β-peptide (Aβ), which assumes a β-pleated sheet configuration, causing it to aggregate and form amyloid fibrils (Selkoe, 2008). The accumulation of fibrils leads to amyloid plaques generation in certain neuronal cells, progressively causing

dementia in affected patients. Cleavage by α-secretase, on the other hand, occurs closer to the membrane than β-secretase, so γ-secretase cleavage liberates a shorter fragment that is not amyloidogenic.

2.3.6 Transcriptional properties of CD44-ICD

It is well established that generation of sCD44 by metalloproteases regulates cell migration. On the other hand, generation of the CD44-ICD has effects on transcription. Okamoto and co-workers showed that CD44-ICD localizes to the nucleus (Okamoto *et al*. 2001). CD44-ICD can enhance transcription that is mediated through the TPA-responsive element (TRE), and CD44-ICD translocation to the nucleus is essential for this enhancement. MMP inhibitors block CD44-dependent transcription enhancement as well as a CD44 mutation that removes the intracellular proteolytic cleavage site (Okamoto *et al*. 2001). Therefore, sequential proteolytic cleavage of CD44 and release of CD44-ICD is essential for CD44-dependent transcription enhancement. Using GAL4 transactivation assays, Okamoto and co-workers found that CD44-ICD was able to mediate transcription through CBP/p300, whether this occurs by a direct or indirect interaction remains to be determined (Okamoto *et al*. 2001).

3. AIMS OF THE STUDY

The aim of this study was to verify whether CD44 RIP occurs in thyroid cancer cells and to understand the role of CD44 cleavage in the RET signaling pathway in thyroid cancer. The study is divided in two different parts:

- the RET-mediated cleavage of CD44, giving origin to CD44-ICD;
- the role of CD44-ICD signaling in follicular thyroid cells.

Specific aims were as follows:

1) To check by immunoblot and ELISA assays the presence of CD44 cleavage in PTC.
2) To understand the biochemical mechanism of RET-mediated CD44 cleavage.
3) To assess the biological effects of CD44-ICD in follicular thyroid cells.
4) To evaluate by luciferase reporter assays the CD44-ICD modulation of transcriptional regulation.
5) To finally propose a model to explain the mechanism by which CD44-ICD could participate to transcriptional regulation in thyroid cells.

4. MATERIALS AND METHODS

4.1 TISSUE SAMPLES

Archival frozen thyroid tissue samples from 5 patients affected by PTC (T1-T5) and 2 normal thyroids (N1-N2) were retrieved from the files of the Pathology Department of the University of Pisa (Italy). The study was approved by the Institutional Ethics Committee. Sections (4-μM thick) of paraffin-embedded samples were stained with hematoxylin and eosin for histological examination to ensure that the samples fulfilled the diagnostic criteria required for the identification of PTC (enlarged nuclei with fine dusty chromatin, nuclear grooves, single or multiple micro/macro nucleoli and intranuclear inclusions) (Hedinger *et al.* 1989). According to a previous characterization, 2 of these PTC samples had a RET/PTC1 rearrangement (T2, T3) and 3 had a BRAFV600E mutation (T1, T4, T5) (Melillo *et al.* 2005). Snap-frozen tissue samples were kept in liquid nitrogen for storage at –80°C. For protein extraction tissue were homogenized in lysis buffer in the mixer mill MM 300 apparatus (Retsch GmbH, Haan Germany) using steal beads and centrifuged at 10,000 x g. Protein concentration was estimated and Western blot were performed as reported thereafter.

4.2 CELL LINES

HEK293 cells were grown in Dulbecco's modified Eagle's medium (DMEM) supplemented with 10% fetal calf serum, 2mmol/L of L-glutamine and 100 U/ml penicillin-streptomycin (Invitrogen Groningen, The Netherlands). Human primary cultures of thyroid cells (P5) were obtained from F. Curcio and were cultured as previously described (Curcio *et al.* 1994). The human thyroid cancer cell lines derived from PTC (TPC-1, BCPAP) were

grown in DMEM containing 10% fetal bovine serum. TPC-1 harbors the RET/PTC1 rearrangement; BCPAP harbours the BRAFV600E mutation (Schweppe *et al.* 2008). PC Cl 3 (hereafter referred to as "PC") is a differentiated thyroid follicular cell line derived from 18-month-old Fischer rats. PC cells were cultured in Coon's modified Ham F12 medium supplemented with 5% calf serum, and a mixture of 6 hormones (6H), including thyrotropin (TSH, 10 mU/ml), hydrocortisone (10 nM), insulin (10 μg/ml), apo-transferrin (5 μg/ml), somatostatin (10 ng/ml) and glycyl-histidyl-lysine (10 ng/ml) (Sigma Chemical Co., St. Louis, MO) according to Fusco *et al.* (Fusco *et al.* 1987). PC ICD cell line was obtained by a stable transfection of PC parental cell line with the CD44-ICD construct by the calcium phosphate co-precipitation technique as described previously (Melillo *et al.* 2005). Mass population (pool) of several cell clones as well as single-cell clones were isolated for each transfection by G418 selection. WRO is a follicular thyroid carcinoma human cell line; it was kindly donated by J.A. Fagin. Transient transfections were carried out with the Fugene HD reagent from Roche Diagnostics (Mannheim, Germany) according to the manufacturer's instructions.

4.3 PLASMIDS

The RET/PTC constructs (PTC) used in this study were cloned in pBABE and pCDNA3(Myc-His) (Invitrogen, Groningen, The Netherlands). They encode the short (RET-9) RET spliced form and are described elsewhere (Castellone *et al.* 2003). PTC1 and PTC3 constructs encode the H4-RET and RFG-RET chimeric oncogenes. PTC1(K-) is a kinase-dead mutant, carrying the substitution of the catalytic lysine (residue 758 in full-length RET) with a methionine. PTC1(Y1062F) carries the substitutions of tyrosine 1062 with a phenylalanine. PTC(4YF) is a mutant in which the 4 autophosphorylation sites

(Y826, Y1015, Y1029, Y1062 in full-length RET) of the carboxyl-terminal tail are mutated to phenylalanines; in PTC(3YF), the Y1062 has been added back. These mutants were generated by site-directed mutagenesis using the QuikChange mutagenesis kit (Stratagene, La Jolla, CA, USA). BRAFV600E was obtained by site-directed mutagenesis kit (Stratagene, La Jolla, CA, USA), also. HRAS(V12) plasmid is described elsewhere (Melillo *et al.* 2005). The CD44 plasmid kindly provided by S. Manié (Lyon, France) was cloned into pDEST47 vector (with GFP coding sequence) (Pellettier *et al.* 2006), CD44-ICD was cloned both in pDEST47 (GFP-tagged ICD) and in pDEST40 (V5-tagged ICD).

4.4 PROTEIN STUDIES

Immunoblotting experiments were performed according to standard procedures. Briefly, cells were harvested and lysed in a buffer containing 50 mM HEPES; pH 7.5, 1% Triton X-100, 150 mM NaCl, 1 mM EGTA, 10%glycerol, 1.5 mM $MgCl_2$, 10 mM NaF, 10 mM sodium pyrophosphate, 1 mM Na_3VO_4, 2 mM PMSF, 10 μg/ml aprotinin, leupeptin. After clarification by centrifugation at 10,000 x g for 20 min, lysates containing comparable amounts of proteins, estimated by a modified Bradford assay (Bio-Rad, Munich, Germany), were subjected to Western blot. Membranes were probed with the indicated antibodies. Immune complexes were detected with the enhanced chemiluminescence kit (ECL, Amersham Pharmacia Biotech). Signal intensity was analyzed with the Phosphorimager (Typhoon 8600, Amersham Pharmacia Biotech) interfaced with the ImageQuant software. For immunoprecipitations, after preclearing with protein-G or protein-A sepharose beads, the lysates were incubated overnight at 4°C with 2 μg of antibody. Antibody-antigen complexes were collected with 40 μl of protein-G or protein-A sepharose beads for 2h at 4°C with gentle rotation. The samples were

centrifuged, washed, eluted in sample buffer and run on SDS-polyacrylamide gel. Nuclear extraction was performed as described elsewhere (Feliciello *et al.* 1997). Briefly, cells were harvested in lysis buffer (10 mM Tris-HCl pH 7.9, 10 mM KCl, 1.5 mM MgCl2, 1 mM dithiothreitol (DTT), 1 mM phenylmethylsulphonylfluoride (PMSF), supplemented with 60 mM NaF, 60mM β-glycerophosphate and protease inhibitors (aprotinin, leupeptin and pepstatin; 40 mg/ml) and lysed by shearing with 15 passages through a 26-gauge needle mounted in a 1 ml syringe. Nuclei were recovered by centrifugation at 3,000 x g for 10 min. Nuclear proteins were extracted in 50 mM Tris-HCl, pH 7.5, containing 0.3M sucrose, 0.42 M KCl, 5 mM MgCl2, 0.1 mM EDTA, 20% glycerol, 2 mM DTT, 0.1 mM PMSF, 60 mM NaF, 60 mM β-glycerophosphate, leupeptin and aprotinin. Cytosolic fractions were recovered after membrane fraction removal by 100,000 x g ultracentrifugation.

4.5 ANTIBODIES AND COMPOUNDS

Anti-RET is an affinity-purified polyclonal antibody raised against the tyrosine kinase protein fragment of human RET. Anti-phospho p44/42 MAPK (#9102), recognizing MAPK (ERK1/2) when phosphorylated either individually or dually on Thr202 and Tyr204, anti-p44/42 MAPK (#9101) were purchased from Cell Signaling (Beverly, MA, USA). Anti-tubulin (#T9036) was from Sigma Chemical Company (St. Louis, MO, USA). Anti-phospho-CREB (S133) (#06-519), anti-CREB (#06-863), anti-PP2A (#05-421) were from Upstate Biotechnology Inc. (Lake Placid, NY, USA). Anti-p300 (sc-584), anti-GFP antibody (sc-8334), anti-c-Myc antibody (sc-40), anti-cyclin D1 (sc-718) were from Santa Cruz Biotechnology (Santa Cruz, CA, USA). Antibody against cytosolic portion of CD44 (α-CD44cyto) was kindly provided by S. Manié (Lyon, France) (Pelletier *et al.* 2006). Secondary antibodies coupled to horseradish peroxidase were from Amersham Pharmacia Biotech (Little Chalfort, UK). MEK1/2-inhibitor U0126 was from Cell Signaling and used at

10 μM final concentration. The metalloprotease-inhibitor BB94 was from British Biotech (Oxford, UK). The γ-secretase inhibitors COMP X/ InSolution™ γ-Secretase Inhibitor X and DAPT, the 3',5' cyclic-AMP analog N6-benzoyl-cAMP, the Adenylate Cyclase (AC) activator Forskolin, the PKA-inhibitor H-89 were from Calbiochem (La Jolla, CA, USA). The RET tyrosine kinase inhibitor ZD6474 was kindly provided by Astra Zeneca Pharmaceuticals (Macclesfield, United Kingdom). For each compound the used concentrations are indicated in the figures.

4.6 CELL GROWTH AND STAINING

For growth curves, 15,000 cells were seeded in triplicate and counted at the indicated time points. PC cells were maintained in medium supplemented with 5% calf serum and with 5 hormones mix (without TSH). The medium was changed every 2 days. DNA synthesis rate was measured by the 5'-bromo-3'-deoxyuridine (BrdU) Labeling and Detection Kit from Boehringer Mannheim (Germany). Briefly, cells were seeded on glass coverslips, pulsed for 1 h with BrdU (final concentration 10 μM), fixed and permeabilized. Coverslips were incubated with anti-BrdU mouse monoclonal and rhodamine-conjugated secondary antibodies (Jackson ImmunoResearch Laboratories, Philadelphia, Pennsylvania) and mounted in Moviol on glass slides. Cell nuclei were identified by Hoechst 33258 (final concentration 1 μg/ml; Sigma Chemicals Co) staining. The fluorescent signal was visualized with an epifluorescent microscope (Axiovert 2, Zeiss) (equipped with a 100X lens) interfaced with the image analyzer software KS300 (Zeiss). At least 100 cells were counted in five different microscopic fields; results were average fractions of BrdU-positive cells ± SD.

4.7 ELISA ASSAY

Extracellular shedding of the soluble ectodomain of human standard CD44 (CD44st) was measured using the Instant ELISA (Bender MedSystems, Vienna, Austria) according to manufacturer's instructions. Conditioned media from cell cultures were analyzed in triplicate at 450 nM with an ELISA reader (Model 550 microplate reader, Bio-Rad).

4.8 PULL DOWN ASSAY

The GST-CD44-ICD was generated by the Invitrogen Gateway technique using as donor the pDEST47-CD44-ICD vector and as recipient the empty vector pDEST15. The GST-CD44-ICD vector codes for a chimeric protein with CD44-ICD fused to the glutathione S-transferase (GST). GST-CD44-ICD was purified from pDEST15-CD44-ICD transformed bacterial lysates using glutathione-Sepharose beads according to standard procedures. To perform the assay, cells were serum starved for 18 h and lysed in ice-cold buffer. Protein lysates (2 mg) were incubated for 2 h with 30 μg of GST-CD44-ICD fusion protein after 2 h of preclearing with glutathione Sepharose beads. Pellet beads were collected by centrifugation (1,000 x g) for three minutes and washed with lysis buffer. The beads were finally resuspended in 2X Laemmli buffer and subjected to Western blotting.

4.9 REPORTER ASSAY

All the *Firefly* luciferase reporters were kindly provided by S.J. Gutkind (NIH, Bethesda, MD). The pGL3-CRE (cAMP response element), pGL3-NFKB (nuclear factor kappa B), pGL3-AP-1 (activator protein 1), pGL3-SRF (serum response factor), pGL3-Gli (Glioma-associated oncogene homologue,

Sonic hedgehog pathway) reporter contains five repetition of the same site (respectively CRE, NFKB, AP-1, SRF and Gli responsive elements) upstream the Firefly luciferase cDNA. To evaluate the TCF/LEF transcriptional activity, we used a pair of luciferase reporter constructs, TOP-FLASH and its negative control FOP-FLASH (Upstate Biotechnology). TOP-FLASH contains three copies of the TCF/LEF binding site (AAGATCAAAGGGGGT) upstream of the thymidine kinase minimal promoter; FOP-FLASH contains a mutated TCF/LEF binding site (AAGGCCAAAGGGGGT). TCF/LEF activity was determined by the TOP-FLASH:FOP-FLASH ratio. Finally, the pGL3-CycD1 reporter contains a cyclin D1 natural promoter (Albanese *et al.* 1995). Twenty-four hours after seeding, the cells were transiently transfected in triplicate with one of these reporters together with pRL-null, a plasmid expressing the enzyme *Renilla* luciferase, used as an internal control, according to manufacturer's instruction (Promega Corporation, Madison, WI, USA). Forty-eight hours after transfection cells were serum-starved overnight. *Firefly* and *Renilla* luciferase activities were assayed using the Dual-Luciferase Reporter System (Promega Corporation). Light emission was quantitated using a Berthold Technologies luminometer (Centro LB 960, Bad Wildbad, Germany) and expressed as a percentage of residual activity compared to untreated cells. In all cases, the total amount of transfected plasmid DNA was normalized with empty vector DNA-transfected cells. Average results of three independent assays ± SD are indicated. Student's t test was used to assess statistical significance.

4.10 CHROMATIN IMMUNOPRECIPITATION (ChIP)

Chromatin was extracted from CD44-ICD or empty vector transfected HEK293 cells. Nuclear extracts were isolated and then fragmented through sonication. ChIP was performed by the chromatin immunoprecipitation assay kit (Upstate Biotechnology Inc.), following manufacturer's instructions. Briefly, chromatin was fixed by directly adding formaldehyde (1% v/v) to the

cell culture medium. Transcription factor-bound chromatin was immunoprecipitated with mock or CREB antibodies, cross-linking was reversed. Then input DNAs and immunoprecipitated DNAs were analyzed by PCR using primers spanning the CRE site of the human cyclin D1 promoter. The primers used to amplify the promoter sequences were:

CRE-forward (5'-AACGTCACACGGACTACAGG-3');

CRE-reverse (5'-TGTTCCATGGCTGGGGCTCTT-3');

The results were representative of three different independent experiments.

4.11 RNA SILENCING

The small inhibitor duplex RNAs (siRNA) were from Dharmacon (Lafayette, CO, USA) and are ON-target plus SMARTpool:

siCD44 human: #L-009999-00;

siCREB human: #L-003619-00-0005;

siCREB rat: #L-092995-00-0010.

The siCONTROL Non-targeting Pool (#D-001206-13-05) was used as a negative control. Cells were transfected with 100nM siRNAs using Dharmafect reagent following the manufacturer's instructions. The day before transfection, the cells were plated in 35 mm dishes at 40% of confluence in DMEM supplemented with 10% FBS and without antibiotics.

Sh29merRNA constructs against human CD44 were from OriGene Technologies (Rockville, MD, USA): TR314080 IDs: TI356313, TI356314, TI356316. shRNA pRS plasmid TR20003 was used as a negative control. Transfection was performed in 100 mm dishes using Fugene HD reagent (Roche, Mannheim, Germany) with 4 μg of each shRNA construct. Cells were harvested 48 hours after siRNA or shRNA transfection.

4.12 STATISTICAL ANALYSIS

The Student's t test was used for statistical analysis. All p values were two sided and differences were significant when $p < 0.05$.

5. RESULTS

5.1 CD44-ICD is overexpressed in human PTC.

Our group has previously demonstrated that OPN, one of the CD44 ligands, is among the most heavily induced transcripts in thyroid follicular cells transformed by RET/PTC and BRAF oncogenes (Melillo *et al.* 2005). Interestingly thyroid transformed cells also feature CD44 mRNA upregulation, in particular v3 and v6 containing variants (Castellone *et al.* 2004). Upregulation of both OPN and CD44 was also found in thyroid carcinoma cell lines spontaneously harboring RET/PTC oncogenes (Castellone *et al.* 2004). Moreover PTC carrying mutations at the level of the RET-RAS-BRAF-MAPK signaling cascade featured upregulation of both OPN and CD44 v6 mRNA and such an upregulation correlated with the presence of lymph node metastasis; in particular (Guarino *et al.* 2005).

Ectodomain shedding of CD44 has been demonstrated in various cancer cell lines (Okamoto *et al.* 1999a) and in tumor specimens (Okamoto *et al.* 2002), releasing ectoCD44 and membrane-bound CD44-CTF. Recent work has revealed that further CD44-CTF proteolytic processing occurs within the residual CD44 transmembrane and cytoplasmic domains, releasing intracellularly the CD44-ICD (**Fig. 7** in the Background section).

Thus, to better understand the role of CD44 in PTC, we investigated the presence of its cleaved form, CD44-ICD, in a small set of primary PTC samples (T1-T5); normal thyroid samples (N1, N2) were used as control. To this aim, we determined the presence of full-length CD44 and CD44-ICD by Western blot with an anti-CD44cyto (which recognizes the cytosolic region of CD44) polyclonal antibody. To normalize the samples we used the anti-tubulin monoclonal antibody. Both full-length and low molecular weight (< 17 kDa) CD44 (corresponding to the molecular weight of CD44-ICD), were upregulated in PTC samples compared to normal tissues (**Fig. 8A**). Instead,

CD44-CTF was not detected, suggesting a very short half life, perhaps due to rapid conversion to CD44-ICD.

To test whether CD44-ICD overexpression was also a feature of human thyroid cancer cell lines, we determined the expression of CD44-ICD in a primary normal thyroid cell line P5 (Curcio *et al*. 1994) and in two cancer cell lines, TPC-1 and BCPAP, derived from human PTC. These PTC cell lines feature RET/PTC1 rearrangement (TPC-1) or BRAFV600E mutation (BCPAP) (Schweppe *et al*. 2008). Both cell lines tested, but not normal thyrocytes, expressed CD44-ICD (**Fig. 8B**).

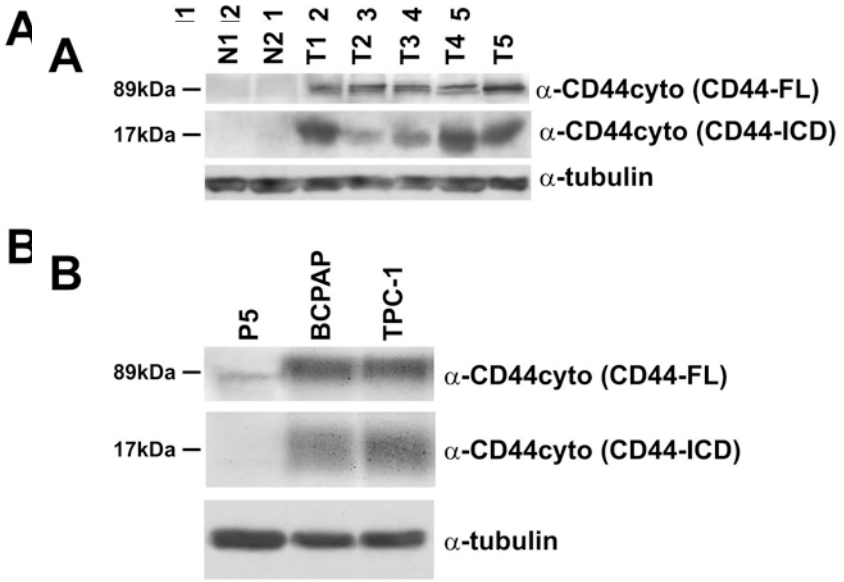

Figure 8 - CD44-ICD is overexpressed in PTC specimens and in PTC cell lines.
A) Protein lysates (100 µg) extracted from the indicated tissue samples underwent Western blotting with anti-CD44cyto (against cytosolic region of CD44)-specific antibodies. Immunocomplexes were revealed by enhanced chemiluminescence. Equal protein loading was ascertained by anti-tubulin immunoblot. N: normal samples; T: papillary tumor samples.
B) Western blot with anti-CD44cyto of protein lysates from PTC cell lines. Normalization of the levels of total proteins was verified by anti-tubulin blot. P5: normal thyroid follicular cells; BCPAP: PTC cell line harboring BRAFV600E mutation; TPC-1: PTC cell line harboring RET/PTC mutation.

5.2 Thyroid oncogenes induce CD44 cleavage.

We used several chemical inhibitors to test their ability to block the generation of the CD44-ICD. We treated for 24 hours the cells with the broad-spectrum metalloprotease inhibitor BB94 or two different γ-secretase inhibitors, COMP X and DAPT. Furthermore, to understand the role played by the oncoproteins expressed by TPC-1 and BCPAP, we treated cells with the RET kinase inhibitor ZD6474 or the MEK-inhibitor, U0126. As shown in **figure 9A**, the broad-spectrum metalloprotease inhibitor BB94 downregulated CD44-ICD, presumably blocking the cleavage of CD44; an accumulation of full length CD44 was not detectable likely for the high abundance of this protein even in untreated cells. COMP X and DAPT, two different γ-secretase inhibitors, reduced the amount of CD44-ICD by blocking the conversion of CD44-CTF to CD44-ICD; indeed, as expected, they increased the amount of CD44-CTF (**Fig. 9A**).

Interestingly, the abrogation of RET/PTC kinase activity by ZD6474 in TPC-1 cells and BRAFV600E and RET/PTC signaling by a MEK-inhibitor U0126, in both TPC-1 and BCPAP cells, downregulated CD44-ICD without causing an accumulation of CD44-CTF, similar to BB94 (**Fig. 9A**). ZD6474 had no effect in BCPAP cells (not shown). This indicates that CD44 regulated proteolysis (RIP) is sustained by oncogene signals in thyroid cancer cells and suggests that metalloprotease–mediated cleavage is the primary (but not necessarily the only) level of such an induction.

To confirm these results, an ELISA analysis of culture supernatants revealed that treatment with BB94, ZD6474 or U0126, blocked the shedding of ectoCD44 (sCD44st, soluble standard CD44) into the cell culture media (**Fig. 9B**). Virtually, no CD44 shedding was measured in normal P5 cells (not shown). The fact that ectoCD44 accumulation parallels CD44-ICD accumulation suggests that oncoproteins are indeed stimulating the CD44

cleavage rather than simply stabilizing CD44-ICD.

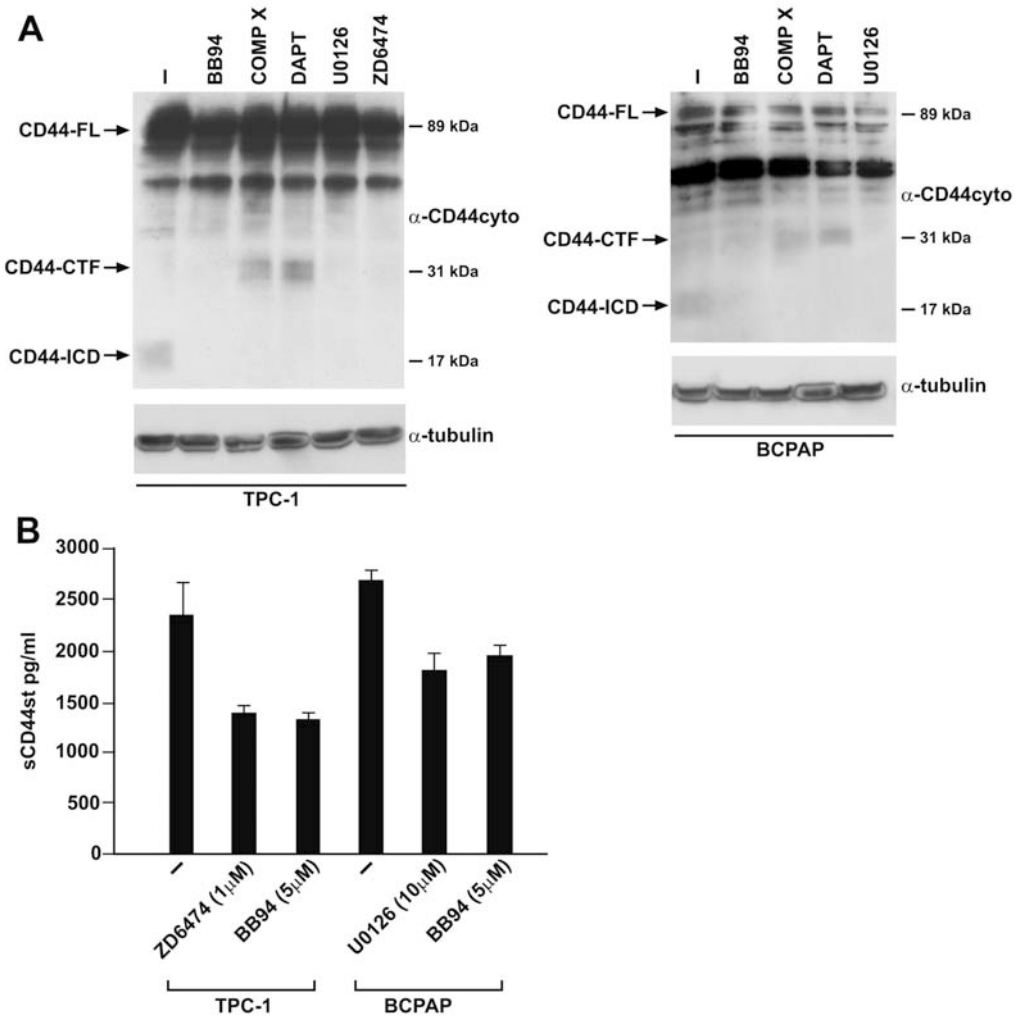

Figure 9 - CD44 cleavage depends on oncogene-induced metalloprotease and γ-secretase activities.

A) Western blot analysis with anti-CD44cyto of BCPAP and TPC-1 cells upon the indicated treatments. Each treatment blocked release of CD44-ICD; COMP-X and DAPT treatments stabilize CD44-CTF by blocking γ-secretase activity.

B) ELISA analysis of extracellular CD44 (ectoCD44 or sCD44st, soluble standard CD44) fragment-shedding. BB94, a metalloprotease inhibitor, ZD6474, a RET/PTC kinase inhibitor, and UO126, a MEK inhibitor, blocked the CD44 shedding.

All together, these data show that CD44-ICD is cleaved by metalloprotease and γ-secretase activities in thyroid cancer cells and point-out to RET/PTC and BRAFV600E oncogenes as activators of this process. It remains to be clarified whether oncogenes promote CD44 cleavage by acting at the level of metalloproteases (as an example stimulating their expression or activity) or rather at the level of the CD44 substrate (as an examples through post-translational modifications or membrane partitioning) or both.

5.3 ERK signaling triggers CD44 cleavage.

To investigate the signaling mechanism of oncogene-induced CD44 cleavage, we co-transfected a GFP-tagged full-length CD44 construct with different RET/PTC mutants in HEK293 cells. The RET catalytic lysine (K758) and major RET autophosphorylation sites (Y826, Y1015, Y1029, Y1062) are indicated in **figure 10A**. We used plasmids encoding the two most frequent RET/PTC rearrangements, RET/PTC1 (PTC1) and RET/PTC3 (PTC3), and the different RET/PTC mutants illustrated in **figure 10A**. The co-transfection of CD44 together with PTC1 or PTC3 myc-tagged expressing plasmids induced the generation of the CD44-ICD fragment (**Fig. 10B**), further indicating that RET/PTC is able to stimulate the cleavage of CD44.

Moreover the RET/PTC-mediated CD44 cleavage depended on RET kinase activity and integrity of tyrosine 1062; in fact, CD44-ICD did not form when the RET/PTC 4YF (tyrosines Y826-1015-1029-1062 mutated to phenylalanine) mutant was used; instead, CD44 cleavage was rescued when Y1062 was added back (3YF) to the 4YF mutant (**Fig. 10C**). Y1062 triggers several signaling cascades downstream RET/PTC, including the ERK and PI3K ones (Manié *et al*. 2001). To investigate the role of Y1062 signaling in the CD44 cleavage, we treated RET/PTC1 transfected HEK293 cells with MEK (U0126) or PI3K (LY294002) inhibitors. Interestingly, U0126 (**Fig. 10D**), but not LY294002 (data not shown) blocked CD44-ICD generation. We also found that transient expression of the myc-tagged constitutively active forms of RAS, (RASV12) and BRAF (BRAFV600E), induced the CD44 cleavage (**Fig. 10D**). Taken together, these results demonstrate that RET/PTC-RAS-BRAF signaling cascade triggers the CD44 cleavage.

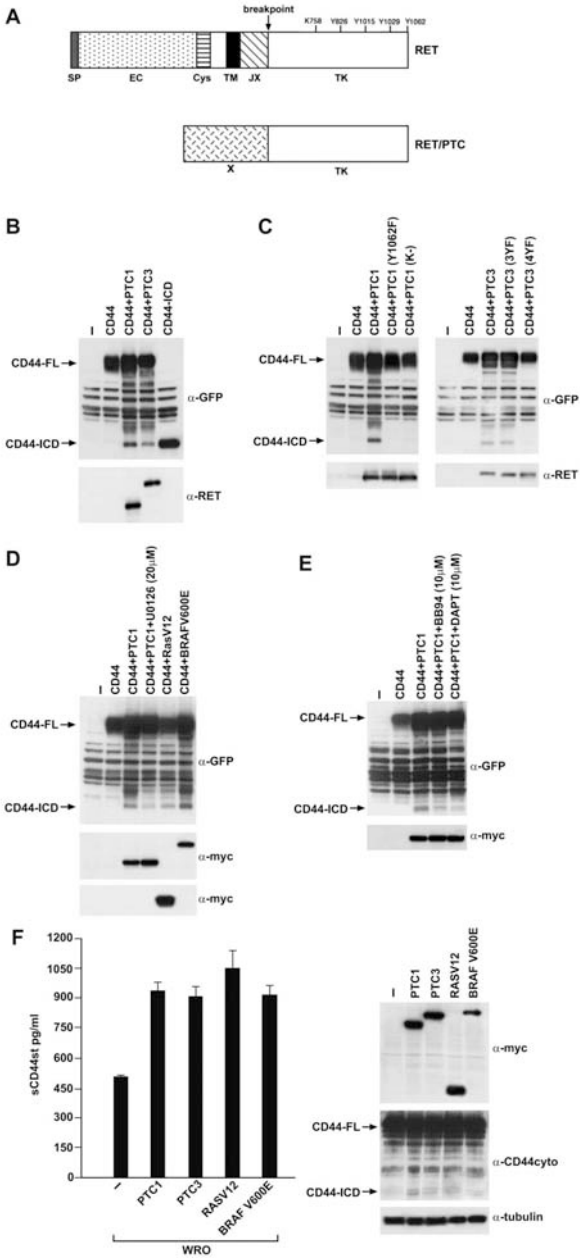

Figure 10 - The RET/PTC-RAS-BRAF cascade triggers CD44 cleavage.

A) Schematic representation of RET and RET/PTC proteins. SP, signal peptide; EC, extracellular; Cys, cysteine rich; TM, transmembrane; JX, juxtamembrane; TK, tyrosine kinase. The catalytic lysine (K758) and major RET autophosphorylation sites are indicated. **B)** Transient transfections in HEK293 cells of RET/PTC1 (PTC1) or RET/PTC3 (PTC3) with GFP-tagged full-length CD44. **C)** The RET/PTC-mediated cleavage of CD44 depends on RET kinase activity and integrity of tyrosine 1062; the

cleavage is restored when Y1062 is added-back (3F). **D)** RAS/RAF/MEK pathway induces the CD44 shedding, as shown by the expression of active RAS and BRAF and the effects of MEK-inhibitor UO126. **E)** The RET/PTC-induced cleavage is blocked by the BB94, a metalloprotease inhibitor, and by DAPT, a γ-secretase inhibitor.

To test whether RET/PTC induced the CD44 cleavage through metalloprotease and γ-secretase activity we treated the RET/PTC-transfected HEK293 cells with BB94 and DAPT. As shown in **figure 10E**, RET/PTC-induced cleavage of CD44 did not occur in the presence of the two inhibitors.

Finally, to further verify the role of RET/PTC in CD44 cleavage, we used a follicular thyroid cancer cell line, WRO, that expresses high levels of endogenous CD44. Upon transient transfection of myc-tagged-PTC1, -PTC3, -RASV12 and -BRAFV600E, the cleavage of endogenous CD44 with shedding of ectoCD44 and generation of CD44-ICD was induced, as demonstrated by ELISA (**Fig. 10F,** left panel) and immunoblot (**Fig. 10F,** right panel).

5.4 CD44-ICD has mitogenic activity in thyrocytes.

To study the effects of CD44-ICD in thyroid cells, we stably expressed GFP-tagged CD44-ICD in the thyroid PC Cl 3 cells (hereafter referred to as "PC"), a continuous line of normal follicular thyroid cells, derived from Fischer rats, that constitutes a good model system to study differentiation and growth regulation in an epithelial thyroid cell setting. PC cells require a mixture of 6 hormones (6H), including thyrotropic hormone (TSH), for proliferation (Fusco *et al*. 1987). A mass population (PC ICD pool) and of one representative clone (PC ICD #1) expressing CD44-ICD (**Fig. 11A**) showed a morphologically transformed cell phenotype and a more rapid cell growth, compared to the parental PC cells (data not shown). Importantly, the PC ICD cells lost the dependence on TSH for proliferation, as demonstrated by **figure 11B**. DNA synthesis, by the BrdU incorporation assay, was measured upon 1 hour BrdU pulse. The average results of 3 independent experiments are reported in figure **11C**. Parental PC cells deprived of TSH virtually did not incorporate BrdU, while BrdU incorporation rate was strongly increased in PC ICD cells.

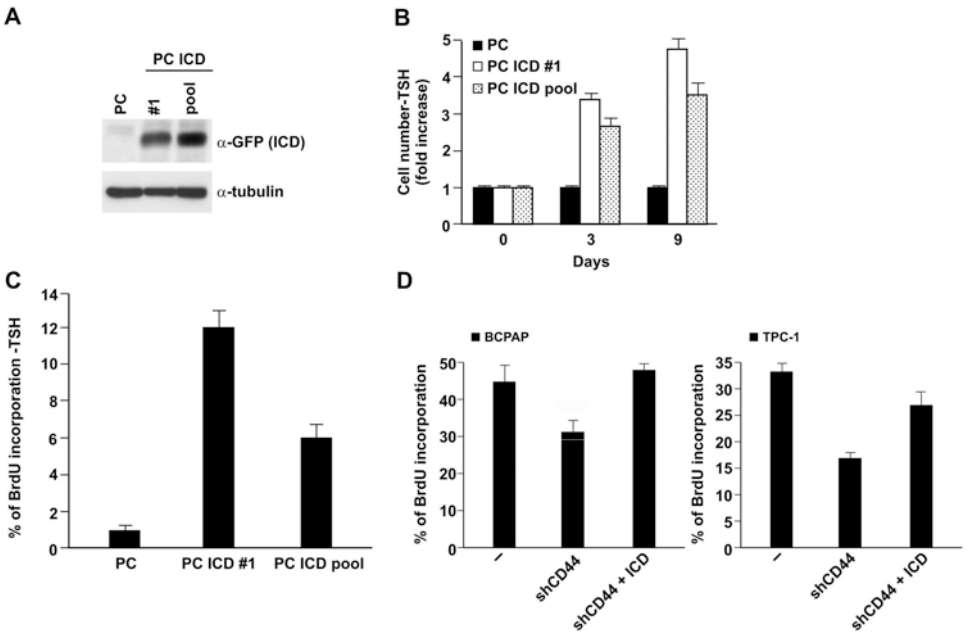

Figure 11 - CD44-ICD has mitogenic activity in thyrocytes

A) Normal rat follicular thyroid PC cells were stably transfected with CD44-ICD (GFP-tagged), several clones and one mass population were isolated by G418 selection. Immunoblot with anti-GFP was performed to test the transgene expression. Normalization was checked with anti-tubulin.

B) Proliferation of the PC ICD cells was measured in the absence of TSH by counting the cells at different time points. The ratio of ICD-expressing versus parental number cells was calculated.

C) Percentage of BrdU positive cells in the absence of TSH in PC ICD cells versus PC parental cells.

D) Fraction of BrdU incorporation in BCPAP and TPC-1 transfected with shCD44 plasmid with or without a CD44-ICD-expression vector (refractory to shCD44 RNAi).

To verify CD44-ICD mitogenic capability also in human thyroid cancer cells, endogenous CD44 was silenced by a transient transfection of a shCD44 plasmid in BCPAP and TPC-1 cells. Cells were co-transfected by a CD44-ICD-expression vector (refractory to human shCD44 RNAi because of rat origin) and the efficiency of CD44 silencing as well as CD44-ICD expression levels were verified by Western blot (data not shown). DNA synthesis was measured by BrDU incorporation assay (**Fig. 11D**). CD44 silencing reduced BrdU incorporation rate and adoptive CD44-ICD expression was able to rescue DNA synthesis rate (**Fig. 11D**).

5.5 CD44-ICD stimulates CRE-mediated transcription.

To address the mechanisms of CD44-ICD mediated signaling, we analysed the CD44-ICD capability to trans-activate luciferase reporter transcription mediated by a panel of promoter elements in HEK293 cells. As a positive control, co-transfection of the same reporters with the correspondent known activator was performed (data not shown). We used reporter plasmids expressing luciferase under the control of AP-1 (activating protein-1), SRF (serum response factor), TCF (ternary complex factor), Gli (Glioma-associated oncogene homologue), the NFKB (nuclear factor kappa B) and the CRE (cAMP-responsive element) DNA elements (Marinissen *et al*. 2004; Iavarone *et al*. 2003; Castellone *et al*. 2005).

CD44-ICD strongly (about 10 fold) and specifically activated CRE reporter (**Fig. 12A**). To verify this capability also in a thyroid cell system, we used transiently transfected PC cells with virtually identical results (**Fig. 12B**). Finally, the CRE reporter was also activated in the stably transfected PC ICD cells compared to parental cells (**Fig. 12C**).

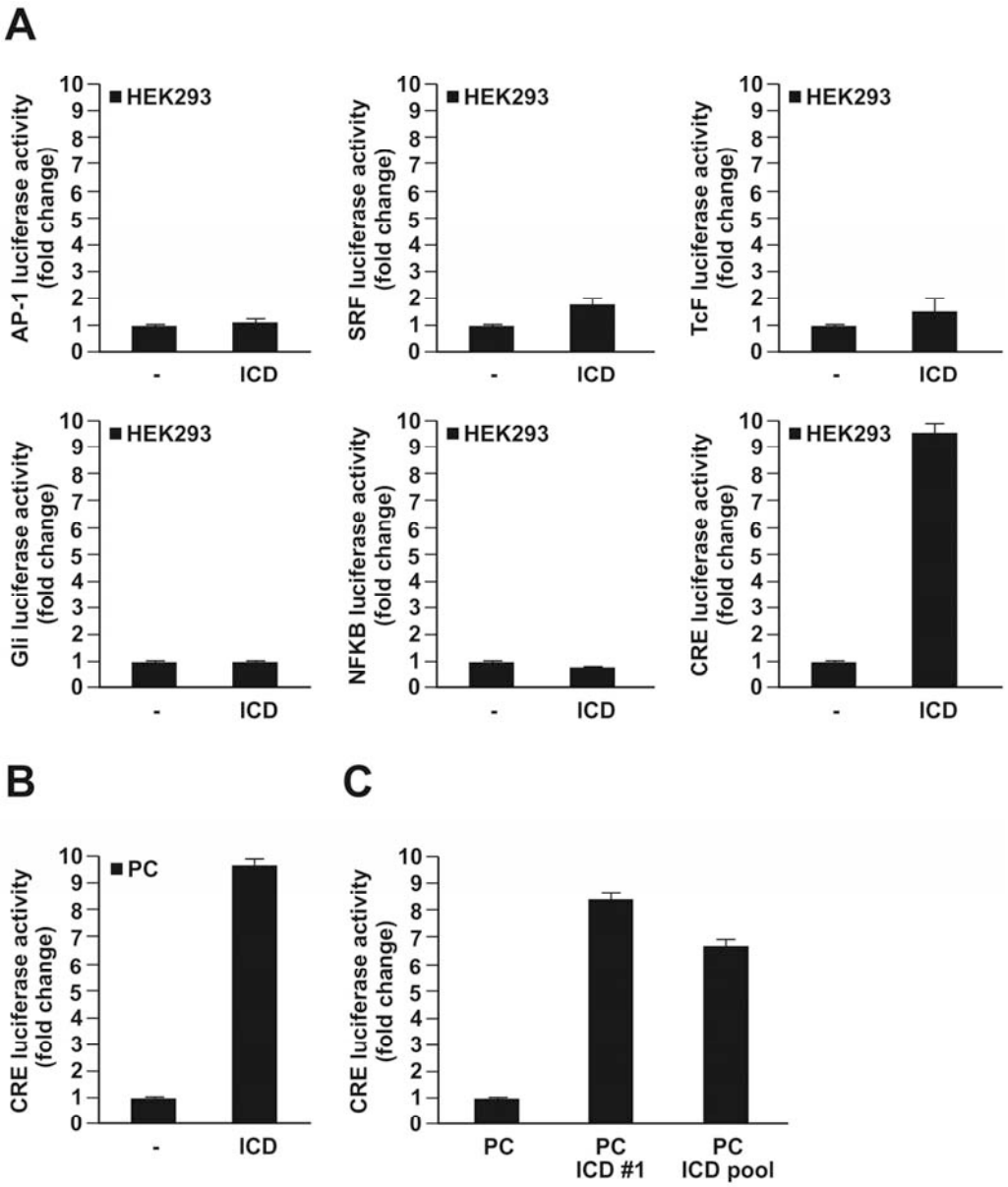

Figure 12 - CD44-ICD stimulates CRE-LUC transcription.

A) Effects on various reporters of CD44-ICD (ICD) in HEK293 cells.

B) CRE-LUC reporter assay in PC cells transiently transfected with CD44-ICD.

C) CRE-LUC reporter assay in a clone (PC ICD #1) and a mass population (PC ICD pool) of stably expressing CD44-ICD.

5.6 CD44-ICD sustains CREB and p300-mediated CycD1 expression.

The activation of the CRE element suggested the involvement of the transcription activating protein CREB (cAMP-responsive element binding protein) in the signaling mediated by CD44-ICD in thyroid cells. To determine whether CD44-ICD can activate also a natural promoter containing the CRE element, we studied the effect of the transient transfection of CD44-ICD in HEK293 and PC cells on Cyclin D1 luciferase promoter (cycD1). Cyclin D1 is a prototypic CREB target and a CRE element, located upstream of the mRNA start site (at -58 bp), has a key role in both basal and induced cyclin D1 expression (Albanese *et al*. 1995; Boulon *et al*. 2002). PC cells were kept without TSH for 48h after the transfection to reduce the TSH-dependent Cyclin D1 promoter activity. CD44-ICD stimulated cycD1 promoter luciferase transcription (about 4 fold) in HEK293 and PC cells (**Fig. 13A**).

To investigate the involvement of CREB in the CD44-ICD-mediated cyclin D1 promoter activation, a chromatin-immunoprecipitation assay (ChIP) was performed to measure CREB binding to the region of the cyclin D1 promoter that contains CRE. For PCR, we used a primer pair spanning the CRE site (**Fig. 13B**). Binding of CREB to the cyclin D1 promoter was greatly enhanced upon CD44-ICD expression (**Fig. 13B**).

We assessed the role of CREB in CD44-ICD-mediated cycD1 promoter activity by silencing endogenous CREB by RNA-interference (siCREB) in CD44-ICD-transfected HEK293 and PC cells, a control siRNA was also used. The results of the luciferase assays confirmed that CREB is necessary for the CD44-ICD-mediated activation of cyclin D1 promoter (**Fig. 13C**).

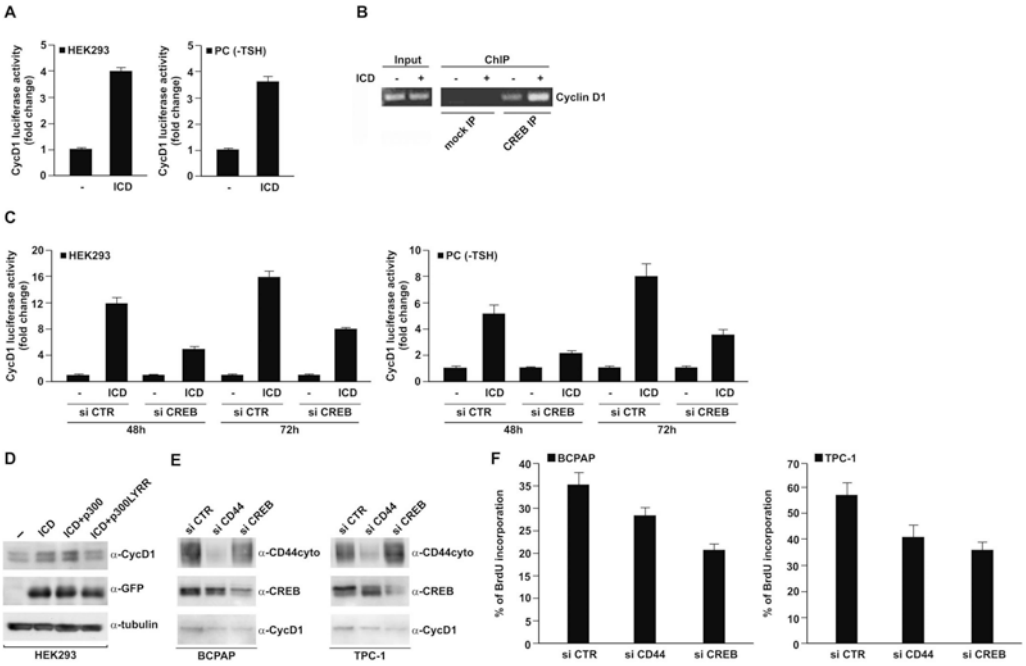

Figure 13 - CD44-ICD sustains CREB and p300-mediated CycD1 expression.
A) CycD1-LUC reporter assay in ICD-transiently transfected HEK293 and PC cells.
B) Chromatin immunoprecipitation assay in ICD-transiently transfected HEK293 cells. Input DNA levels are shown for normalization. Mock or CREB antibodies immunoprecipitated chromatin was analysed by semiquantitative PCR with human cycD1 promoter primers spanning CRE site.
C) CycD1-LUC reporter assay in ICD-transiently transfected HEK293 and PC cells upon CREB silencing by RNAi. RNA interference was performed with control (siCTR) siRNA or CREB (siCREB) siRNA; cells were harvested at the indicated time points.
D) Immunoblot stained with CycD1 antibody of HEK293 cells transfected with ICD and with p300 or p300LYRR dominant negative mutant. ICD expression was tested with anti-GFP. Anti-tubulin was used as a control.
E) Immunoblot stained with CycD1 antibody of BCPAP and TPC-1 cells treated with siCD44 or siCREB. The efficiency of interference was tested by immunoblot with anti-CD44cyto and anti-CREB.
F) BrdU incorporation rate in BCPAP and TPC-1 cells treated with siCD44 and siCREB.

CBP/p300 is a general transcriptional co-activator, in particular involved in CREB-mediated gene transcription, being recruited to S133 phosphorylated CREB (Chrivia *et al.* 1993; Johannessen, 2004; Mayr *et al.* 2001). Previous data demonstrated that CD44-ICD is able to potentiate transactivation of

promoters through CBP/p300 (Okamoto *et al.* 2001). We checked if CD44-ICD increased the expression of cyclin D1, in a p300 dependent manner. To this aim, we co-transfected the GFP-tagged CD44-ICD either with p300 or a p300-dominant negative expression vector (LYRR) (Di Agostino *et al*. 2006). As shown in **figure 13D**, p300 modestly increased the ICD-induced cyclin D1 expression, while the p300-dominant negative potently blocked cyclin D1 upregulation.

Finally, we confirmed the involvement of CREB in the CD44-ICD mediated expression of cyclin D1 also in human derived thyroid cancer cells BCPAP and TPC-1. Downregulation of CREB, as well CD44, by RNA interference (siCREB) blunted the expression of cyclin D1 in both cell lines (**Fig. 13E**). Importantly, the reduction of cyclin D1 expression following downregulation of CREB or CD44 by RNAi, paralleled the decrement of DNA synthesis of cell lines measured by BrDU incorporation (**Fig. 13F**).

5.7 CD44-ICD increases levels of phosphoCREB.

To explore how CREB is involved in the signaling mediated by CD44-ICD, we analysed CREB phosphorylation at serine 133, its principal activation site, in nuclear extracts of HEK293 cells transfected with CD44-ICD. Forskolin (FSK) (40μM for 30 minutes) stimulation was used as a positive control to stimulate CREB phosphorylation (**Fig. 14A**). Total CREB nuclear levels were measured for normalization. The phospho-CREB antibody recognizes, besides CREB (43kDa), also CREM (30 kDa) and ATF-1 (38 kDa); the arrow indicates CREB and ATF-1. Expression of CD44-ICD induced a robust increase of CREB S133 phosphorylation (**Fig. 14A,** left panel).

S133 phosphorylated CREB binds CREB binding protein (CBP/p300) resulting in a transcriptionally active complex (Mayr *et al*. 2001). We analysed stoichiometry of CREB-p300 binding by immunoprecipitating CREB from nuclear extracts of HEK293 cells transfected with CD44-ICD and staining the immunoblot with p300. Total levels of p300 and CREB proteins are shown for normalization. CD44-ICD strongly increased CREB-p300 interaction (**Fig. 14A,** right panel).

We also analysed the level of S133 CREB phosphorylation in BCPAP and TPC-1 cells compared to normal thyroid follicular cells (P5). As shown in **figure 14B**, CREB phosphorylation was almost undetectable in P5 cells while BCPAP and TPC-1 showed high levels of CREB phosphorylation.

We applied CD44 RNA interference, to determine CD44 contribution. CREB phosphorylation in the human PTC cell lines partially depended on CD44 expression (**Fig. 14C**). Levels of CREB phosphorylation were also measured upon transfection of in the human PTC cells treated with the shCD44 plasmid. CREB phosphorylation strongly depended on CD44-ICD because it was efficiently rescued by V5- CD44-ICD (**Fig. 14D**). Finally, blocking CD44 cleavage by the metalloprotease-inhibitor (BB94) or γ-secretase-inhibitor

(DAPT) reduced the levels of CREB phosphorylation (**Fig. 14E**). ERK phosphorylation was measured as control of inhibition specificity.

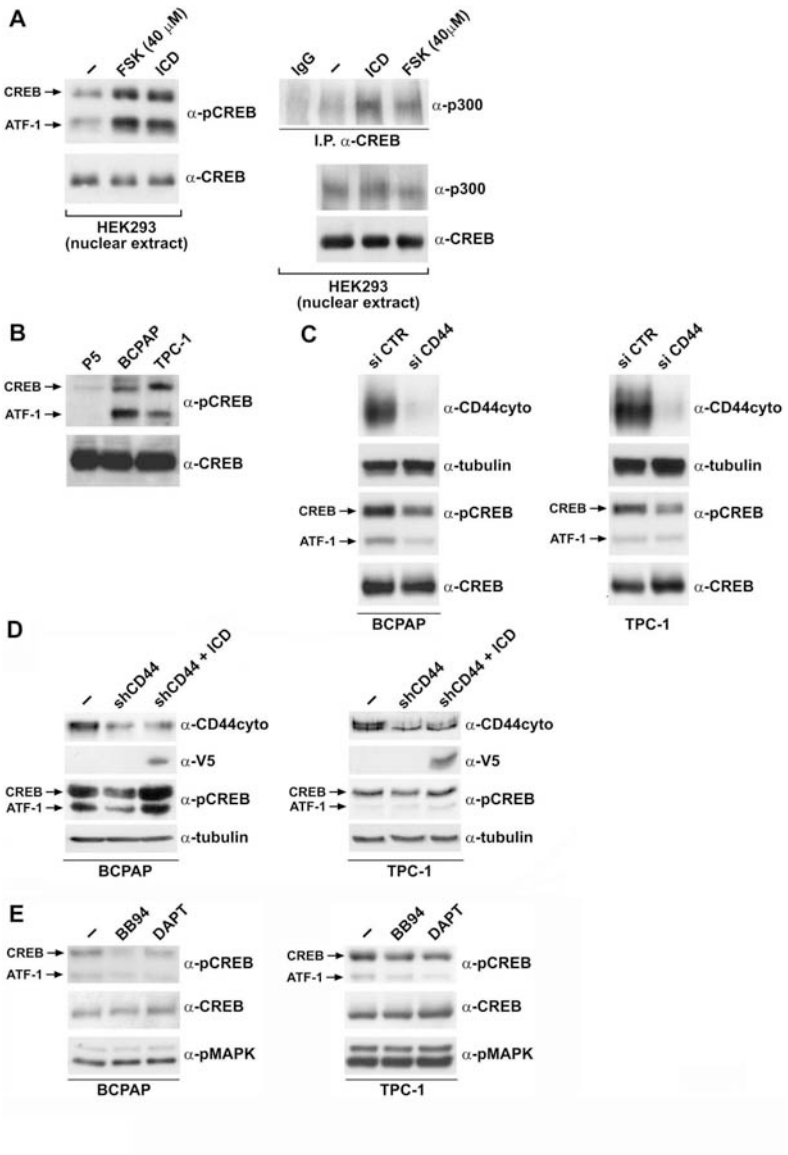

Figure 14 - CD44-ICD induces CREB-phosphorylation.

A) Immunoblot with pS133CREB antibody of nuclear extracts of HEK293 cells stimulated with forskolin (FSK) or transfected with CD44-ICD (ICD). Anti-CREB was used for normalization. p300 antibody stain of CREB-immunocomplexes in HEK293 nuclear extracts. B) pS133CREB levels in normal (P5) and BCPAP and TPC-1 cells. Anti-CREB antibody was used to normalize. C) pS133CREB levels in BCPAP and TPC-1 cells treated with siCD44. The RNAi efficiency was tested by CD44cyto antibody. Anti-tubulin and anti-CREB were used for normalization. D) pS133CREB levels in cells transfected with shCD44 with or without V5-tagged CD44-ICD (refractory to shCD44 RNAi). E) pS133CREB levels in BCPAP and TPC-1 cells treated with BB94 or DAPT. Anti-CREB was used for normalization. Anti-phosphoMAPK was used to assess the specificity of treatments.

5.8 CD44-ICD forms a complex with CREB.

It is known that CD44-ICD can translocate into the nucleus and that this translocation is necessary to activate CD44-ICD-mediated transcription (Okamoto *et al*. 2001). To understand the mechanism by which CD44-ICD induces CREB-phosphorylation, we analysed whether CD44-ICD and CREB formed a protein complex. Anti-CREB (**Fig. 15A,** left panel) and anti-phospho-CREB (**Fig. 15A,** right panel) immunocomplexes of HEK293 cells transfected with V5-tagged CD44-ICD were stained with V5 antibody. V5-CD44-ICD interacted with total CREB and in particular with the phosphorylated pS133 form. The mirror experiment was performed by immunoprecipitating GFP-tagged CD44-ICD and immunoblotting with anti-CREB antibody. This experiment was performed on total lysates and purified cytosolic and nuclear fractions. The CREB-CD44-ICD complex was detected in both the fractions but was more abundant in the nuclear fraction, parallel to CREB protein distribution (**Fig. 15B**).

The CREB-CD44-ICD interaction was also demonstrated in the human PTC cells, by immunoprecipitating endogenous pS133-phosphorylated CREB and staining the blot with anti-CD44cyto antibody (**Fig. 15C**). Moreover, we carried-out a pull-down experiment by using as a bait GST (as negative control) and recombinant CD44-ICD-GST protein. GST-CD44-ICD was able to pull-down the active form of CREB (pS133CREB) in both BCPAP and TPC-1 cell lysates (**Fig. 15D**). Interestingly, GST-CD44-ICD was also able to pull-down PP1 and PP2A phosphatases, that physiologically bind and de-phosphorylate pS133 CREB (Ugi *et al.* 2002) (**Fig. 15D**).

Finally, to verify if the interaction between CREB and CD44-ICD was direct or mediated by other proteins, we performed a pull-down assay by using an *in vitro* recombinant CREB protein and CD44-ICD-GST. As shown in **figure 15E**, the two recombinant proteins, CREB and CD44-ICD, readily

interacted *in vitro*.

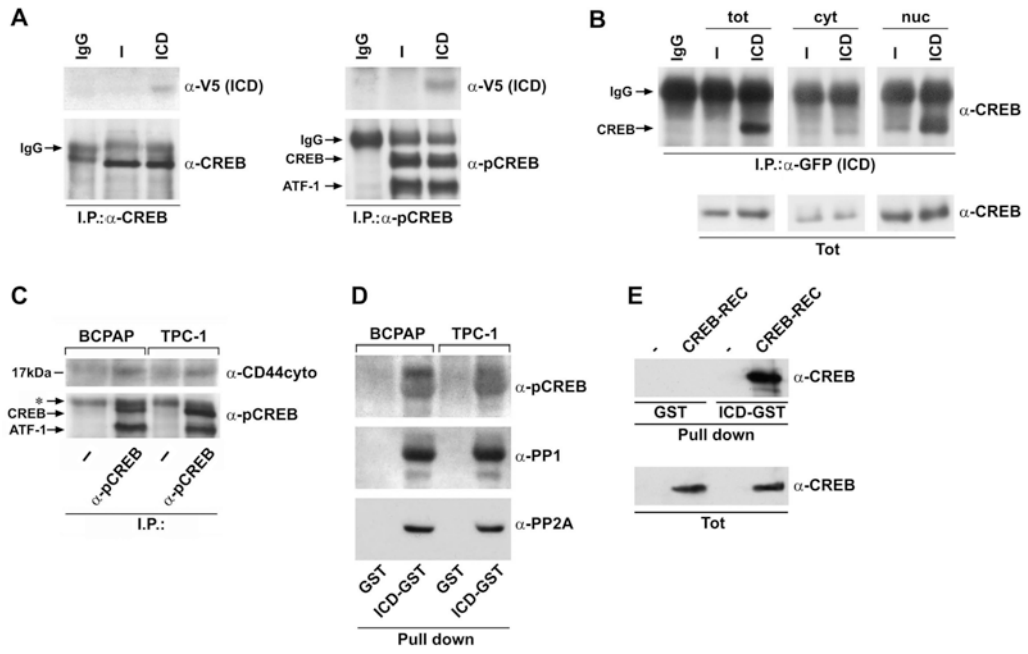

Figure 15 - CD44-ICD binds CREB.

A) Immunoblot analysis with V5 antibody of CREB (left panel) and phosphoCREB (right panel) immunoprecipitates from HEK293 transfected or not with V5-tagged CD44-ICD (ICD). Equal amounts of pCREB were used for the assay in the right panel. Anti-CREB antibody was used for normalization. The immunoglobulin (IgG) band is indicated.

B) Immunoblot with anti-CREB of GFP-immunoprecipitated total (tot), cytosolic (cyt) and nuclear (nuc) fractions of HEK293 transfected or not with GFP-tagged CD44-ICD (ICD). Normalization was performed with CREB antibody.

C) Immunoblot with CD44cyto antibody of phosphoCREB immunocomplexes from BCPAP and TPC-1 cells. Anti-phosphoCREB was used for normalization. In the 1st and 3rd lane the immunoprecipitation was performed without primary antibody. A non-specific band was indicated by the asterisk.

D) CD44-ICD was produced as GST-fusion protein (ICD-GST) and used to pull-down phosphoCREB, PP1 and PP2A from BCPAP and TPC-1 protein lysates. Pull-down with GST backbone was used as a control.

E) Pull-down with 30 μg of ICD-GST or GST (as a control) of 1 μg of recombinant CREB (CREB-REC). Immunoblot of pulled-down samples and of an aliquot of input CREB-REC was stained with CREB antibody.

5.9 CD44-ICD binds preferentially the phosphorylated form of CREB and delays CREB rate of dephosphorylation.

To better understand the mechanism by which CD44-ICD induces CREB phosphorylation we used different inhibitors against known CREB kinases (Johannessen *et al*. 2004). We inhibited the kinase activity of PKA by treating CD44-ICD transfected HEK293 cells for two hours with the compound H89 or by cotransfection of CD44-ICD with a plasmid encoding PKA-specific peptide inhibitor (PKi) (Feliciello *et al*. 1997). Since RSK and MSK, two MEK downstream kinases, are able to phosphorylate CREB on S133, we also treated CD44-ICD transfected cells for two hours with MEK-inhibitor U0126. Nuclear extracts were analysed by Western blot with anti phospho-CREB antibody and normalized with anti-CREB (**Fig. 16A**). The inhibition of both PKA and MEK efficiently blocked CD44-ICD-induced CREB phosphorylation.

We hypothesized that rather than promoting the activity of a specific CREB kinase, CD44-ICD may instead negatively affects the rate of CREB de-phosphorylation. To verify this possibility, we stimulated serum-starved HEK293 cells for 40 minutes with cAMP-analogue (N6-benzoyl-cAMP) to induce CREB phosphorylation. A preferential binding of CD44-ICD to pS133CREB was detected; accordingly, CD44-ICD-GST pulled-down a larger amount of CREB upon induction of CREB phosphorylation (**Fig. 16B**). It is possible that binding to CD44-ICD either sterically or allosterically inhibit CREB interaction with PP1/PP2A phosphatases this leading to a long half-life of pS133 CREB. To start verifying this hypothesis, we induced CREB phosphorylation with N6-benzoyl-cAMP in the presence or not of CD44-ICD and followed in a time-course experiment pS133 CREB. Anti-CREB antibody was used for normalization. **Fig. 16C** shows that CD44-ICD expression is able to delay the rate of CREB dephosphorylation.

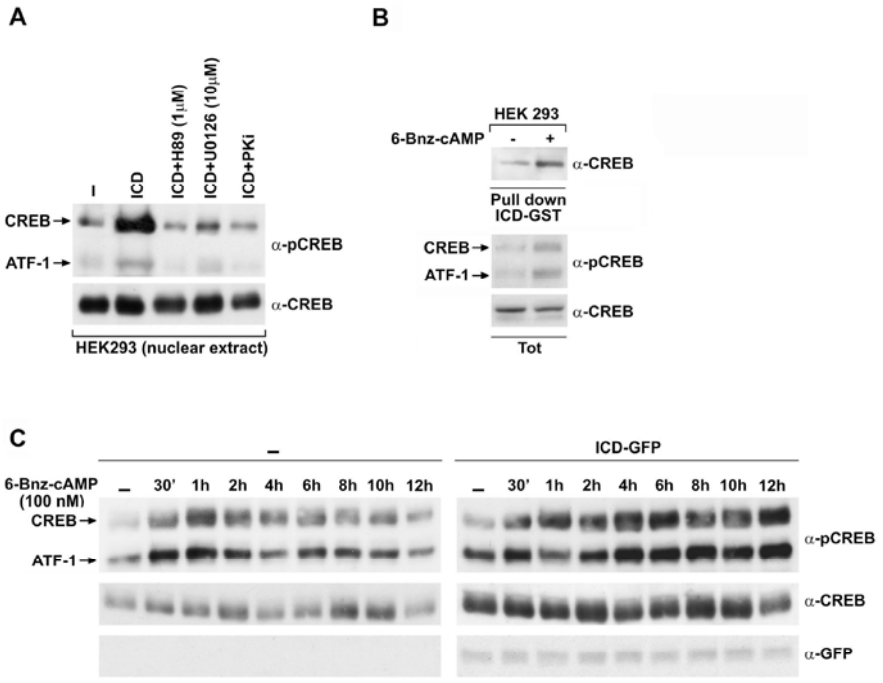

Figure 16 - CD44-ICD binds preferentially the phosphorylated form of CREB and reduces CREB rate of dephosphorylation.

A) Immunoblot analysis with phosphoCREB antibody from nuclear extract of CD44-ICD transfected HEK293 cells. The cells were treated for 2 hours with PKA inhibitor (H89) or MEK-inhibitor (U0126). Lane 4 shows cells transfected with PKA inhibiting peptide (PKi). Anti-CREB was used for normalization.

B) CD44-ICD-GST (ICD-GST) was used to pull down CREB from protein lysates of HEK293 treated for 1 hour with cAMP analogue (N6-benzoyl-cAMP, 100 μM). Immunoblot was performed with the indicated antibodies. The efficiency of N6-benzoyl-cAMP treatment on CREB phosphorylation was checked by phosphoCREB antibody.

C) Immunoblot analysis of CREB phosphorylation of HEK293 cells upon N6-benzoyl-cAMP treatment. GFP-tagged CD44-ICD (ICD) transfected cells were treated with N6-benzoyl-cAMP and harvested at different time points. Anti-GFP was used to check the efficiency of transfection. The normalization was performed with CREB antibody.

6. DISCUSSION AND CONCLUSIONS

Thyroid cancer is often associated to the oncogenic conversion of genes (RET, RAS and BRAF) acting in the ERK signaling pathway. In this dissertation, we have explored functional interaction between such oncogenes and CD44. It was previously known that CD44 is involved in the mitogenic and invasive phenotype of papillary thyroid carcinomas (Melillo *et al*. 2005; Guarino, *et al*. 2005; Castellone *et al*. 2004) and that CD44 undergoes regulated intramembrane proteolysis in various cancer cell lines (Okamoto *et al*. 2001) and human tumors (Okamoto *et al*. 2002). Here we have shown that the CD44-ICD fragment is expressed in human PTC tissue samples and in PTC cell lines harboring RET/PTC or BRAFV600E mutations.

As previously demonstrated in other cellular systems (Okamoto *et al*. 1999a; Pelletier *et al*. 2006), our study shows, by using different chemical inhibitors, that in transformed thyroid cells the release of the ICD fragment from CD44 depends on metalloprotease and γ-secretase activities. The increased production of the extracellular ectoCD44 fragment indicates that metalloprotease-mediated cleavage is at least one level at which induction of CD44 cleavage takes place in thyroid cancer cells. Multiple signaling pathways have been described to regulate the CD44 cleavage: the activation of PKC, the influx of extracellular Ca^{2+}, members of the Rho family of GTPases and the RAS oncoprotein (Okamoto *et al*. 1999b; Kawano *et al*. 2000). In particular, it has been shown that RAS oncoprotein induces CD44 cleavage through PI3K and the Rho family of GTPases, allowing cell migration (Kawano *et al*. 2000; Nagano and Saya, 2004). Here we demonstrate that RET/PTC signaling induces CD44 cleavage through the RAS/BRAF/MEK pathway. Such signaling cascade may stimulate metalloprotease-mediated CD44 cleavage at different levels, such as i) stimulation of metalloprotease expression or activity (Inamoto *et al*. 2007), ii) post-translational modification of CD44, including altered plasma membrane distribution, in turn making the molecule more

susceptible to proteolysis (Pelletier *et al*. 2006), iii) production of CD44 ligands, such as chondroitin sulfate or hyaluronan in turn, able to promote CD44 cleavage (Sugahara *et al*. 2003, 2005, 2008). Metalloprotease up-regulation is likely an important event in RET/PTC-mediated CD44 cleavage as we could previously show that RET/PTC and BRAF up-regulate transcription of some metalloproteases (Melillo *et al*. 2005). However, this does not exclude additional mechanisms. In addition to increasing kinetics of CD44 cleavage, RET/PTC mediated signaling may also increase the half life of CD44-ICD; accordingly, our preliminary data indicate that CD44-ICD expression is still detectable up to 24 hours inhibition of *de novo* protein synthesis in CD44-ICD transfected cells expressing RET/PTC (data not shown). Likely, a combination of these factors contributes to CD44-ICD accumulation in thyroid cancer cells. However, it is important to note that the increased expression of CD44-ICD in transformed compared with non transformed cells is not merely a consequence of the increased expression level of full-length CD44, because it was noted also upon adoptive expression of exogenous CD44 in cells transfected with RET/PTC, RAS V12 or BRAFV600E but not in mock transfected cells.

Concerning the role of CD44-ICD in thyroid cells, here we have demonstrated that CD44-ICD triggers autonomous proliferation of normal thyrocytes in the absence of TSH and is required for the proliferation of the transformed thyroid cells as well. It has been previously demonstrated that CD44-ICD is able to translocate to the nucleus and potentiate gene transcription (Okamoto *et al*. 2001). Our results demonstrated that CD44-ICD stimulates CRE-mediated transcription, thus targeting a major mitogenic signaling cascade for thyroid follicular cells. Indeed, PKA-mediated CREB activation and stimulation of CRE-mediated gene transcription is one of the prominent mechanisms of mitogenic TSH effects in thyroid cells (Kupperman *et al*. 1993). CREB-mediated stimulation of CRE-containing gene promoters may ultimately lead to the up-regulation of cell cycle regulated genes such as

type D cyclins (Albanese *et al.* 1995; Motti *et al.* 2003). Moreover, cyclin D1 is able to trigger TSH-independent proliferation of normal thyrocytes (Kimura *et al.* 2001; Medina and Santisteban 2000). In addition, the expression of a dominant-negative CREB mutant in FRTL-5 rat thyroid follicular cells leads to a reduction of TSH-stimulated cell proliferation and cAMP-mediated gene transcription (Woloshin *et al.* 1992). Furthermore, the expression of a dominant negative CREB in transgenic mice thyroids induces dwarfism and hypothyroidism by reducing expression of thyroid-specific genes and transcription factors (Nguyen *et al.* 2000).

Consistent with the mitogenic effect of CD44-ICD, we found that its expression sustains CREB-mediated cyclin D1 expression in thyroid cells. CD44-ICD was previously reported to potentiate transactivation by the transcriptional coactivator CBP/p300 (Okamoto *et al.* 2001). Accordingly, by using a p300 dominant negative mutant, we demonstrated that the CD44-ICD-mediated overexpression of cyclin D1 is dependent on p300. The mechanism by which CD44-ICD promotes CREB-mediated gene transcription remains to be clarified. Phosphorylation on S133 is a hallmark of CREB activation and allows CBP/p300 binding to CREB thereby facilitating DNA unwinding and recruitment of basal transcriptional machinery (Mayr *et al.* 2001; Chrivia *et al.* 1993; Arias *et al.* 1994). We show that CD44-ICD induces CREB phosphorylation at S133. Furthermore, CD44-ICD formed a protein complex with CREB. It is possible that this interaction either favors CREB S133 phosphorylation or attenuates CREB pS133 de-phosphorylation. We favor the second possibility because on one hand we did not detect a CREB kinase activity in the CD44-ICD/CREB complex (data not shown) and on the other hand we noted a preferential binding of CD44-ICD to phosphorylated form of CREB and the capability of CD44-ICD to delay the rate of CREB dephosphorylation. PP1 and PP2A phosphatases have been reported to de-phosphorylate CREB S133 (Wadzinski *et al.* 1993; Wheat *et al.* 1994). It

remains to be clarified whether CD44-ICD/CREB interaction prevents phosphorylated CREB binding to PP1 and PP2A or protect phosphoCREB from PP1 and PP2A activity. According with such a model, RET signaling is able to directly promote S133 CREB phosphorylation via ERK mediated activation of CREB kinases (likely RSK or MSK) (Hyashi *et al*. 2000); in this framework, via CD44 cleavage RET signaling will also stabilize phosphoS133-CREB, thereby fostering its transcriptional activity.

Likely, CD44-ICD cooperates with other signaling cascades activated by RET/PTC to mediate mitogenic activity. For instance, RET/PTC triggered CREB phosphorylation cooperates with beta-catenin stimulation in promoting the proliferation of thyroid cells (Castellone *et al*. 2008). Several points remain to be clarified, including i) whether CD44-ICD sits on CRE-containing promoters together with CREB; ii) mechanism of CD44-ICD nuclear import; iv) whether the formation of CREB-CD44-ICD complex modifies the panel of CREB transcriptional targets. Finally, it should not be disregarded that CD44-ICD release is not the only result of CD44 proteolysis and ectoCD44 shedding indeed the cleavage may also modulate cell migration and metastasis formation of thyroid cancer cells as previously shown for other cancer systems (Ponta *et al*. 2003).

Altogether, these findings unveil a novel signaling cascade involved in sustaining the mitogenic phenotype of thyroid cancer cells. In principle, this pathway offers the possibility of detecting thyroid cancer burden by measuring ectoCD44 levels in patient blood. Moreover, this pathway is amenable to pharmacological intervention. CD44 cleavage is mediated by metalloproteases and gamma-secretases and both enzymes can be pharmacologically inhibited (Ramnath and Creaven, 2004). For instance, in tumors of epithelial origin, inhibition of TNF-α sheddase may prevent paracrine activation of the epidermal growth factor receptor (EGFR), resulting in inhibition of cancer cell growth (Borrell-Pages *et al*. 2003). The ability of combination between γ-secretase inhibitors and kinase inhibitors to improve efficacy and specificity of

cancer therapy was already shown. For instance, in T-cell acute lymphoblastic leukemia patients carrying ABL1 rearrangement and presenting γ-secretase-dependent cleavage of mutated Notch1, a synergistic anti-proliferative effects was reported for the combined treatment with γ-secretase inhibitors to prevent Notch cleavage, and tyrosine kinase inhibitor imatinib to prevent ABL activity (De Keersmaecker *et al*. 2008). Our study suggests that CD44 cleavage may be another potential therapeutic target in thyroid cancer cells sustaining oncogenic activation of RET, RAS and BRAF.

7. ACKNOWLEDGEMENTS

First and foremost I would like to thank Prof. Giancarlo Vecchio, coordinator of the International Doctorate Program and head of the Dipartimento di Biologia e Patologia Cellulare e Molecolare "L. Califano", where this study was carried out.

There are many people in our department that provided me with help and friendship since 2003 when I joined this institution as a student in Biotechnology. I want to take this opportunity to thank them for precious advices as well as for every time saying a warm hello! These people are too numerous to mention, however I am nonetheless, very grateful. There are, however, a number of people who I am indebted to and would like to acknowledge.

I am grateful to Prof. Massimo Santoro for giving me the opportunity to participate in very interesting projects in his lab, for always being enthusiastic, helpful and supportive.

My sincere thanks go to Dr. Valentina De Falco for teaching me everything I know about good-bench-work-practice, for her constant support, for tireless discussions about experiments, even when it was really time to go!!

I wish to express my gratitude to Dr. Serge Manié for fruitful collaboration and exchanges about CD44 story. Also, I thank professor Mark Billaud and Dr. Serge Manié for hospitality in their lab in Lyon, where I found a pleasant welcome.

I wish to express my gratitude to Dr. Donatella Vitagliano for her precious support and for her sense of humor!!

I would also like to thank all the other researchers in Massimo's lab: Prof. Giuliana Salvatore, Dr. Nello Cerrato, Dr. Mariolina Castellone, Dr. Annamaria Cirafici, Dr. Paolo Salerno, from everyone of them I learned a piece of my small knowledge pack.

Then I would like to mention young colleagues and students: Mara Cantisani, Roberto Bellelli, Simona Ventre … they never forget me at coffee time!!

Moreover, I want to appreciate all foreign guests in Massimo's lab: Mikko Laukkanen, Lilja Laatikainen, Magesh Muthu, Manikandan Mayakannan for always encouraging me and also helping me with English….!!

I cannot end without thanking all my family and my friends; in particular I'm grateful to my parents and Carmine. On their constant encouragement and love I have relied since everything started. To them I dedicate my work.

8. REFERENCES

- Adeniran AJ, Zhu Z, Gandhi M, Steward DL, Fidler JP, Giordano TJ, Biddinger PW, Nikiforov YE. Correlation between genetic alterations and microscopic features, clinical manifestations, and prognostic characteristics of thyroid papillary carcinomas. Am J Surg Pathol 2006;30:216-22.
- Ain KB. Anaplastic thyroid carcinoma: a therapeutic challenge. Semin Surg Oncol 1999;16: 64-9.
- Albanese C, Johnson J, Watanabe G, Eklund N, Vu D, Arnold A, Pestell RG. Transforming p21ras mutants and c-Ets-2 activate the cyclin D1 promoter through distinguishable regions. J Biol Chem. 1995 Oct 6;270(40):23589-97.
- Arias J, Alberts AS, Brindle P, Claret FX, Smeal T, Karin M, Feramisco J, Montminy M. Activation of cAMP and mitogen responsive genes relies on a common nuclear factor. Nature. 1994 Jul 21;370(6486):226-9.
- Asai N, Murakami H, Iwashita T, Takahashi M. A mutation at tyrosine 1062 in MEN2A-Ret and MEN2B-Ret impairs their transforming activity and association with shc adaptor proteins. J Biol Chem 1996;271:17644-9.
- Begum S, Rosenbaum E, Henrique R, Cohen Y, Sidransky D, Westra WH. BRAF mutations in anaplastic thyroid carcinoma: implications for tumor origin, diagnosis and treatment. Mod Pathol. 2004 Nov;17(11):1359-63.
- Berg EL, Goldstein LA, Jutila MA, Nakache M, Picker LJ, Streeter PR, Wu NW, Zhou D, Butcher EC. Homing receptors and vascular addressins: cell adhesion molecules that direct lymphocyte traffic. Immunol Rev. 1989 Apr;108:5-18.
- Borganzone I, Butti MG, Coronelli S, Borrello MG, Santoro M, Mondellini P, Pilotti S, Fusco A, Della Porta G, Pierotti MA. Frequent activation of ret protooncogene by fusion with a new activating gene in papillary thyroid carcinomas. Cancer Res 1994;54:2979-2985.
- Borrell-Pagès M, Rojo F, Albanell J, Baselga J, Arribas J. TACE is required for the activation of the EGFR by TGF-alpha in tumors. EMBO J. 2003 Mar 3;22(5):1114-24.
- Boulon S, Dantonel JC, Binet V, Vié A, Blanchard JM, Hipskind RA, Philips A. Oct-1 potentiates CREB-driven cyclin D1 promoter activation via a phospho-CREB- and CREB binding protein-independent mechanism. Mol Cell Biol. 2002 Nov;22(22):7769-79.
- Capezzone M, Marchisotta S, Cantara S, Busonero G, Brilli L, Pazaitou-Panayiotou K, Carli AF, Caruso G, Toti P, Capitani S, Pammolli A, Pacini F. Familial non-medullary thyroid carcinoma displays the features of clinical anticipation suggestive of a distinct biological entity. Endocr Relat Cancer. 2008 Dec;15(4):1075-1081.
- Carta C, Moretti S, Passeri L, Barbi F, Avenia N, Cavaliere A, Monacelli M, Macchiarulo A, Santeusanio F, Tartaglia M, Puxeddu E. Genotyping of an Italian papillary thyroid carcinoma cohort revealed high prevalence of BRAF mutations, absence of RAS mutations and allowed the detection of a new mutation of BRAF oncoprotein (BRAF(V599lns)). Clin Endocrinol (Oxf) 2006;64:105-9.
- Castellone MD, Celetti A, Guarino V, Cirafici AM, Basolo F, Giannini R, Medico E, Kruhoffer M, Orntoft TF, Curcio F, Fusco A, Melillo RM, Santoro M. Autocrine stimulation by osteopontin plays a pivotal role in the expression of the mitogenic and invasive phenotype of RET/PTC-transformed thyroid cells. Oncogene. 2004 Mar 18;23(12):2188-96.
- Castellone MD, Teramoto H, Williams BO, Druey KM, Gutkind JS. Prostaglandin E2 promotes colon cancer cell growth through a Gs-axin-beta-catenin signaling axis. Science. 2005 Dec 2;310(5753):1504-10.

- Castellone MD, De Falco V, Rao DM, Bellelli R, Muthu M, Basolo F, Fusco A, Gutkind JS, Santoro M. The β-catenin Axis Integrates Multiple Signals Downstream From RET/PTC and Leads to Cell Proliferation. Cancer Res 2008 (in press).
- Castro P, Rebocho AP, Soares RJ, Magalhães J, Roque L, Trovisco V, Vieira de Castro I, Cardoso-de-Oliveira M, Fonseca E, Soares P, Sobrinho-Simões M. PAX8-PPARgamma rearrangement is frequently detected in the follicular variant of papillary thyroid carcinoma. J Clin Endocrinol Metab. 2006 Jan;91(1):213-20.
- Chrivia JC, Kwok RP, Lamb N, Hagiwara M, Montminy MR, Goodman RH. Phosphorylated CREB binds specifically to the nuclear protein CBP. Nature. 1993 Oct 28;365(6449):855-9.
- Ciampi R, Knauf JA, Kerler R, Gandhi M, Zhu Z, Nikiforova MN, Rabes HM, Fagin JA, Nikiforov YE. Oncogenic AKAP9-BRAF fusion is a novel mechanism of MAPK pathway activation in thyroid cancer. J Clin Invest 2005;115:94-101.
- Ciampi R, Nikiforov YE. RET/PTC rearrangements and BRAF mutations in thyroid tumorigenesis. Endocrinology 2007;148:936-41.
- Conkright MD, Montminy M. CREB: the unindicted cancer co-conspirator. Trends Cell Biol. 2005 Sep;15(9):457-9.
- Cote GJ, Gagel RF. Lessons learned from the management of a rare genetic cancer. N Engl J Med 2003;349:1566-8.
- Curcio F, Ambesi-Impiombato FS, Perrella G, Coon HG. Long-term culture and functional characterization of follicular cells from adult normal human thyroids. Proc Natl Acad Sci U S A. 1994 Sep 13;91(19):9004-8.
- De Falco V, Guarino V, Malorni L, Cirafici AM, Troglio F, Erreni M, Pelicci G, Santoro M, Melillo RM. RAI(ShcC/N-Shc)-dependent recuitment of GAB 1 to RET oncoproteins potentiates PI3-K signaling in thyroid tumors. Oncogene 2005;24:6303-6313.
- De Keersmaecker K, Lahortiga I, Mentens N, Folens C, Van Neste L, Bekaert S, Vandenberghe P, Odero MD, Marynen P, Cools J. In vitro validation of gamma-secretase inhibitors alone or in combination with other anti-cancer drugs for the treatment of T-cell acute lymphoblastic leukemia. Haematologica. 2008 Apr;93(4):533-42.
- De Vita G, Zannini M, Cirafici AM, Melillo RM, Di Lauro R, Fusco A, Santoro M. Expression of RET/PTC1 oncogene impairs the activity of TTF-1 and Pax-8 thyroid transcription factors. Cell Growth Differ 1998;9:97-103.
- DeLellis RA, Williams ED. Thyroid and parathyroid tumors. In Tumors of Endocrine Organs, World Health Organization Classification of Tumors. DeLellis RA, Lloyd RV, Heitz PU and Eng C. 2004 (eds), p. 51-56.
- DeLellis RA. Pathology and genetics of thyroid carcinoma. J Surg Oncol 2006;94:662-9.
- Di Agostino S, Strano S, Emiliozzi V, Zerbini V, Mottolese M, Sacchi A, Blandino G, Piaggio G. Gain of function of mutant p53: the mutant p53/NF-Y protein complex reveals an aberrant transcriptional mechanism of cell cycle regulation. Cancer Cell. 2006 Sep;10(3):191-202.
- Dianzani U, Malavasi F. Lymphocyte adhesion to endothelium. Crit Rev Immunol. 1995;15(2):167-200.
- Dremier S, Coulonval K, Perpete S, Vandeput F, Fortemaison N, Van Keymeulen A, Deleu S, Ledent C, Clément S, Schurmans S, Dumont JE, Lamy F, Roger PP, Maenhaut C. The role of cyclic AMP and its effect on protein kinase A in the mitogenic action of thyrotropin on the thyroid cell. Ann N Y Acad Sci. 2002 Jun;968:106-21.

- Durante C, Haddy N, Baudin E, Leboulleux S, Hartl D, Travagli JP, Caillou B, Ricard M, Lumbroso JD, De Vathaire F, Schlumberger M. Long-term outcome of 444 patients with distant metastases from papillary and follicular thyroid carcinoma: benefits and limits of radioiodine therapy. J Clin Endocrinol Metab 2006;91:2892-9.
- Dworet JH, Meinkoth JL. Interference with 3',5'-cyclic adenosine monophosphate response element binding protein stimulates apoptosis through aberrant cell cycle progression and checkpoint activation. Mol Endocrinol. 2006 May;20(5):1112-20.
- Elisei R, Cosci B, Romei C, Bottici V, Renzini G, Molinaro E, Agate L, Vivaldi A, Faviana P, Basolo F, Miccoli P, Berti P, Pacini F, Pinchera A. Prognostic significance of somatic RET oncogene mutations in sporadic medullary thyroid cancer: a 10-year follow-up study. J Clin Endocrinol Metab. 2008b Mar;93(3):682-7
- Elisei R, Romei C, Cosci B, Agate L, Bottici V, Molinaro E, Sculli M, Miccoli P, Basolo F, Grasso L, Pacini F, Pinchera A. RET genetic screening in patients with medullary thyroid cancer and their relatives: experience with 807 individuals at one center. J Clin Endocrinol Metab. 2007 Dec;92(12):4725-9.
- Elisei R, Ugolini C, Viola D, Lupi C, Biagini A, Giannini R, Romei C, Miccoli P, Pinchera A, Basolo F. BRAF(V600E) mutation and outcome of patients with papillary thyroid carcinoma: a 15-year median follow-up study. J Clin Endocrinol Metab. 2008a Oct;93(10):3943-9.
- Fabien N, Fusco A, Santoro M, Barbier Y, Dubois PM, Paulin C Description of a human papillary thyroid carcinoma cell line. Morphologic study and expression of tumoral markers. Cancer. 1994 Apr 15;73(8):2206-12.
- Feliciello A, Li Y, Avvedimento EV, Gottesman ME, Rubin CS. A-kinase anchor protein 75 increases the rate and magnitude of cAMP signaling to the nucleus. Curr Biol. 1997 Dec 1;7(12):1011-4.
- Frattini M, Ferrario C, Bressan P, Balestra D, De Cecco L, Mondellini P, Bongarzone I, Collini P, Gariboldi M, Pilotti S, Pierotti MA, Greco A. Alternative mutations of BRAF, RET and NTRK1 are associated with similar but distinct gene expression patterns in papillary thyroid cancer. Oncogene 2004 ;23:7436-40.
- Frêche B, Guillaumot P, Charmetant J, Pelletier L, Luquain C, Christiansen D, Billaud M, Manié SN. Inducible dimerization of RET reveals a specific AKT deregulation in oncogenic signaling. J Biol Chem 2005;280:36584-91.
- Fujita Y, Kitagawa M, Nakamura S, Azuma K, Ishii G, Higashi M, Kishi H, Hiwasa T, Koda K, Nakajima N, Harigaya K. CD44 signaling through focal adhesion kinase and its anti-apoptotic effect. FEBS Lett. 2002 Sep 25;528(1-3):101-8.
- Fusco A, Berlingieri MT, Di Fiore PP, Portella G, Grieco M, Vecchio G. One- and two-step transformations of rat thyroid epithelial cells by retroviral oncogenes. Mol Cell Biol 1987;7:3365-70.
- Fusco A, Chiappetta G, Hui P, Garcia-Rostan G, Golden L, Kinder BK, Dillon DA, Giuliano A, Cirafici AM, Santoro M, Rosai J, Tallini G. Assessment of RET/PTC oncogene activation and clonality in thyroid nodules with incomplete morphological evidence of papillary carcinoma: a search for the early precursors of papillary thyroid cancer. Am J Pathol 2002;160:2157-67.
- Fusco A, Grieco M, Santoro M, Berlingieri MT, Pilotti S, Pierotti MA, Della Porta G, Vecchio G. A new oncogene in human thyroid papillary carcinomas and their lymph-nodal metastases. Nature 1987;328:170-172.
- Galandrini R, Albi N, Tripodi G, Zarcone D, Terenzi A, Moretta A, Grossi CE, Velardi A. Antibodies to CD44 trigger effector functions of human T cell clones. J Immunol. 1993 May 15;150(10):4225-35.
- García-Rostán G, Camp RL, Herrero A, Carcangiu ML, Rimm DL, Tallini G. Beta-catenin dysregulation in thyroid neoplasms: down-regulation, aberrant nuclear expression, and CTNNB1 exon 3 mutations are markers for aggressive tumor phenotypes and poor prognosis. Am J Pathol 2001;158:987-96.

- García-Rostán G, Costa AM, Pereira-Castro I, Salvatore G, Hernandez R, Hermsem MJ, Herrero A, Fusco A, Cameselle-Teijeiro J, Santoro M. Mutation of the PIK3CA gene in anaplastic thyroid cancer. Cancer Res 2005;65:10199-207.
- Garcia-Rostan G, Zhao H, Camp RL, Pollan M, Herrero A, Pardo J, Wu R, Carcangiu ML, Costa J, Tallini G. ras mutations are associated with aggressive tumor phenotypes and poor prognosis in thyroid cancer. J Clin Oncol. 2003 Sep 1;21(17):3226-35.
- Ghaffari S, Dougherty GJ, Eaves AC, Eaves CJ. Diverse effects of anti-CD44 antibodies on the stromal cell-mediated support of normal but not leukaemic (CML) haemopoiesis in vitro. Br J Haematol. 1997 Apr;97(1):22-8.
- Ghaffari S, Smadja-Joffe F, Oostendorp R, Lévesque JP, Dougherty G, Eaves A, Eaves C. CD44 isoforms in normal and leukemic hematopoiesis. Exp Hematol. 1999 Jun;27(6):978-93.
- Gimm O. Thyroid cancer. Cancer Lett. 2001 Feb 26;163(2):143-56.
- Gonzalez GA, Montminy MR. Cyclic AMP stimulates somatostatin gene transcription by phosphorylation of CREB at serine 133. Cell. 1989 Nov 17;59(4):675-80.
- Goshen R, Ariel I, Shuster S, Hochberg A, Vlodavsky I, de Groot N, Ben-Rafael Z, Stern R. Hyaluronan, CD44 and its variant exons in human trophoblast invasion and placental angiogenesis. Mol Hum Reprod. 1996 Sep;2(9):685-91.
- Greco A, Mariani C, Miranda C, Lupas A, Pagliardini S, Pomati M, Pierotti MA. The DNA rearrangement that generates the TRK-T3 oncogene involves a novel gene on chromosome 3 whose product has a potential coiled-coil domain. Mol Cell Biol. 1995 Nov;15(11):6118-27.
- Greco A, Mariani C, Miranda C, Pagliardini S, Pierotti MA. Characterization of the NTRK1 genomic region involved in chromosomal rearrangements generating TRK oncogenes. Genomics. 1993 Nov;18(2):397-400.
- Greco A, Miranda C, Pagliardini S, Fusetti L, Bongarzone I, Pierotti MA. Chromosome 1 rearrangements involving the genes TPR and NTRK1 produce structurally different thyroid-specific TRK oncogenes. Genes Chromosomes Cancer. 1997 Jun;19(2):112-23.
- Grieco M, Santoro M, Berlingieri MT, Melillo RM, Donghi R, Borganzone I, Pierotti MA, Della Porta G, Fusco A, Vecchio G. PTC is a novel rearranged form of the ret proto-oncogene and is frequently detected in vivo in human thyroid papillary carcinomas. Cell 1990;60:557-563.
- Guarino V, Faviana P, Salvatore G, Castellone MD, Cirafici AM, De Falco V, Celetti A, Giannini R, Basolo F, Melillo RM, Santoro M. Osteopontin is overexpressed in human papillary thyroid carcinomas and enhances thyroid carcinoma cell invasiveness. J Clin Endocrinol Metab. 2005 Sep;90(9):5270-8.
- Günthert U, Schwärzler C, Wittig B, Laman J, Ruiz P, Stauder R, Bloem A, Smadja-Joffe F, Zöller M, Rolink A. Functional involvement of CD44, a family of cell adhesion molecules, in immune responses, tumour progression and haematopoiesis. Adv Exp Med Biol. 1998;451:43-9.
- Guy R, Yefenof E, Naor D, Dorogin A, Zilberman Y. CD44 co-stimulates apoptosis in thymic lymphomas and T cell hybridomas. Cell Immunol. 2002 Mar-Apr;216(1-2):82-92.
- Hayashi H, Ichihara M, Iwashita T, Murakami H, Shimono Y, Kawai K, Kurokawa K, Murakumo Y, Imai T, Funahashi H, Nakao A, Takahashi M. Characterization of intracellular signals via tyrosine 1062 in RET activated by glial cell line-derived neurotrophic factor. Oncogene. 2000 Sep 14;19(39):4469-75.
- Hedinger C, Williams ED, Sobin LH. The WHO histological classification of thyroid tumors: a commentary on the second edition. Cancer. 1989 Mar 1;63(5):908-11.

- Hou P, Liu D, Shan Y, Hu S, Studeman K, Condouris S, Wang Y, Trink A, El-Naggar AK, Tallini G, Vasko V, Xing M. Genetic alterations and their relationship in the phosphatidylinositol 3-kinase/Akt pathway in thyroid cancer. Clin Cancer Res. 2007 Feb 15;13(4):1161-70.
- Hundahl SA, Fleming ID, Fremgen AM, Menck HR. A National Cancer Data Base report on 53,856 cases of thyroid carcinoma treated in the U.S., 1985-1995. Cancer 1998 Dec 15;83(12):2638-48.
- Iavarone C, Catania A, Marinissen MJ, Visconti R, Acunzo M, Tarantino C, Carlomagno MS, Bruni CB, Gutkind JS, Chiariello M. The platelet-derived growth factor controls c-myc expression through a JNK- and AP-1-dependent signaling pathway. J Biol Chem. 2003 Dec 12;278(50):50024-30.
- Impey S, McCorkle SR, Cha-Molstad H, Dwyer JM, Yochum GS, Boss JM, McWeeney S, Dunn JJ, Mandel G, Goodman RH. Defining the CREB regulon: a genome-wide analysis of transcription factor regulatory regions. Cell. 2004 Dec 29;119(7):1041-54.
- Inamoto T, Azuma H, Sakamoto T, Kiyama S, Ubai T, Kotake Y, Watanabe M, Katsuoka Y. Invasive ability of human renal cell carcinoma cell line Caki-2 is accelerated by gamma-aminobutyric acid, via sustained activation of ERK1/2 inducible matrix metalloproteinases.
  Cancer Invest. 2007 Oct;25(7):574-83.
- Isacke CM, Yarwood H. The hyaluronan receptor, CD44. Int J Biochem Cell Biol. 2002 Jul;34(7):718-21.
- Jalkanen S, Jalkanen M. Lymphocyte CD44 binds the COOH-terminal heparin-binding domain of fibronectin. J Cell Biol. 1992 Feb;116(3):817-25.
- Jemal A, Siegel R, Ward E, Hao Y, Xu J, Murray T, Thun MJ. Cancer statistics, 2008. CA Cancer J Clin. 2008 Mar-Apr;58(2):71-96.
- Johannessen M, Delghandi MP, Moens U. What turns CREB on? Cell Signal. 2004 Nov;16(11):1211-27.
- Jothy S. CD44 and its partners in metastasis. Clin Exp Metastasis. 2003;20(3):195-201.
- Jung HS, Kim DW, Jo YS, Chung HK, Song JH, Park JS, Park KC, Park SH, Hwang JH, Jo KW, Shong M 2005 Regulation of protein kinase B tyrosine phosphorylation by thyroid-specific oncogenic RET/PTC kinases. Mol Endocrinol 19:2748-2759.
- Kaya G, Rodriguez I, Jorcano JL, Vassalli P, Stamenkovic I. Cutaneous delayed-type hypersensitivity response is inhibited in transgenic mice with keratinocyte-specific CD44 expression defect. J Invest Dermatol. 1999 Jul;113(1):137-8.
- Kaya G, Rodriguez I, Jorcano JL, Vassalli P, Stamenkovic I. Selective suppression of CD44 in keratinocytes of mice bearing an antisense CD44 transgene driven by a tissue-specific promoter disrupts hyaluronate metabolism in the skin and impairs keratinocyte proliferation. Genes Dev. 1997 Apr 15;11(8):996-1007.
- Kimura ET, Nikiforova MN, Zhu Z, Knauf JA, Nikiforov YE, Fagin JA. High prevalence of BRAF mutations in thyroid cancer: genetic evidence for constitutive activation of the RET/PTC-RAS-BRAF signalling pathway in papillary thyroid carcinoma. Cancer Res 2003;63:1454-1457.
- Kimura T, Van Keymeulen A, Golstein J, Fusco A, Dumont JE, Roger PP. Regulation of thyroid cell proliferation by TSH and other factors: a critical evaluation of in vitro models. Endocr Rev. 2001 Oct;22(5):631-56.
- Kimura T, Van Keymeulen A, Golstein J, Fusco A, Dumont JE, Roger PP. Regulation of thyroid cell proliferation by TSH and other factors: a critical evaluation of in vitro models. Endocr Rev. 2001 Oct;22(5):631-56.
- Kinashi T, Springer TA. Adhesion molecules in hematopoietic cells. Blood Cells. 1994;20(1):25-44.

- Knauf JA, Kuroda H, Basu S, Fagin JA. RET/PTC-induced dedifferentiation of thyroid cells is mediated through Y1062 signaling through SHC-RAS-MAP kinase. Oncogene 2003;22:4406-4412.
- Knauf JA, Ma X, Smith EP, Zhang L, Mitsutake N, Liao XH, Refetoff S, Nikiforov YE, Fagin JA. Targeted expression of BRAFV600E in thyroid cells of transgenic mice results in papillary thyroid cancers that undergo dedifferentiation. Cancer Res 2005 15;65:4238-45.
- Knudson CB, Knudson W. Hyaluronan-binding proteins in development, tissue homeostasis, and disease. FASEB J. 1993 Oct;7(13):1233-41.
- Kohn LD, Shimura H, Shimura Y, Hidaka A, Giuliani C, Napolitano G, Ohmori M, Laglia G, Saji M. The thyrotropin receptor. Vitam Horm. 1995;50:287-384.
- Kondo T, Ezzat S, Asa SL. Pathogenetic mechanisms in thyroid follicular-cell neoplasia. Nat Rev Cancer 2006;6:292–306.
- Kroll TG, Sarraf P, Pecciarini L, Chen CJ, Mueller E, Spiegelman BM, Fletcher JA. PAX8-PPARgamma1 fusion oncogene in human thyroid carcinoma. Science 2000;289:1357-60.
- Lammer C, Wagerer S, Saffrich R, Mertens D, Ansorge W, Hoffmann I. The cdc25B phosphatase is essential for the G2/M phase transition in human cells. J Cell Sci 1998;111:2445-53.
- Larsen PR, Kronenberg HM, Melmed S, Polonsky KS. Williams textbook of Endocrinology. 10th edition 2003. Saunders Ed.
- Leboulleux S, Baudin E, Travagli JP, Schlumberger M. Medullary thyroid carcinoma. Clin Endocrinol (Oxf) 2004;61:299-310.
- Leboulleux S, Rubino C, Baudin E, Caillou B, Hartl DM, Bidart JM, Travagli JP, Schlumberger M. Prognostic factors for persistent or recurrent disease of papillary thyroid carcinoma with neck lymph node metastases and/or tumor extension beyond the thyroid capsule at initial diagnosis. J Clin Endocrinol Metab 2005;90:5723-9.
- Ledent C, Parmentier M, Maenhaut C, Taton M, Pirson I, Lamy F, Roger P, Dumont JE. The TSH cyclic AMP cascade in the control of thyroid cell proliferation: the story of a concept. Thyroidology. 1991 Dec;3(3):97-101.
- Lesley J, Hyman R. CD44 structure and function. Front Biosci. 1998 Jul 1;3:d616-30.
- Lewinsohn DM, Nagler A, Ginzton N, Greenberg P, Butcher EC. Hematopoietic progenitor cell expression of the H-CAM (CD44) homing-associated adhesion molecule. Blood. 1990 Feb 1;75(3):589-95.
- Liaw D, Marsh DJ, Li J, Dahia PL, Wang SI, Zheng Z, Bose S, Call KM, Tsou HC, Peacocke M, Eng C, Parsons R.Germline mutations of the PTEN gene in Cowden disease, an inherited breast and thyroid cancer sindrome. Nat Genet. 1997 May;16(1):64-7.
- Lin HY, Harris TL, Flannery MS, Aruffo A, Kaji EH, Gorn A, Kolakowski LF Jr, Lodish HF, Goldring SR. Expression cloning of an adenylate cyclase-coupled calcitonin receptor. Science. 1991 Nov 15;254(5034):1022-4.
- Liu Z, Hou P, Ji M, Guan H, Studeman K, Jensen K, Vasko V, El-Naggar AK, Xing M. Highly prevalent genetic alterations in receptor tyrosine kinases and phosphatidylinositol 3-kinase/akt and mitogen-activated protein kinase pathways in anaplastic and follicular thyroid cancers. J Clin Endocrinol Metab. 2008 Aug;93(8):3106-16.
- Long MW. Blood cell cytoadhesion molecules. Exp Hematol. 1992 Mar;20(3):288-301.
- Lui WO, Zeng L, Rehrmann V, Deshpande S, Tretiakova M, Kaplan EL, Leibiger I, Leibiger B, Enberg U, Höög A, Larsson C, Kroll TG. CREB3L2-PPARgamma fusion mutation identifies a thyroid signaling pathway regulated by intramembrane proteolysis. Cancer Res. 2008 Sep 1;68(17):7156-64.

- Lupi C, Giannini R, Ugolini C, Proietti A, Berti P, Minuto M, Materazzi G, Elisei R, Santoro M, Miccoli P, Basolo F. Association of BRAF V600E Mutation with Poor Clinicopathological Outcomes in 500 Consecutive Cases of Papillary Thyroid Carcinoma. J Clin Endocrinol Metab 2007;92:4085-90.
- Malchoff CD, Malchoff DM. Familial nonmedullary thyroid carcinoma. Cancer Control. 2006 Apr;13(2):106-10.
- Manié S, Santoro M, Fusco A, Billaud M. The RET receptor: function in development and dysfunction in congenital malformation. Trends Genet 2001;17:580-9.
- Marhaba R, Bourouba M, Zöller M. CD44v7 interferes with activation-induced cell death by up-regulation of anti-apoptotic gene expression. J Leukoc Biol. 2003 Jul;74(1):135-48.
- Marhaba R, Zöller M. CD44 in cancer progression: adhesion, migration and growth regulation. J Mol Histol. 2004 Mar;35(3):211-31.
- Marinissen MJ, Chiariello M, Tanos T, Bernard O, Narumiya S, Gutkind JS. The small GTP-binding protein RhoA regulates c-jun by a ROCK-JNK signaling axis. Mol Cell. 2004 Apr 9;14(1):29-41.
- Marx SJ. Molecular genetics of multiple endocrine neoplasia types 1 and 2. Nat Rev Cancer. 2005 May;5(5):367-75. Review. Erratum in: Nat Rev Cancer. 2005 Aug;5(8):663.
- Mayr B, Montminy M. Transcriptional regulation by the phosphorylation-dependent factor CREB. Nat Rev Mol Cell Biol. 2001 Aug;2(8):599-609.
- Mayr BM, Canettieri G, Montminy MR. Distinct effects of cAMP and mitogenic signals on CREB-binding protein recruitment impart specificity to target gene activation via CREB. Proc Natl Acad Sci U S A. 2001 Sep 11;98(19):10936-41.
- Mazzaferri EL. 1993 Management of a solitary thyroid nodule. N Engl J Med. 328:553–559.
- McKallip RJ, Do Y, Fisher MT, Robertson JL, Nagarkatti PS, Nagarkatti M. Role of CD44 in activation-induced cell death: CD44-deficient mice exhibit enhanced T cell response to conventional and superantigens. Int Immunol. 2002 Sep;14(9):1015-26.
- Medina DL, Santisteban P. Thyrotropin-dependent proliferation of in vitro rat thyroid cell systems. Eur J Endocrinol. 2000 Aug;143(2):161-78.
- Melillo RM, Castellone MD, Guarino V, Da Falco V, Cirafici AM, Salvatore G, Caiazzo F, Basolo F, Giannini R, Kruhoffer M, Orntoft T, Fusco A, Santoro M. The RET/PTC-RAS-BRAF linear signaling cascade mediates the motile and mitogenic phenotype of thyroid cancer cells. J Clin Invest 2005;115:1068-1081.
- Melillo RM, Santoro M, Ong SH, Billaud M, Fusco A, Hadari YR, Schlessinger J, Lax I. Docking protein FRS2 links the protein tyrosine kinase RET and its oncogenic forms with the mitogen-activated protein kinase signaling cascade. Mol Cell Biol 2001;21:4177-87.
- Miccoli P, Minuto MN, Ugolini C, Molinaro E, Basolo F, Berti P, Pinchera A, Elisei R. Clinically unpredictable prognostic factors in the outcome of medullary thyroid cancer. Endocr Relat Cancer. 2007 Dec;14(4):1099-105.
- Missero C, Cobellis G, De Felice M, Di Lauro R. Molecular events involved in differentiation of thyroid follicular cells. Mol Cell Endocrinol. 1998 May 25;140(1-2):37-43.
- Mitsutake N, Knauf JA, Mitsutake S, Mesa C, Jr., Zhang L, Fagin JA. Conditional BRAFV600E expression induces DNA synthesis, apoptosis, dedifferentiation, and chromosomal instability in thyroid PCCL3 cells. Cancer Res 2005;65:2465-2473.
- Miyagi E, Braga-Basaria M, Hardy E, Vasko V, Burman KD, Jhiang S, Saji M, Ringel MD. Chronic expression of RET/PTC3 enhances basal insulin-stimulated PI3 kinase/AKT signaling and increases IRS-2 expression in FRTL-5 thyroid cells. Mol Carcinog 2004;41:98-107.

- Miyake N, Maeta H, Horie S, Kitamura Y, Nanba E, Kobayashi K, Terada T. Absence of mutations in the beta-catenin and adenomatous polyposis coli genes in papillary and follicular thyroid carcinomas. Pathol Int 2001;51:680-5.
- Montminy MR, Bilezikjian LM. Binding of a nuclear protein to the cyclic-AMP response element of the somatostatin gene. Nature. 1987 Jul 9-15;328(6126):175-8.
- Motti ML, Boccia A, Belletti B, Bruni P, Troncone G, Cito L, Monaco M, Chiappetta G, Baldassarre G, Palombini L, Fusco A, Viglietto G. Critical role of cyclin D3 in TSH-dependent growth of thyrocytes and in hyperproliferative diseases of the thyroid gland. Oncogene 2003 Oct 23;22(48):7576-86.
- Murakami D, Okamoto I, Nagano O, Kawano Y, Tomita T, Iwatsubo T, De Strooper B, Yumoto E, Saya H. Presenilin-dependent gamma-secretase activity mediates the intramembranous cleavage of CD44. Oncogene. 2003 Mar 13;22(10):1511-6.
- Nagano O, Saya H. Mechanism and biological significance of CD44 cleavage. Cancer Sci. 2004 Dec;95(12):930-5.
- Nagayama Y, Yamashita S, Hirayu H, Izumi M, Uga T, Ishikawa N, Ito K, Nagataki S. Regulation of thyroid peroxidase and thyroglobulin gene expression by thyrotropin in cultured human thyroid cells. J Clin Endocrinol Metab. 1989 Jun;68(6):1155-9.
- Namba H, Nakashima M, Hayashi T, Hayashida N, Maeda S, Rogounovitch TI, Ohtsuru A, Saenko VA, Kanematsu T, Yamashita S. Clinical implication of hot spot BRAF mutation, V599E, in papillary thyroid cancers. J Clin Endocrinol Metab 2003;88:4393-7.
- Naor D, Nedvetzki S, Golan I, Melnik L, Faitelson Y. CD44 in cancer. Crit Rev Clin Lab Sci. 2002 Nov;39(6):527-79.
- Naor, D., Sionov, R. V. & Ish-Shalom, D. in Advances in Cancer Research Vol. 70 (eds Vande Woude, G. F. & Klein, G.) 243–318 (Academic, San Diego, 1997).
- Nguyen LQ, Kopp P, Martinson F, Stanfield K, Roth SI, Jameson JL. A dominant negative CREB (cAMP response element-binding protein) isoform inhibits thyrocyte growth, thyroid-specific gene expression, differentiation, and function. Mol Endocrinol. 2000 Sep;14(9):1448-61.
- Nikiforov YE. Genetic alterations involved in the transition from-well differentiated to poorly differentiated and anaplastic thyroid carcinoma. Endocr Pathos Winter 2004;15:319-27.
- Nikiforova MN, Kimura ET, Gandhi M, Biddinger PW, Knauf JA, Basolo F, Zhu Z, Giannini R, Salvatore G, Fusco A, Santoro M, Fagin JA, Nikiforov YE. BRAF mutations in thyroid tumors are restricted to papillary carcinomas and anaplastic or poorly differentiated carcinomas arising from papillary carcinomas. J Clin Enocrinol Metab 2003a; 88:5399-5404.
- Nikiforova MN, Lynch RA, Biddinger PW, Alexander EK, Dorn GW 2nd, Tallini G, Kroll TG, Nikiforov YE. RAS point mutations and PAX8-PPAR gamma rearrangement in thyroid tumors: evidencefor distinct molecular pathways in thyroid follicular carcinoma. J Clin Endocrinol Metab 2003b;88:2318-26.
- Nikiforova MN, Stringer JR, Blough R, Medvedovic M, Fagin JA, Nikiforov YE. Proximity of chromosomal loci that participate in radiation-induced rearrangements in human cells. Science. 2000 Oct 6;290(5489):138-41.
- Nosé V. Familial Non-Medullary Thyroid Carcinoma: An Update. Endocr Pathol. 2008 Oct 18.
- Ohmori M, Endo T, Harii N, Onaya T. A novel thyroid transcription factor is essential for thyrotropin-induced up-regulation of Na+/I- symporter gene expression. Mol Endocrinol. 1998 May;12(5):727-36.
- Okamoto I, Kawano Y, Tsuiki H, Sasaki J, Nakao M, Matsumoto M, Suga M, Ando M, Nakajima M, Saya H. CD44 cleavage induced by a membrane-associated metalloprotease plays a critical role in tumor cell migration. Oncogene. 1999a Feb 18;18(7):1435-46.

- Okamoto I, Kawano Y, Matsumoto M, Suga M, Kaibuchi K, Ando M, Saya H. Regulated CD44 cleavage under the control of protein kinase C, calcium influx, and the Rho family of small G proteins. J Biol Chem. 1999b Sep 3;274(36):25525-34.
- Okamoto I, Kawano Y, Murakami D, Sasayama T, Araki N, Miki T, Wong AJ, Saya H. Proteolytic release of CD44 intracellular domain and its role in the CD44 signaling pathway. J Cell Biol. 2001 Nov 26;155(5):755-62.
- Okamoto I, Tsuiki H, Kenyon LC, Godwin AK, Emlet DR, Holgado-Madruga M, Lanham IS, Joynes CJ, Vo KT, Guha A, Matsumoto M, Ushio Y, Saya H, Wong AJ. Proteolytic cleavage of the CD44 adhesion molecule in multiple human tumors. Am J Pathol. 2002 Feb;160(2):441-7.
- Ordonez N, Baloch Z, Matias-Guiu X, *et al*. Undifferentiated (anaplastic) carcinoma. In: Tumours of Endocrine Organs, World Health Organization Classification of Tumors. DeLellis RA, Lloyd RV, Heitz PU and Eng C. 2004 (eds), p. 77-80.
- Ortiz L, Zannini M, Di Lauro R, Santisteban P. Transcriptional control of the forkhead thyroid transcription factor TTF-2 by thyrotropin, insulin, and insulin-like growth factor I. J Biol Chem. 1997 Sep 12;272(37):23334-9.
- Pacini F, Schlumberger M, Dralle H, Elisei R, Smit JW, Wiersinga W; European Thyroid Cancer Taskforce. European consensus for the management of patients with differentiated thyroid carcinoma of the follicular epithelium. Eur J Endocrinol. 2006 Jun;154(6):787-803.
- Parma J, Van Sande J, Swillens S, Tonacchera M, Dumont J, Vassart G. Somatic mutations causing constitutive activity of the thyrotropin receptor are the major cause of hyperfunctioning thyroid adenomas: identification of additional mutations activating both the cyclic adenosine 3',5'-monophosphate and inositol phosphate-Ca2+ cascades. Mol Endocrinol. 1995 Jun;9(6):725-33.
- Pasieka JL. Anaplastic thyroid cancer. Curr Opin Oncol 2003;15:78-83.
- Pelicci G, Troglio F, Bodini A, Melillo RM, Pettirossi V, Coda L, De Giuseppe A, Santoro M, Pelicci PG. The neuron-specific Rai (ShcC) adaptor protein inhibits apoptosis by coupling Ret to the phosphatidylinositol 3-kinase/Akt signaling pathway. Mol Cell Biol 2002;20:7351-63.
- Pelletier L, Guillaumot P, Frêche B, Luquain C, Christiansen D, Brugière S, Garin J, Manié SN. Gamma-secretase-dependent proteolysis of CD44 promotes neoplastic transformation of rat fibroblastic cells. Cancer Res. 2006 Apr 1;66(7):3681-7.
- Picker LJ, Nakache M, Butcher EC. Monoclonal antibodies to human lymphocyte homing receptors define a novel class of adhesion molecules on diverse cell types. J Cell Biol. 1989 Aug;109(2):927-37.
- Ponta H, Sherman L, Herrlich PA. CD44: from adhesion molecules to signalling regulators. Nat Rev Mol Cell Biol. 2003 Jan;4(1):33-45.
- Powell DJ, Jr., Russell J, Nibu K, Li G, Rhee E, Liao M, Goldstein M, Keane WM, Santoro M, Fusco A, Rothstein JL. The RET/PTC3 oncogene: metastatic solid-type papillary carcinomas in murine thyroids. Cancer Res 1998;58:5523-5528.
- Pulcrano M, Boukheris H, Talbot M, Caillou B, Dupuy C, Virion A, De Vathaire F, Schlumberger M. Poorly differentiated follicular thyroid carcinoma: prognostic factors and relevance of histological classification. Thyroid 2007;17:639-46.
- Puré E, Cuff CA. A crucial role for CD44 in inflammation. Trends Mol Med. 2001 May;7(5):213-21.
- Ramnath N, Creaven PJ. Matrix metalloproteinase inhibitors. Curr Oncol Rep. 2004 Mar;6(2):96-102.
- recoGreco A, Roccato E, Pierotti MA. TRK oncogenes in papillary thyroid carcinoma. Cancer Treat Res. 2004;122:207-19.

- Riesco-Eizaguirre G, Gutiérrez-Martínez P, García-Cabezas MA, Nistal M, Santisteban P. The oncogene BRAF V600E is associated with a high risk of recurrence and less differentiated papillary thyroid carcinoma due to the impairment of Na+/I- targeting to the membrane. Endocr Relat Cancer 2006;13:257-69.
- Romei C, Ciampi R, Faviana P, Agate L, Molinaro E, Bottici V, Basolo F, Miccoli P, Pacini F, Pinchera A, Elisei R. BRAFV600E mutation, but not RET/PTC rearrangements, is correlated with a lower expression of both thyroperoxidase and sodium iodide symporter genes in papillary thyroid cancer. Endocr Relat Cancer. 2008 Jun;15(2):511-20.
- Rossi DL, Acebrón A, Santisteban P. Function of the homeo and paired domain proteins TTF-1 and Pax-8 in thyroid cell proliferation. J Biol Chem. 1995 Sep 29;270(39):23139-42.
- Ruiz P, Schwärzler C, Günthert U. CD44 isoforms during differentiation and development. Bioessays. 1995 Jan;17(1):17-24.
- Salvatore G, Nappi TC, Salerno P, Jiang Y, Garbi C, Ugolini C, Miccoli P, Basolo F, Castellone MD, Cirafici AM, Melillo RM, Fusco A, Bittner ML, Santoro M. A cell proliferation and chromosomal instability signature in anaplastic thyroid carcinoma. Cancer Res. 2007 Nov 1;67(21):10148-58.
- Santoro M, Carlomagno F, Romano A, Bottaro DP, Dathan NA, Grieco M, Fusco A, Vecchio G, Matoskova B, Kraus MH, *et al.* Activation of RET as a dominant transforming gene by germline mutations of MEN2A and MEN2B. Science 1995;267:381-3.
- Santoro M, Carlomagno F. Drug insight: Small-molecule inhibitors of protein kinases in the treatment of thyroid cancer. Nat Clin Pract Endocrinol Metab. 2006 Jan;2(1):42-52.
- Santoro M, Chiappetta G, Cerrato A, Salvatore D, Zhang L, Manzo G, Picone A, Portella G, Santelli G, Vecchio G, Fusco A. Development of thyroid papillary carcinomas secondary to tissue-specific expression of the RET/PTC1 oncogene in transgenic mice. Oncogene 1996;12:1821-1826.
- Santoro M, Dathan NA, Berlingieri MT, Borganzone I, Paulin C, Grieco M, Pierotti MA, Vecchio G, Fusco A. Molecular characterization of RET/PTC3; a novel rearranged version of the RET proto-oncogene in human thyroid papillary carcinoma. Oncogene 1994;9:509-516.
- Santoro M, Melillo RM, Carlomagno F, Vechio G, Fusco A. Minireview: RET: normal and abnormal functions. Endocrinology 2004;145:5448-51.
- Santoro M, Melillo RM, Grieco M, Berlingieri MT, Vecchio G, Fusco A. The TRK and RET tyrosine kinase oncogenes cooperate with ras in the neoplastic transformation of a rat thyroid epithelial cell line. Cell Growth Differ. 1993 Feb;4(2):77-84.
- Schlumberger M, Carlomagno F, Baudin E, Bidart JM, Santoro M. New therapeutic approaches to treat medullary thyroid carcinoma. Nat Clin Pract Endocrinol Metab. 2008 Jan;4(1):22-32.
- Schlumberger MJ. Papillary and follicular thyroid carcinoma. N Engl J Med 1998;338:297-306.
- Schweppe RE, Klopper JP, Korch C, Pugazhenthi U, Benezra M, Knauf JA, Fagin JA, Marlow LA, Copland JA, Smallridge RC, Haugen BR. Deoxyribonucleic Acid profiling analysis of 40 human thyroid cancer cell lines reveals cross-contamination resulting in cell line redundancy and misidentification. J Clin Endocrinol Metab. 2008 Nov;93(11):4331-41.
- Screaton GR, Bell MV, Jackson DG, Cornelis FB, Gerth U, Bell JI. Genomic structure of DNA encoding the lymphocyte homing receptor CD44 reveals at least 12 alternatively spliced exons. Proc Natl Acad Sci U S A. 1992 Dec 15;89(24):12160-4.

- Segouffin-Cariou C, Billaud M. Transforming ability of MEN2A-RET requires activation of the phosphatidylinositol 3-kinase/AKT signaling pathway. J Biol Chem 2000;275:3568-76.
- Selkoe DJ. Biochemistry and Molecular Biology of Amyloid beta-Protein and the Mechanism of Alzheimer's Disease. Handb Clin Neurol. 2008;89:245-60.
- Seth A, Gote L, Nagarkatti M, Nagarkatti PS. T-cell-receptor-independent activation of cytolytic activity of cytotoxic T lymphocytes mediated through CD44 and gp90MEL-14. Proc Natl Acad Sci U S A. 1991 Sep 1;88(17):7877-81.
- Shaywitz AJ, Greenberg ME.CREB: a stimulus-induced transcription factor activated by a diverse array of extracellular signals. Annu Rev Biochem. 1999;68:821-61.
- Sherman L, Sleeman J, Dall P, Hekele A, Moll J, Ponta H, Herrlich P. The CD44 proteins in embryonic development and in cancer. Curr Top Microbiol Immunol. 1996;213 (Pt 1):249-69.
- Sherman L, Wainwright D, Ponta H, Herrlich P. A splice variant of CD44 expressed in the apical ectodermal ridge presents fibroblast growth factors to limb mesenchyme and is required for limb outgrowth. Genes Dev. 1998 Apr 1;12(7):1058-71.
- Sherman SI. Thyroid carcinoma. Lancet 2003;361:501-11.
- Shimizu Y, Shaw S. Lymphocyte interactions with extracellular matrix. FASEB J. 1991 Jun;5(9):2292-9.
- Smallridge R, Marlow L, Copland J. Anaplastic thyroid cancer: molecular pathogenesis and emerging therapies. Endocr Relat Cancer. 2008
- Soares P, Trovisco V, Rocha AS, Lima J, Castro P, Preto A, Maximo V, Botelho T, Seruca R, Sobrinho-Simoes M. BRAF mutations and RET/PTC rearrangements are alternative events in the etiopathogenesis of papillary thyroid carcinoma. Oncogene 2003;22:4578-4580.
- Squarize CH, Castilho RM, Sriuranpong V, Pinto DS Jr, Gutkind JS. Molecular cross-talk between the NFkappaB and STAT3 signaling pathways in head and neck squamous cell carcinoma. Neoplasia. 2006 Sep;8(9):733-46.
- Stamenkovic I, Aruffo A, Amiot M, Seed B. The hematopoietic and epithelial forms of CD44 are distinct polypeptides with different adhesion potentials for hyaluronate-bearing cells. EMBO J. 1991 Feb;10(2):343-8.
- Sturgeon C, Clark OH. Familial nonmedullary thyroid cancer. Thyroid. 2005 Jun;15(6):588-93.
- Sugahara KN, Hirata T, Hayasaka H, Stern R, Murai T, Miyasaka M. Tumor cells enhance their own CD44 cleavage and motility by generating hyaluronan fragments. J Biol Chem. 2006 Mar 3;281(9):5861-8. Epub 2005 Dec 29.
- Sugahara KN, Murai T, Nishinakamura H, Kawashima H, Saya H, Miyasaka M. Hyaluronan oligosaccharides induce CD44 cleavage and promote cell migration in CD44-expressing tumor cells.J Biol Chem. 2003 Aug 22;278(34):32259-65. Epub 2003 Jun 11.
- Sugahara KN, Hirata T, Tanaka T, Ogino S, Takeda M, Terasawa H, Shimada I, Tamura J, ten Dam GB, van Kuppevelt TH, Miyasaka M. Chondroitin sulfate E fragments enhance CD44 cleavage and CD44-dependent motility in tumor cells. Cancer Res. 2008 Sep 1;68(17):7191-9.
- Takahashi M, Ritz J, Cooper GM. Activation of a novel human transforming gene, ret, by DNA rearrangement. Cell 1985;42:581-588.
- Tan PH, Santos EB, Rossbach HC, Sandmaier BM. Enhancement of natural killer activity by an antibody to CD44. J Immunol. 1993 Feb 1;150(3):812-20.

- Thomas GA, Bunnell H, Cook HA, Williams ED, Nerovnya A, Cherstvoy ED, Tronko ND, Bogdanova TI, Chiappetta G, Viglietto G, Pentimalli F, Salvatore G, Fusco A, Santoro M, Vecchio G. High prevalence of RET/PTC rearrangements in Ukrainian and Belarussian post-Chernobyl thyroid papillary carcinomas: a strong correlation between RET/PTC3 and the solid-follicular variant. J Clin Endocrinol Metab 1999; 84: 4232-4238.
- Thorne RF, Legg JW, Isacke CM. The role of the CD44 transmembrane and cytoplasmic domains in co-ordinating adhesive and signalling events. J Cell Sci. 2004 Jan 26;117(Pt 3):373-80.
- Trovisco V, Vieira de Castro I, Soares P, Máximo V, Silva P, Magalhães J, Abrosimov A, Guiu XM, Sobrinho-Simões M. BRAF mutations are associated with some histological types of papillary thyroid carcinoma. J Pathol 2004;202:247-51.
- Ugi S, Imamura T, Ricketts W, Olefsky JM. Protein phosphatase 2A forms a molecular complex with Shc and regulates Shc tyrosine phosphorylation and downstream mitogenic signaling. Mol Cell Biol. 2002 Apr;22(7):2375-87.
- Ugolini C, Giannini R, Lupi C, Salvatore G, Miccoli P, Proietti A, Elisei R, Santoro M, Basolo F. Presence of BRAF V600E in very early stages of papillary thyroid carcinoma. Thyroid 2007;17:381-8.
- Van Renterghem P, Vassart G, Christophe D. Pax 8 expression in primary cultured dog thyrocyte is increased by cyclic AMP. Biochim Biophys Acta. 1996 Jun 3;1307(1):97-103.
- Vitagliano D, Carlomagno F, Motti ML, Viglietto G, Nikiforov YE, Nikiforova MN, Hershman JM, Ryan AJ, Fusco A, Melillo RM, Santoro M. Regulation of p27Kip1 protein levels contributes to mitogenic effects of the RET/PTC kinase in thyroid carcinoma cells. Cancer Res 2004;64:3823-9.
- Volante M, Collini P, Nikiforov YE, Sakamoto A, Kakudo K, Katoh R, Lloyd RV, LiVolsi VA, Papotti M, Sobrinho-Simoes M, Bussolati G, Rosai J. Poorly differentiated thyroid carcinoma: the Turin proposal for the use of uniform diagnostic criteria and an algorithmic diagnostic approach. Am J Surg Pathol. 2007 Aug;31(8):1256-64.
- Volpato CB, Martínez-Alfaro M, Corvi R, Gabus C, Sauvaigo S, Ferrari P, Bonora E, De Grandi A, Romeo G. Enhanced sensitivity of the RET proto-oncogene to ionizing radiation in vitro. Cancer Res. 2008 Nov 1;68(21):8986-92.
- Wadzinski BE, Wheat WH, Jaspers S, Peruski LF Jr, Lickteig RL, Johnson GL, Klemm DJ. Nuclear protein phosphatase 2A dephosphorylates protein kinase A-phosphorylated CREB and regulates CREB transcriptional stimulation. Mol Cell Biol. 1993 May;13(5):2822-34.
- Wan PT, Garnett MJ, Roe SM, Lee S, Niculescu-Duvaz D, Good VM, Jones CM, Marshall CJ, Springer CJ, Barford D, Marais R. Mechanism of activation of the RAF-ERK signaling pathway by oncogenic mutations of B-RAF. Cell 2004;116:855-867.
- Wang W Functional studies of adhesion molecules on CD4-CD8- double negative T cells of autoimmune MRL/Mp-lpr/mice. Hokkaido Igaku Zasshi. 1993 Sep;68(5):755-66.
- Wayner EA, Carter WG, Piotrowicz RS, Kunicki TJ. The function of multiple extracellular matrix receptors in mediating cell adhesion to extracellular matrix: preparation of monoclonal antibodies to the fibronectin receptor that specifically inhibit cell adhesion to fibronectin and react with platelet glycoproteins Ic-IIa. J Cell Biol. 1988 Nov;107(5):1881-91.
- Weinberg RA. p53 and apoptosis: master guardian and executioner. In: Weinberg RA. The biology of cancer. New York: Garland Science, Taylor & Francis group; 2007. p. 307-356.
- Wellbrock C, Karasarides M, Marais R. Tha RAF take center stage. Nat Rev Mol Cell Biol 2004;5:875-885.

- Wheat WH, Roesler WJ, Klemm DJ. Simian virus 40 small tumor antigen inhibits dephosphorylation of protein kinase A-phosphorylated CREB and regulates CREB transcriptional stimulation. Mol Cell Biol. 1994 Sep;14(9):5881-90.
- Williams D. Cancer after nuclear fallout: lessons from the Chernobyl accident. Nat Rev Cancer. 2002 Jul;2(7):543-9.
- Wittig BM, Johansson B, Zöller M, Schwärzler C, Günthert U. Abrogation of experimental colitis correlates with increased apoptosis in mice deficient for CD44 variant exon 7 (CD44v7). J Exp Med. 2000 Jun 19;191(12):2053-64.
- Woloshin PI, Walton KM, Rehfuss RP, Goodman RH, Cone RD. 3',5'-cyclic adenosine monophosphate-regulated enhancer binding (CREB) activity is required for normal growth and differentiated phenotype in the FRTL5 thyroid follicular cell line. Mol Endocrinol. 1992 Oct;6(10):1725-33.
- Wu G, Mambo E, Guo Z, Hu S, Huang X, Gollin SM, Trink B, Ladenson PW, Sidransky D, Xing M. Uncommon mutation, but common amplifications, of the PIK3CA gene in thyroid tumors. J Clin Endocrinol Metab 2005;90:4688-93.
- Xing M, Westra WH, Tufano RP, Cohen Y, Rosenbaum E, Rhoden KJ, Carson KA, Vasko V, Larin A, Tallini G, Tolaney S, Holt EH, Hui P, Umbricht CB, Basaria S, Ewertz M, Tufaro AP, Califano JA, Ringel MD, Zeiger MA, Sidransky D, Ladenson PW. BRAF mutation predicts a poorer clinical prognosis for papillary thyroid cancer. J Clin Endocrinol Metab 2005;90:6373-9.
- Xing M. BRAF mutation in papillary thyroid cancer: pathogenic role, molecular bases, and clinical implications. Endocr Rev. 2007 Dec;28(7):742-62.
- Yang H, Binns RM. CD44 is involved in porcine natural cytotoxicity. Cell Immunol. 1993 Jul;149(2):227-36.
- Yang T, Namba H, Hara T, Takmura N, Nagayama Y, Fukata S, Ishikawa N, Kuma K, Ito K, Yamashita S. p53 induced by ionizing radiation mediates DNA end-jointing activity, but not apoptosis of thyroid cells. Oncogene. 1997 Apr 3;14(13):1511-9.
- Yasuda M, Nakano K, Yasumoto K, Tanaka Y. CD44: functional relevance to inflammation and malignancy. Histol Histopathol. 2002;17(3):945-50.
- Zhang X, Odom DT, Koo SH, Conkright MD, Canettieri G, Best J, Chen H, Jenner R, Herbolsheimer E, Jacobsen E, Kadam S, Ecker JR, Emerson B, Hogenesch JB, Unterman T, Young RA, Montminy M. Genome-wide analysis of cAMP-response element binding protein occupancy, phosphorylation, and target gene activation in human tissues. Proc Natl Acad Sci U S A. 2005 Mar 22;102(12):4459-64.
- Zhu Z, Gandhi M, Nikiforova MN, Fischer AH, Nikiforov YE. Molecular profile and clinical-pathologic features of the follicular variant of papillary thyroid carcinoma. An unusually high prevalence of ras mutations. Am J Clin Pathol. 2003 Jul;120(1):71-7.

Attached manuscript #II

De Falco V, Giannini R, **Tamburrino A**, Ugolini C, Lupi C, Puxeddu E, Santoro M, Basolo F.

Functional Characterization of the Novel T599I-VKSRdel BRAF Mutation in a Follicular Variant Papillary Thyroid Carcinoma.

J Clin Endocrinol Metab. 2008 Nov;93(11):4398-402.

Functional Characterization of the Novel T599I-VKSRdel BRAF Mutation in a Follicular Variant Papillary Thyroid Carcinoma

Valentina De Falco, Riccardo Giannini, Anna Tamburrino, Clara Ugolini, Cristiana Lupi, Efisio Puxeddu, Massimo Santoro, and Fulvio Basolo

Istituto di Endocrinologia ed Oncologia Sperimentale del CNR (V.D.F., A.T., M.S.), Dipartimento di Biologia e Patologia Cellulare e Molecolare, Università di Napoli Federico II, 80131 Naples, Italy; Department of Surgery (R.G., C.U., C.L., F.B.), University of Pisa, 56127 Pisa, Italy; and Dipartimento di Medicina Interna (E.P.), Università degli Studi di Perugia, 06123 Perugia, Italy

Context: Mutations in BRAF are rare in the follicular variant of papillary thyroid carcinoma (FV-PTC).

Objective: We identified and functionally characterized a novel T599I-VKSR(600–603)del BRAF mutation in a FV-PTC patient. We analyzed *in vitro* the effects of this novel mutation in comparison with other thyroid cancer-associated mutations.

Design: Expression vectors for the BRAF mutants were generated and their *in vitro* kinase activity, signaling along the MAPK pathway, and capability of stimulating transcription from an AP1-responsive reporter evaluated.

Results: BRAF kinase and signaling were increased to a similar extent by the T599I-VKSR (600–603)del, V600E, and K601E mutations. Instead, the G474R, a mutation previously found in a FV-PTC, knocked down the BRAF kinase and its intracellular signaling. Some cancer-associated low-activity BRAF mutants stimulate the MAPK cascade via CRAF; however, the G474R protein lacked also this property.

Conclusion: The T599I-VKSR(600–603)del is a novel gain-of-function mutation that targets BRAF in FV-PTC. Moreover, G474R is the first example of a mutation knocking down enzymatic BRAF activity in a FV-PTC. These findings underscore the importance of functional studies to characterize the role of BRAF mutations associated with thyroid cancer. **(*J Clin Endocrinol Metab* 93: 4398–4402, 2008)**

Point mutations in BRAF are the most common genetic event in papillary thyroid carcinoma (PTC) and can initiate thyroid carcinogenesis *in vivo* (1–4). V600E is the most frequent mutation in thyroid cancer. Less frequent are the K601E (5), V599ins (6), G474R (7), and G469R (8) point mutations as well as complex genetic alterations such as the AKAP9-BRAF rearrangement (9), the V600E-K601del (10, 11), and V600D-FLAGT601–605ins (12).

There are three main PTC subtypes: the tall cell variant (TCV)-PTC, conventional variant (CV)-PTC, and follicular variant (FV)-PTC. BRAF is mutated in about 77% of TCV-PTC cases, in 60% of CV-PTC cases, and in only 12% of FV-PTC cases (3). Moreover, there is an association between PTC subtypes and particular BRAF mutations. Although V600E accounts for most BRAF-mutated cases of CV-PTC and TCV-PTC, mutants K601E (7% of patients) and G474R (in only one patient) are associated with FV-PTC (3, 5, 7, 13).

Under basal conditions, hydrophobic interactions between the activation loop (A-loop), in the C-lobe, and the glycine-rich phosphate-binding loop (P-loop), in the N-lobe, of the BRAF kinase stabilize its inactive conformation. Oncogenic mutations mostly cluster at the A- and P-loops and destabilize the inactive

0021-972X/08/$15.00/0

Printed in U.S.A.

doi: 10.1210/jc.2008-0887 Received April 23, 2008. Accepted August 1, 2008.

First Published Online August 12, 2008

Abbreviations: A-loop, Activation loop; CV, conventional variant; FV, follicular variant; MEK, MAPK kinase; P-loop, phosphate-binding loop; PTC, papillary thyroid carcinoma; TCV, tall cell variant.

conformation, thereby promoting constitutive activity of the enzyme (14). Functionally, cancer-associated BRAF mutants can be divided into three categories: high activity (exemplified by V600E in the A-loop), low activity (exemplified by G466E/V in the P-loop and G596R in the A-loop), and rare impaired activity (exemplified by D594V in the A-loop) (14, 15). These mutants differ in the extent and mechanism of MAPK kinase (MEK), the BRAF downstream kinase, activation. Low-activity mutants, which have impaired MEK kinase activity, can activate MEK indirectly by binding and allosterically activating CRAF. High-activity BRAF mutants signal directly to MEK (although they can also activate MEK through CRAF). No effect has yet been ascribed to impaired-activity BRAF mutants (14, 15).

Patients and Methods

Thyroid sample

The patient (a 23-yr-old woman) had a 2-cm thyroid nodule and was treated at the Institute of Endocrinology of the University of Pisa with Ethics Committee approval (16). Histological diagnosis, encapsulated FV-PTC stage pT1NxMx with a neoplastic blood embolus, was made in a blinded fashion by two pathologists (C.U. and F.B.) according to the World Health Organization guidelines (17). She belonged to a series of 500 PTC patients treated at the same institution (16). Among these samples, 230 were micro-PTC, 82 were CV-PTC, 114 were FV-PTC, 40 were TCV-PTC, and 34 belonged to other variants; 219 and three of the PTC samples of this series had the V600E or the K601E mutation, respectively. The BRAF mutant cases were 90 micro-PTC, 56 CV-PTC, 32 TCV-PTC, 21 FV-PTC, and 15 other subtypes. The K601E mutation was found in one FV-PTC and in two micro-PTC with a FV-PTC pattern (16).

Detection of BRAF mutation

DNA was isolated by using QIAGEN spin columns (QIAGEN GmbH, Hilden, Germany) and processed for PCR amplification. Single-strand conformation polymorphism and sequencing were carried out as described elsewhere (16).

Expression vectors and cell transfections

BRAF and CRAF expression vectors were kindly donated by C. J. Marshall. The T599I-VKSRdel mutant was generated by PCR. The thyroid cancer-associated (V600E, G474R, and K601E), the melanoma-associated (G596R), and the kinase-dead K483M (BRAF K-) BRAF constructs were obtained by site-directed mutagenesis (Stratagene, La Jolla, CA). The constructs were myc-tagged and cloned in the pEF vector. The mutations were confirmed by DNA sequencing. HEK293 cells were grown in DMEM supplemented with 10% fetal calf serum (Invitrogen, Carlsbad, CA). PC Cl 3 (hereafter referred to as PC), a differentiated rat thyroid follicular cell line, was cultured in Coon's modified Ham F12 medium supplemented with 5% calf serum and a mixture of six hormones (6H), including TSH as described (18). Transfections were carried out with the Lipofectamine reagent according to the manufacturer's instructions (GIBCO, Paisley, PA). In HEK293, green fluorescent protein transfection was used to measure transfection efficacy (about 30%).

Protein studies

Immunoblotting experiments were performed according to standard procedures. Signal intensity was evaluated with the Phosphorimager (Typhoon 8600; Amersham Pharmacia Biotech, Little Chalfont, UK) interfaced with the ImageQuant software. Anti-phospho-p44/42 MAPK (9102), anti-p44/42 MAPK (9101), anti-phospho-p90RSK (90-kDa ribosomal S6 kinase) (9344), anti-p90RSK (9347), anti-phospho-MEK1/2 (MAPK 1 and 2) (9121), and anti-MEK1/2 (9122) were from Cell Signaling (Beverly, MA). Anti-BRAF (sc-9002) was from Santa Cruz Biotechnology (Santa Cruz, CA). Monoclonal anti-α-tubulin was from Sigma Chemical Co. (St. Louis, MO). Secondary antibodies coupled to horseradish peroxidase were from Santa Cruz Biotechnology. For the BRAF kinase assay, HEK293 cells were transiently transfected with the indicated constructs, cultured for 18 h in serum-deprived medium, and harvested 48 h after transfection. BRAF kinase was immunoprecipitated with anti-myc and resuspended in a kinase buffer containing 100 mM $MgCl_2$, 20 μM ATP, and 0.5 μg recombinant glutathione S-transferase-MEK. After 15 min incubation at 30 C, reactions were stopped by adding 2× Laemmli buffer. Proteins were then subjected to 10% SDS-PAGE and immunoblotted with anti-phospho-MEK1/2 antibody. Immunoblots with anti-MEK antibodies served as loading controls.

Luciferase assays

HEK293 cells were transiently transfected with BRAF vectors and the AP1-Luc reporter containing six AP1 binding sites upstream from the *Firefly* luciferase cDNA (Stratagene, Garden Grove, CA). Twenty-four hours after transfection, cells were serum starved and harvested 48 h after transfection. Ten nanograms of pRL-null (a plasmid expressing the enzyme *Renilla* luciferase from *Renilla reniformis*) were used for normalization. *Firefly* and *Renilla* luciferase activities were assayed using the Dual-Luciferase reporter system (Promega Corp., Madison, WI) in protein extracts normalized for equal level expression of the BRAF constructs and expressed as fold increase with respect to empty vector-transfected cells. Average results of three independent assays ± SD are indicated.

Statistical analysis

The two-tailed unpaired Student's *t* test (normal distributions and equal variances) was used for statistical analysis (GraphPad InStat software program, version 3.06.3; GraphPad, San Diego, CA). Differences were significant when $P < 0.001$.

Results

Identification of the T599I-VKSRdel mutation in BRAF

We identified a novel BRAF mutation in a FV-PTC (Fig. 1A). The mutation was a heterozygous 14-bp deletion with a 2-bp insertion. This resulted in a complex amino acid change consisting in replacement of threonine 599 with isoleucine and deletion of valine 600, lysine 601, serine 602, and arginine 603 [T599I-VKSR (600–603)del, abbreviated to T599I-VKSRdel] (Fig. 1, B and C).

Functional characterization of the T599I-VKSRdel mutation

After being phosphorylated by RAF kinases at serine 217 and 221, MEK1/2 phosphorylates threonine 202 and tyrosine 204 of p44 and p42 MAPK (ERK1 and 2). In turn, p90RSK is a p44/p42 MAPK substrate. We transiently expressed the BRAF T599I-VKSRdel mutant and other BRAF alleles previously identified in thyroid carcinoma (V600E, K601E, and G474R) in HEK293 and evaluated their effect on the MAPK cascade using immunoblotting with phosphospecific antibodies. Forty-eight hours after transfection, V600E, K601E, and T599I-VKSRdel expression resulted in higher phosphorylation levels of MEK1/2 (2.8-, 2.4-, and 4-fold, respectively), p44/42 MAPK (3-, 2.5-, and 3-fold,

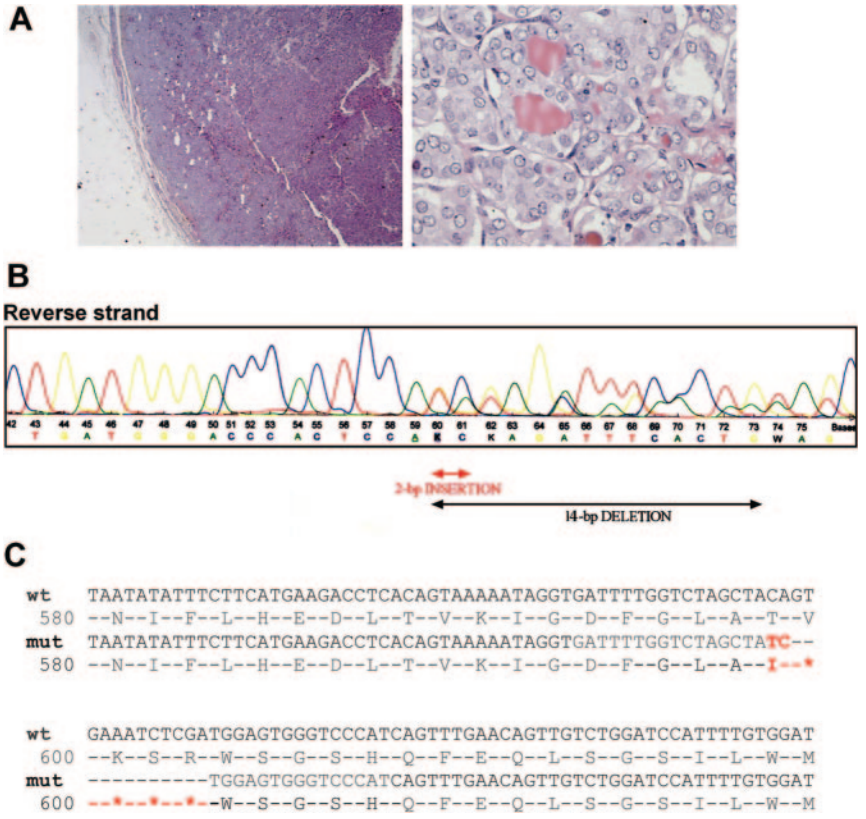

FIG. 1. A, Representative hematoxylin- and eosin-stained sections of the FV-PTC at ×1.6 (*left*) and ×40 (*right*) magnification; B, sequence analysis (reverse strand) of the BRAF exon 15 region containing the T599I-VKSR (600–603)del mutation (K represents T/G overlap; W represents T/A overlap); C, partial BRAF exon 15 sequence of the mutated (mut) sample aligned with the wild-type (wt) sequence; mutated residues are in *bold*, and deleted residues are marked with an *asterisk*.

respectively), and RSK (3-, 2.7-, and 1.8-fold, respectively) compared with wild-type BRAF ($P < 0.001$) (Fig. 2B). Differently, the activity of G474R was impaired compared with wild-type BRAF (2.5-fold reduction of both phospho-MEK and phospho-MAPK) and virtually indistinguishable from that of kinase-dead BRAF (Fig. 2B). Accordingly, in an *in vitro* immunocomplex phosphorylation assay, V600E, K601E, and T599I-VKSRdel exerted strong kinase activity, whereas G474R exerted no activity (Fig. 2C).

We measured AP1-luciferase stimulation by the various BRAF mutants. As shown in Fig. 2D, V600E, K601E, and T599I-VKSRdel stimulated AP1-Luc by more than 2.5-fold with respect to wild-type BRAF ($P < 0.001$). The difference between them was not significant ($P > 0.01$). Instead, G474R was approximately 50-fold less active than wild-type BRAF ($P < 0.001$) (Fig. 2D).

Although unable to signal to MEK directly, low-activity BRAF mutants (exemplified by G466E/V and G596R) can induce MEK phosphorylation *in trans* by allosterically activating CRAF. We tested whether G474R retained the ability to cooperate with CRAF. G474R was coexpressed in HEK293 cells in combination with a suboptimal CRAF dose, which alone is unable to stimulate MAPK. The G596R mutant, previously reported to activate MEK through CRAF (14, 15), was used as control. Overexpressed wild-type BRAF exerted modest levels of MEK stimulation that was not further potentiated by CRAF (Fig. 2E). G596R, although inactive alone, triggered MEK and MAPK phosphorylation in the presence of CRAF. G474R was not able to active the MEK/ERK pathway also when coexpressed with CRAF (Fig. 2E).

BRAF V600E drives TSH-independent proliferation of thyroid PC cells (18). Thus, equal numbers (25,000) of marker-selected PC cells transfected with V600E, T599I-VKSRdel, or G474R mutants were plated in triplicate in the absence of TSH and counted 7 d later. Empty vector-transfected cells did not proliferate; BRAF(V600E) cells were able to proliferate (cell number increased by 4.5-fold) in the absence of TSH. The BRAF(T599I-VKSRdel) also triggered TSH-independent proliferation (cell numbers increased by 3.5-fold). Although to a lesser extent (2.5-fold), also G474R was able to mediate a modest TSH-independent proliferation.

Discussion

Here we show that the newly identified T599I-VKSRdel mutant activates the kinase function and signaling ability of BRAF. Interestingly, while this manuscript was under revision, a second patient with the T599I-VKSRdel mutation was found in the frame of a routine analysis for BRAF mutations at the University of Pisa; also in this case (a 46-yr-old women), the tumor sample was a small (T1) encapsulated FV-PTC. T599I-VKSRdel targets the A-loop of BRAF, which is also targeted by most activating mutations (V600E, K601E, V599ins, V600E-K601del, and V600D-FLAGT601–605ins). It is likely that all these mutations disturb the interaction +between the A- and P-loops that normally keep BRAF under check, thereby activating its catalytic function (14). In contrast, the other FV-PTC-associated mutant (G474R), targeting the glycine-rich loop, impaired BRAF kinase. G474R has been identified only in one FV-PTC (7), and to the best of our knowledge, it has not been described in other tumor types. It remains unclear whether G474R is only a passenger mutation or whether it signals in a kinase-independent manner through pathway(s) alternative to the MAPK one. The observation that *in vitro* G474R is able to drive, albeit at low levels, TSH-independent thyroid cell proliferation suggests that it may contribute to thyroid tumorigenesis in a kinase-independent manner. *In vivo* experiments may help to address this issue.

In conclusion, the identification of T599I-VKSRdel confirms that FV-PTC often harbor BRAF mutations other than the classic V600E one, information to be taken into account to optimize the search of BRAF mutations in thyroid cancer patients.

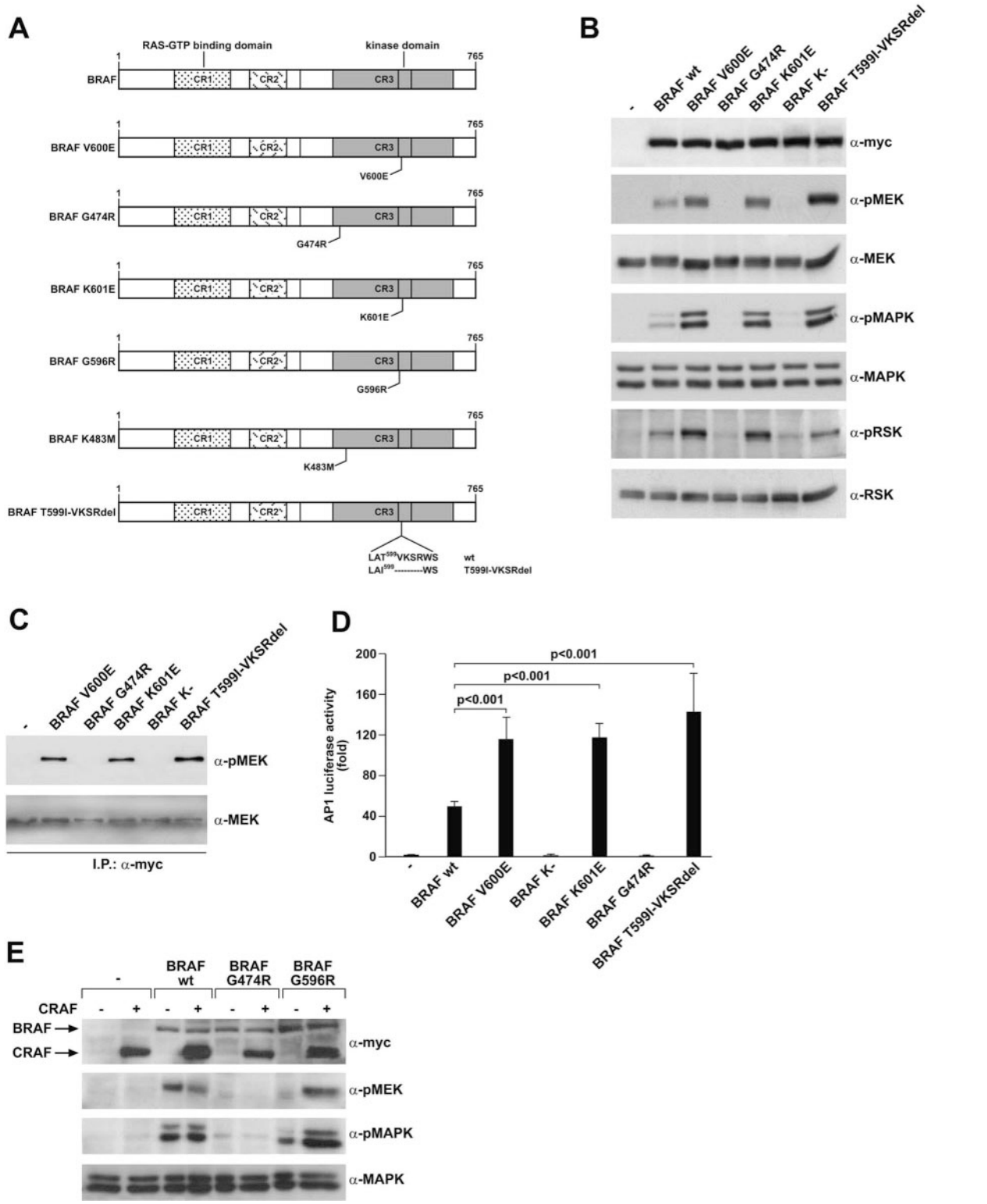

FIG. 2. A, Schematic representation of the BRAF protein structure and the various mutants used in this study. CR1, -2, and -3 represent conserved regions; CR3 is a kinase domain; A represents an activation loop. B, HEK293 cells expressing the indicated BRAF mutants were kept in serum-deprived medium (18 h) and harvested. Total cell lysates (50 μg) were immunoblotted with the indicated phosphospecific antibodies. Total amounts of MEK, MAPK, and RSK are shown for normalization. The results were quantified at the Phosphorimager. Data are representative of at least three different experiments. C, Protein lysates (500 μg) were immunoprecipitated with anti-BRAF and subjected to a kinase assay with recombinant glutathione S-transferase-MEK. Data are representative of at least three different experiments. D, HEK293 cells were transiently transfected with BRAF mutant-expressing vectors and the AP1-Luc reporter. Average results of three independent Luciferase assays ± SD are expressed as fold increase compared with empty vector-transfected (−) cells. Statistical significance was assessed with the Student's *t* test. E, HEK293 cells expressing the indicated BRAF mutants, and when indicated CRAF, were kept in serum-deprived medium and harvested. Total cell lysates (50 μg) were immunoblotted with the indicated antibodies. Data are representative of at least three different experiments.

Acknowledgments

We thank Jean Ann Gilder for text editing and Ciotola Presentation for the artwork.

Address all correspondence and requests for reprints to: Massimo Santoro, Dipartimento di Biologia e Patologia Cellulare e Molecolare, "L. Califano", Universita' Federico II di Napoli, via S. Pansini 5, 80131 Naples, Italy. E-mail: masantor@unina.it.

This study was supported by the Associazione Italiana per la Ricerca sul Cancro and the Naples Oncogenomic Center and by grants from Italian Ministero della Salute and Ministero dell'Università e della Ricerca.

Disclosure Statement: The authors have declared no conflict of interest.

References

1. **Groussin L, Fagin JA** 2006 Significance of BRAF mutations in papillary thyroid carcinoma: prognostic and therapeutic implications. Nat Clin Pract Endocrinol Metab 2:180–181
2. **Ciampi R, Nikiforov YE** 2007 RET/PTC rearrangements and BRAF mutations in thyroid tumorigenesis. Endocrinology 148:936–941
3. **Xing M** 2007 BRAF mutation in papillary thyroid cancer: pathogenic role, molecular bases, and clinical implications. Endocr Rev 28:742–762
4. **Knauf JA, Ma X, Smith EP, Zhang L, Mitsutake N, Liao XH, Refetoff S, Nikiforov YE, Fagin JA** 2005 Targeted expression of BRAFV600E in thyroid cells of transgenic mice results in papillary thyroid cancers that undergo dedifferentiation. Cancer Res 65:4238–4245
5. **Trovisco V, Vieira de Castro I, Soares P, Máximo V, Silva P, Magalhães J, Abrosimov A, Guiu XM, Sobrinho-Simões M** 2004 BRAF mutations are associated with some histological types of papillary thyroid carcinoma. J Pathol 202:247–251
6. **Moretti S, Macchiarulo A, De Falco V, Avenia N, Barbi F, Carta C, Cavaliere A, Melillo RM, Passeri L, Santeusanio F, Tartaglia M, Santoro M, Puxeddu E** 2006 Biochemical and molecular characterization of the novel BRAF(V599Ins) mutation detected in a classic papillary thyroid carcinoma. Oncogene 25:4235–4240
7. **Castro P, Rebocho AP, Soares RJ, Magalhães J, Roque L, Trovisco V, Vieira de Castro I, Cardoso-de-Oliveira M, Fonseca E, Soares P, Sobrinho-Simões M** 2006 PAX8-PPARγ rearrangement is frequently detected in the follicular variant of papillary thyroid carcinoma. J Clin Endocrinol Metab 91:213–220
8. **Koh CS, Ku JL, Park SY, Kim KH, Choi JS, Kim IJ, Park JH, Oh SK, Chung JK, Lee JH, Kim WH, Kim CW, Cho BY, Park JG** 2007 Establishment and characterization of cell lines from three human thyroid carcinomas: responses to all-*trans*-retinoic acid and mutations in the BRAF gene. Mol Cell Endocrinol 264:118–127
9. **Ciampi R, Knauf JA, Kerler R, Gandhi M, Zhu Z, Nikiforova MN, Rabes HM, Fagin JA, Nikiforov YE** 2005 Oncogenic AKAP9-BRAF fusion is a novel mechanism of MAPK pathway activation in thyroid cancer. J Clin Invest 115:94–101
10. **Oler G, Ebina KN, Michaluart Jr P, Kimura ET, Cerutti J** 2005 Investigation of BRAF mutation in a series of papillary thyroid carcinoma and matched-lymph node metastasis reveals a new mutation in metastasis. Clin Endocrinol (Oxf) 62:509–511
11. **Trovisco V, Soares P, Soares R, Magalhaes J, Sa-Couto P, Sobrinho-Simoes M** 2005 A new BRAF gene mutation detected in a case of a solid variant of papillary thyroid carcinoma. Hum Pathol 36:694–697
12. **Hou P, Liu D, Xing M** 2007 Functional characterization of the T1799–1801del and A1799–1816ins BRAF mutations in papillary thyroid cancer. Cell Cycle 6:377–379
13. **Trovisco V, Soares P, Sobrinho-Simões M** 2006 B-RAF mutations in the etiopathogenesis, diagnosis, and prognosis of thyroid carcinomas. Hum Pathol 37:781–786
14. **Wan PT, Garnett MJ, Roe SM, Lee S, Niculescu-Duvaz D, Good VM, Jones CM, Marshall CJ, Springer CJ, Barford D, Marais R** 2004 Mechanism of activation of the RAF-ERK signaling pathway by oncogenic mutations of B-RAF. Cancer Genome Project. Cell 116:855–867
15. **Garnett MJ, Rana S, Paterson H, Barford D, Marais R** 2005 Wild-type and mutant B-RAF activate C-RAF through distinct mechanisms involving heterodimerization. Mol Cell 20:963–969
16. **Lupi C, Giannini R, Ugolini C, Proietti A, Berti P, Minuto M, Materazzi G, Elisei R, Santoro M, Miccoli P, Basolo F** 2007 Association of BRAF V600E mutation with poor clinicopathological outcomes in 500 consecutive cases of papillary thyroid carcinoma. J Clin Endocrinol Metab 92:4085–4090
17. **Hedinger C, Williams ED, Sobin LH** 1989 The WHO histological classification of thyroid tumors: a commentary on the second edition. Cancer 63:908–911
18. **Melillo RM, Castellone MD, Guarino V, De Falco V, Cirafici AM, Salvatore G, Caiazzo F, Basolo F, Giannini R, Kruhoffer M, Orntoft T, Fusco A, Santoro M** 2005 The RET/PTC-RAS-BRAF linear signaling cascade mediates the motile and mitogenic phenotype of thyroid cancer cells. J Clin Invest 115: 1068–1081

Attached manuscript #III

Paolo Salerno, Valentina De Falco, **Anna Tamburrino**, Tito Claudio Nappi, Giancarlo Vecchio, Gideon E. Bollag, Massimo Santoro, Giuliana Salvatore.

Cytostatic activity of PLX4032 and PLX4720 BRAF ATP-competitive inhibitors in BRAF mutant thyroid carcinoma cells.

Manuscript submitted

Cytostatic activity of PLX4032 and PLX4720 BRAF ATP-competitive inhibitors in BRAF mutant thyroid carcinoma cells

Paolo Salerno, Valentina De Falco, **Anna Tamburrino**, Tito Claudio Nappi, Giancarlo Vecchio, Manikandan Mayakannan, Gideon E. Bollag, Massimo Santoro, Giuliana Salvatore.

Dipartimento di Biologia e Patologia Cellulare e Molecolare c/o Istituto di Endocrinologia ed Oncologia Sperimentale CNR, Universita' "Federico II", Naples, 80131, Italy (PS, VDF, AT, TCN, GV, MM, MS); Plexxikon, Inc., 91 Bolivar Drive, Berkeley, CA 94710 (GEB). Dipartimento di Studi delle Istituzioni e dei Sistemi Territoriali, Universita' "Parthenope", Naples, 80133, Italy (GS).

Abbreviated title: PLX4032/PLX4720 effects on thyroid carcinoma cells

Key words: BRAF, thyroid carcinoma, kinase inhibitor, targeted therapy

Corresponding author: Massimo Santoro, Dipartimento di Biologia e Patologia Cellulare e Molecolare, "L. Califano", Università Federico II di Napoli, via S. Pansini 5, 80131 Naples, Italy. Ph: +39-081-7463056; Fax: +39-081-7463037; E-mail: masantor@unina.it

Abstract

Context: BRAF activating mutations are prevalent in papillary and anaplastic thyroid carcinoma**.** The V600E mutation accounts for the vast majority of thyroid carcinoma-associated BRAF mutations. **Objective**: To study the effects of two BRAF ATP-competitive kinase inhibitors, PLX4032 and PLX4720, in thyroid carcinoma cell lines. **Experimental design**: We examined PLX4032 and PLX4720 activity in thyroid carcinoma cell lines (8505C, FB1, BCPAP, SW1736) harboring BRAF V600E oncogene. Normal thyrocytes (PC Cl 3) were used as control. **Results:** Extracellular regulated kinases (ERK) were de-phosphorylated upon PLX4032 and PLX4720 treatment in thyroid carcinoma cells and not in normal thyroid cells. PLX4720 inhibited the proliferation of BRAF mutant cell lines with a half maximal effective concentration (EC_{50}) ranging from 94 (FB1 cells) to 113 (BCPAP cells) nM. PLX4032 EC_{50} ranged from 29 (SW1736 cells) to 78 (BCPAP cells) nM. Importantly, PLX4032 and PLX4720 exerted potent cytostatic effects on carcinoma cell lines, but not in normal thyroid follicular cells. Furthermore, PLX4032 and PLX4720 treatment induced a block in the G1-S transition of the cell cycle and an altered expression of genes involved in the control of cell-cycle progression. These effects were observed also with a MEK inhibitor, PD0325901, indicating they are indeed mediated by ERK pathway inhibition. **Conclusions**: This study provides additional evidence of the potential efficacy of BRAF targeting in BRAF mutant thyroid carcinoma cells.

Introduction

Thyroid cancer incidence has increased significantly during the past decades and it has become one of the ten leading cancer types in female (1). In general, well-differentiated papillary carcinomas (PTC) are curable with total thyroidectomy, ablative doses of radioiodine and thyroid suppressive treatment. However, there is still no effective systemic treatment for PTC patients if their disease does not concentrate radioiodine. Finally, anaplastic thyroid carcinoma (ATC) is a very rare thyroid tumor with a dismal prognosis (2). Thyroid carcinomas are often associated to oncogenic conversion of proteins acting in the ERK cascade. In particular, BRAF mutation has emerged as the most frequent genetic lesion of thyroid carcinoma, identified in 44% of PTC and 25% of ATC samples. The T1799A transversion, leading to V600E amino acid substitution accounts for the vast majority of these cases (3-6).

Several small-molecule RAF kinase inhibitors are being developed. Among these, Sorafenib (BAY 43-9006) is a multitarget ATP competitive inhibitor that, *in vitro,* inhibits RAF kinases and a set of tyrosine kinases. Results from a phase II clinical trial of sorafenib in advanced thyroid cancer have been recently reported (7, 8). RAF (9) and MEK (10-13) kinase targeting with different compounds (AAL-881 and LBT-613 for RAF and PD0325901, CI-1040, and AZD6244 for MEK) also proved efficacy in thyroid carcinoma cell models. Importantly, BRAF mutation was demonstrated to be a molecular determinant of high MEK blockade responsiveness (9-13). Recently, a 7-azaindole, named PLX4720, was discovered as a novel selective inhibitor of RAF kinases (14). PLX4720 inhibited BRAF V600E with a half maximal inhibitory concentration (IC_{50}) of 13 nM. It also inhibited mutant (Y340D and Y341D) CRAF with an IC_{50} of 6.7 nM. Importantly, the compound inhibited less efficiently wild type BRAF (10-fold higher concentration than BRAF V600E) and was selective against a panel of 70 kinases. A related compound, PLX4032, also selectively targeted BRAF V600E (IC_{50} = 44

nM); besides BRAF, only BRK showed PLX4032 inhibition with an IC_{50} = 240 nM out of a series of 65 different kinases (14). Sala and coworkers reported that PLX4032 had modest anti-proliferative effects (IC_{50} > 10,000 nM) in BRAF wild type and RET/PTC1-positive TPC1 thyroid cancer cells, while it was active in BRAF mutant ARO and NPA cells recently reported not to be of thyroid origin (15, 16). Here, we studied the *in vitro* efficacy of PLX4720 and PLX4032 in a panel of thyroid carcinoma cell lines harboring BRAF V600E oncogene and in normal thyroid follicular cells.

Materials and Methods

Reagents-PLX4720 and PLX4032 were provided by Plexxikon, Inc, Berkely, CA, USA. The compounds were dissolved in dimethyl sulfoxide (DMSO) at a concentration of 50 mM. Anti-phospho p44/42 (#9101) specific for MAPK (ERK1/2) phosphorylated at Thr202/Tyr204, anti-p44/42 MAPK (#9102), anti-phospho MEK1/2 (#9121) specific for MEK1/2 phosphorylated at Ser217/Ser221 and anti-MEK1/2 (#9122) antibodies were from Cell Signaling (Beverly, MA), anti-BRAF (sc-9002) antibody was from Santa Cruz Biotechnology (Santa Cruz).

Cell cultures-The human thyroid carcinoma cell lines 8505C, FB1, SW1736 and BCPAP were grown in Dulbecco's modified Eagle's medium (DMEM) (Invitrogen, Groningen, The Netherlands) containing 10% fetal bovine serum. The Fischer rat-derived differentiated thyroid follicular cell line PC Cl 3 (hereafter referred as “PC”) was grown in Coon’s modified Ham F12 medium supplemented with 5% calf serum and a mixture of six hormones (6H) (Sigma Chemical Co., St. Louis, MO).

Cell proliferation-For cell proliferation assay, $5x10^4$ cells were plated in 35-mm dishes in low serum (2.5% for carcinoma cell lines, 1.25% for normal rat cells). The day after plating, compounds or vehicle were added. The medium was changed every 2 days and cells were counted in triplicate every day. Cell counts after 96 hours treatment were used for half maximal effective concentrations (EC_{50}) calculation (Graph Pad InStat software program, version 3.06.3, San Diego, CA).

Cell cycle analysis- $5x10^5$ cells were plated in 100-mm dishes in low serum. The day after plating, compounds or vehicle were added; at the indicated time intervals, cells were harvested and fixed in 70% ethanol for 4 hours. After washing with PBS, cells were treated with RNAse A (100 U/ml) and stained with propidium iodide (25 μg/ml) (Sigma) for 30 min. Samples were analyzed with a CyAn ADP flow cytometer interfaced with the Summit V4.2 software (DakoCytomation, Carpinteria, CO).

Protein studies-Immunoblotting experiments were performed according to standard procedures. Antigens were revealed by an enhanced chemiluminescence detection kit (ECL, Amersham Pharmacia Biotech, Little Chalfort, UK). Signal intensity was evaluated with the Phosphor-imager (Typhoon 8600, Amersham Pharmacia Biotech). For the BRAF kinase assay, cells were cultured for 18 hours in low serum medium, thereafter treated with different concentrations (50 and 500 nM) of PLX4032 for 2 hours. BRAF kinase was immunoprecipitated and resuspended in a kinase buffer containing 100 mM $MgCl_2$, 20 μM ATP and 0.5 μg of recombinant GST-MEK. After 15 min incubation at 30°C, reactions were stopped by adding 2X Laemmli buffer. Proteins were then subjected to 10% SDS gel electrophoresis and immunoblotted with anti-phospho-MEK1/2 antibody. Immunoblots with MEK and BRAF antibodies served, respectively, as loading and immunoprecipitating controls.

RNA extraction and RT-PCR

Total RNA was isolated with the RNeasy Kit (Qiagen, Crawley, West Sussex, UK). One μg of RNA from each sample was reverse-transcribed with the QuantiTect® Reverse Transcription (Qiagen) according to manufacturer's instructions. Expression levels of the cell cycle-related genes: cyclin E1 (CCNE1), cyclin E2 (CCNE2), cyclin D1 (CCND1), cyclin D3 (CCND3), cell

division cycle 25 homolog A (CDC25A), minichromosome maintenance complex component 6 (MCM6), minichromosome maintenance complex component 7 (MCM7), cell division cycle 6 homolog (CDC6), proliferating cell nuclear antigen (PCNA), cyclin-dependent kinase inhibitor 1A (CDKN1A), cyclin-dependent kinase inhibitor 1B (CDKN1B) were measured by quantitative RT-PCR, using the Human ProbeLibray^{TM} system (Exiqon, Denmark). PCR reactions were performed in triplicate and fold changes were calculated using the formula: $2^{-(\text{sample 1 } \Delta Ct - \text{sample 2 } \Delta Ct)}$, where ΔCt is the difference between the amplification fluorescent thresholds of the mRNA of interest and the mRNA of RNA polymerase 2A used as an internal reference. Primers sequences are available upon request.

Statistical analysis-Two-tailed unpaired Student's t test (normal distributions and equal variances) was used for statistical analysis. Differences were significant when $P < 0.05$. Statistical analysis and EC_{50} calculation was performed by using the Graph Pad InStat software program, version 3.06.3, San Diego, CA).

Results

PLX4032 and PLX4720 inhibition of ERK phosphorylation in thyroid carcinoma cells harboring BRAF mutation- BRAF V600E-positive PTC (BCPAP) and ATC (8505C, FB1, SW1736) cell lines were used together with normal PC thyrocytes as control (18). Cells were treated with 50-500 nM doses of PLX4720 and PLX4032 for two hours and p44/p42 ERK (MAPK) phosphorylation measured by immunoblot. Both PLX4720 and PLX4032 inhibited MAPK phosphorylation with an IC_{50} ranging 50-100 nM in BRAF mutant cells; no inhibition was observed in normal cells with compounds concentration up to 500 nM (Fig. 1A).

Accordingly, phosphorylation levels of the downstream effector MEK, were reduced in BRAF mutant cells and not in normal thyrocytes (Fig. 1B, upper panel). To verify whether the reduced phosphorylation of ERK was indeed mediated by BRAF inhibition, we performed an *in vitro* BRAF kinase assay. As shown in Fig. 1B (lower panel), at the dose of 50 nM, PLX4032 inhibited BRAF enzymatic activity in the SW1736 and 8505C cells, while up to 500 nM PLX4032 did not inhibit the wild type BRAF kinase in normal thyroid cells.

PLX4032 and PLX4720 inhibition of cell growth in BRAF V600E-positive thyroid carcinoma cells - Cells were treated with different concentrations of PLX4720, PLX4032 or vehicle (NT) and counted daily for four days. The average results of three independent determinations are reported in Fig. 1C. Treatment with PLX4720 caused a dose-dependent growth inhibition of the BRAF mutant cell lines with EC_{50} of 98 (8505C, SW1736), 94 (FB1) and 113 nM (BCPAP). Similarly, PLX4032 inhibited the proliferation with an EC_{50} of 57 (8505C), 29 (SW1736), 54 (FB1), 78 nM (BCPAP). Importantly, at 1,000 nM the EC_{50} for growth inhibition of normal PC cells was not reached yet (Fig. 1C).

The reduced activity of PLX4032 and PLX4720 on normal thyrocytes could be due to their selectivity for mutant BRAF or the reduced dependence of normal cells on ERK pathway for proliferation or both. To discriminate between these possibilities, we used the MEK inhibitor PD0325901 as an alternative tool for ERK pathway inhibition. As shown in Fig. S1A, PD0325901 efficiently inhibited ERK (MAPK) phosphorylation both in SW1736 and PC cells. Importantly, treatment with the compound caused a dose-dependent growth inhibition of SW1736 cell line with a half maximal efficacy concentration (EC_{50}) of 0.4 nM; while 50% of growth inhibition was observed in normal thyrocytes only at concentrations ≥ 50 nM (Fig.

S1B). These findings indicate that BRAF mutant cancer cells are more dependent on ERK pathway than normal thyrocytes.

Characterization of PLX4032 and PLX4720-mediated cell cycle arrest in thyroid carcinoma cells

To characterize the growth inhibitory effect induced by PLX4720 and PLX4032, we performed flow cytometry analysis in SW1736 and control PC cells. SW1736 underwent a marked G1 arrest, starting at 24 hours (Fig. 2A) and lasting up to 48 hours (not shown), upon PLX4032 and PLX4720 (500 nM) treatment. No increase in the sub G1 fraction was detectable, indicating that the treatment is cytostatic, as reported also previously with other agents targeting the BRAF/MEK pathway in thyroid cancer cells (9-13). Importantly, PLX4032 and PLX4720 treatment (500 nM) did not modify cell cycle profile of normal control cells (Fig. 2A). Consistently, the MEK inhibitor PD0325901 arrested SW1736 cells in G1 phase while it did not affect the cell cycle profile of normal thyroid cells (not shown). Further, to better characterize the G1-S transition block, we analyzed by quantitative RT-PCR the expression levels of cell cycle related genes involved in G1-S transition upon PLX4720 and PLX4032 treatment. PLX4720 and PLX4032 induced respectively a reduction of the mRNA levels of CCND1 (6.1 and 9.5 fold), CCND3 (2.5 and 4.1 fold), CCNE1 (2.3 and 2.7 fold), CCNE2 (8.1 and 12.6 fold), PCNA (3.5 and 4.8 fold), CDC25A (4.1 and 6.4 fold), CDC6 (5.7 and 11.3 fold), MCM6 (2.0 and 3.4 fold) and MCM7 (2.3 and 4.2 fold) at 24 hours upon treatment (Fig. 2B). The reductions started at 6 hours and lasted up to 48 hours upon treatment (Fig. 2B). Moreover, increased mRNA levels of the cyclin-dependent kinase inhibitors CDKN1A (4.0 and 4.2 fold) and CDKN1B (1 and 1.5 fold) was observed after 24 hours of PLX4720 and PLX4032

treatment (Fig. 2B). Similar results were obtained using the MEK inhibitor PD0325901 (Fig. 2B).

Discussion

There is currently no effective systemic treatment for iodine-refractory thyroid carcinoma. Based on the high prevalence and the correlation with high tumor stage, BRAF mutation is a promising molecular target (3-6). Although RNAi-mediated genetic knock-down has provided the proof-of-concept that BRAF targeting may be useful, thus far, chemical inhibition with available agents, given their multitarget activity, could only provide correlative experimental evidence of the validity of the approach (15, 17). Here, we show that PLX4032 and PLX4720 inhibited at nM concentration ERK pathway phosphorylation and growth of cancer cells harboring BRAF mutation.

The refractoriness of normal thyroid cells to PLX4032 and PLX4720 may be explained by the reduced activity of the compounds on wild type BRAF, as demonstrated by BRAF kinase assay, and by the lack of addiction of normal cells on BRAF for their proliferation as demonstrated by the experiments with the MEK inhibitor PD0325901. Solit *et al* and Pratilas first reported selectivity of MEK pathway inhibitors for BRAF mutant cancer cell lines (18, 19).

In conclusion, these *in vitro* data, set the stage for potential clinical assessment of PLX4032 and PLX4720 efficacy in BRAF V600E-positive iodine-refractory thyroid cancer patients and suggest cell cycle G1-S related proteins as potential surrogate markers for ERK pathway inibition monitoring in thyroid cancer cells. It should be noted however that in solid tumors blockade of one single signaling pathway is expected to hardly exert a prominent effect on tumor maintenance. Multiple regulatory circuits have been shown to be elicited secondary to

oncogenic pathways ablation that limit the effectiveness of this approach (20, 21). For instance in thyroid cancer cells, ERK pathway inhibition was followed by downregulation of ERK-specific phosphatases that, in turn, restored the ERK phosphorylation (9). Thus, rather than used as single agents, ERK pathway inhibitors could be used in combination with other targeted inhibitors. MEK inhibitors were recently reported to synergize with AKT/mTOR blockade in prostate cancer (22). Thus, the identification of the pathway whose inhibition synergizes with ERK blockade is the next challenge to develop molecular targeting therapeutic approaches in thyroid cancer.

Figure legends

Fig. 1. PLX4720 and PLX4032 in BRAF V600E-positive thyroid carcinoma cells.

1A) The indicated thyroid cell lines (their BRAF status is indicated) were kept in low serum and treated with increasing concentrations of PLX4720 or PLX4032. Two hours later, cells were lysed and analyzed by Western blotting with phosphospecific antibodies. Antibodies that recognize total amount of the same proteins were used for normalization. **1B**, u**pper panel)** Cells were kept in low serum and treated with increasing concentrations of PLX4032. Two hours later, cells were lysed and analyzed by Western blotting with the indicated antibodies. **1B, lower panel**) Protein lysates (500 μg) were immunoprecipitated with anti-BRAF and subjected to a BRAF kinase assay with recombinant GST-MEK. Data are representative of at least three different experiments. **1C)** The indicated cells ($5x10^4$) were plated in triplicate in 35-mm dishes. One day later, different concentrations of PLX4720, PLX4032 or vehicle (NT) were added. Cells were counted at different time points. Each point represents the mean value for the three triplicates and error bars represent 95% confidence intervals. Statistical significance was determined by the two-tailed unpaired Student's *t* test.

Fig.2. Cell cycle effects of PLX4032 and PLX4720 in thyroid cancer cell lines.

2A) SW1736 and PC cells were incubated with PLX4032 (500 nM) and PLX4720 (500 nM) or vehicle (NT) at the indicated time points and cell cycle distribution was determined by flow cytometry. **2B)** SW1736 cells were incubated with PLX4032 (500 nM), PLX4720 (500 nM), PD0325901 (10 nM) or vehicle (NT) at different time points, RNA was extracted and mRNA levels of the indicated genes were measured by quantitative RT-PCR and reported as fold change (logarithmic scale) with respect to vehicle treated cells (NT).

Fig.S1. Inhibition of MEK by PD0325901 in BRAF mutant thyroid carcinoma cells and in normal thyroid cells.

S1A) The indicated cell lines were kept in low serum and treated with increasing concentrations of PD0325901 or vehicle (NT) for 2 hours. Cell lysates were immunoblotted with the indicated antibodies. Total amounts of proteins are shown for normalization. **S1B**) The indicated cell lines ($5x10^4$) were plated in triplicate in 35-mm dishes in low serum. The BRAF status of the different cell lines is represented. One day later, different concentrations of PD0325901 or vehicle (NT) were added. Cells were counted at different time points. Day 0 was the treatment-starting day. Each point represents the mean value of triplicates and error bars represent 95% confidence intervals. Statistical significance was determined by the two-tailed unpaired Student's *t* test.

Acknowledgements

We are grateful to A. Fusco for continuous support and to C.H. Heldin for SW1736 cells. This study was supported by the Associazione Italiana per la Ricerca sul Cancro (AIRC), the Istituto Superiore di Oncologia (ISO), the Italian Ministero della Salute, and Ministero dell'Universita' e della Ricerca (MiUR), the European Union Contract FP6-36495 (GENRISK-T), and the Project Applicazioni Biotecnologiche **(**MoMa**)**. PS was supported by a NOGEC (Naples OncoGEnomic Center) fellowship.

References

1. **Jemal A, Siegel R, Ward E, Hao Y, Xu J, Murray T, Thun MJ** 2008 Cancer statistics, 2008. CA Cancer J Clin 58 71-96.
2. **DeLellis RA, Williams ED** 2004 Thyroid and parathyroid tumors. In Tumours of Endocrine Organs, World Health Organization Classification of Tumors. DeLellis RA, Lloyd RV, Heitz PU and Eng C. (eds), p. 51-56**.**
3. **Kondo T, Ezzat S, Asa SL** 2006 Pathogenetic mechanisms in thyroid follicular-cell neoplasia. Nat Rev Cancer 6:292-306.
4. **Groussin L, Fagin JA** 2006 Significance of BRAF mutations in papillary thyroid carcinoma: prognostic and therapeutic implications. Nat Clin Pract Endocrinol Metab 2:180-1.
5. **Xing M** 2007 BRAF Mutation in Papillary Thyroid Cancer: Pathogenic Role, Molecular Bases, and Clinical Implications. Endocr Rev 28:742-762.
6. **Espinosa AV, Porchia L, Ringel MD** 2007 Targeting BRAF in thyroid cancer. Br J Cancer 96:16-20.
7. **Wilhelm S, Carter C, Lynch M, Lowinger T, Dumas J, Smith RA, Schwartz B, Simantov R, Kelley S** 2006 Discovery and development of sorafenib: a multikinase inhibitor for treating cancer. Nat Rev Drug Discov 5:835-44.
8. **Gupta-Abramson V, Troxel AB, Nellore A, Puttaswamy K, Redlinger M, Ransone K, Mandel SJ, Flaherty KT, Loevner LA, O'Dwyer PJ, Brose MS** 2008 Phase II Trial of Sorafenib in Advanced Thyroid Cancer. J Clin Oncol 26:4714-9.
9. **Ouyang B, Knauf JA, Smith EP, Zhang L, Ramsey T, Yusuff N, Batt D, Fagin JA** 2006 Inhibitors of Raf kinase activity block growth of thyroid cancer cells with RET/PTC or BRAF mutations in vitro and in vivo. Clin Cancer Res 12:1785-93.

10. **Leboeuf R, Baumgartner JE, Benezra M, Malaguarnera R, Solit D, Pratilas CA, Rosen N, Knauf JA, Fagin JA** 2008 BRAFV600E Mutation Is Associated with Preferential Sensitivity to Mitogen-Activated Protein Kinase Kinase Inhibition in Thyroid Cancer Cell Lines. J Clin Endocrinol Metab 93:2194-201.

11. **Liu D, Liu Z, Jiang D, Dackiw AP, Xing M** 2007 Inhibitory effects of the mitogen-activated protein kinase kinase inhibitor CI-1040 on the proliferation and tumor growth of thyroid cancer cells with BRAF or RAS mutations. J Clin Endocrinol Metab 92:4686-95.

12. **Ball DW, Jin N, Rosen DM, Dackiw A, Sidransky D, Xing M, Nelkin BD** 2007 Selective growth inhibition in BRAF mutant thyroid cancer by the mitogen-activated protein kinase kinase 1/2 inhibitor AZD6244. J Clin Endocrinol Metab 92:4712-8.

13. **Liu D, Xing M** 2008 Potent inhibition of thyroid cancer cells by the MEK inhibitor PD0325901 and its potentiation by suppression of the PI3K and NF-kappaB pathways. Thyroid 18:853-64.

14. **Tsai J, Lee JT, Wang W, Zhang J, Cho H, Mamo S, Bremer R, Gillette S, Kong J, Haass NK, Sproesser K, Li L, Smalley KS, Fong D, Zhu YL, Marimuthu A, Nguyen H, Lam B, Liu J, Cheung I, Rice J, Suzuki Y, Luu C, Settachatgul C, Shellooe R,Cantwell J, Kim SH, Schlessinger J, Zhang KY, West BL, Powell B, Habets G, Zhang C, Ibrahim PN, Hirth P, Artis DR, Herlyn M, Bollag G** 2008 Discovery of a selective inhibitor of oncogenic B-Raf kinase with potent antimelanoma activity. Proc Natl Acad Sci U S A 105:3041-6.

15. **Sala E, Mologni L, Truffa S, Gaetano C, Bollag GE, Gambacorti-Passerini C** 2008. BRAF Silencing by Short Hairpin RNA or Chemical Blockade by PLX4032 Leads to Different Responses in Melanoma and Thyroid Carcinoma Cells. Mol Cancer Res 6:751-9.

16. **Schweppe RE, Klopper JP, Korch C, Pugazhenthi U, Benezra M, Knauf JA, Fagin JA, Marlow LA, Copland JA, Smallridge RC, Haugen BR** 2008 Deoxyribonucleic Acid profiling analysis of 40 human thyroid cancer cell lines reveals cross-contamination resulting in cell line redundancy and misidentification. J Clin Endocrinol Metab 93:4331-41.

17. **Salvatore G, De Falco V, Salerno P, Nappi TC, Pepe S, Troncone G, Carlomagno F, Melillo RM, Wilhelm SM, Santoro M** 2006 BRAF is a therapeutic target in aggressive thyroid carcinoma. Clin Cancer Res 12:1623-9.

18. **Solit DB, Garraway LA, Pratilas CA, Sawai A, Getz G, Basso A, Ye Q, Lobo JM, She Y, Osman I, Golub TR, Sebolt-Leopold J, Sellers WR, Rosen N** 2006 BRAF mutation predicts sensitivity to MEK inhibition. Nature 439:358-62.

19. **Pratilas CA, Hanrahan AJ, Halilovic E, Persaud Y, Soh J, Chitale D, Shigematsu H, Yamamoto H, Sawai A, Janakiraman M, Taylor BS, Pao W, Toyooka S, Ladanyi M, Gazdar A, Rosen N, Solit DB**. 2008 Genetic predictors of MEK dependence in non-small cell lung cancer. Cancer Res. 68:9375-83.

20. **Stommel JM, Kimmelman AC, Ying H, Nabioullin R, Ponugoti AH, Wiedemeyer R, Stegh AH, Bradner JE, Ligon KL, Brennan C, Chin L, DePinho RA.** 2007 Coactivation of receptor tyrosine kinases affects the response of tumor cells to targeted therapies. Science 318:287-90.

21. **Grant S**. 2008 Cotargeting survival signaling pathways in cancer. J Clin Invest 118:3003-6.

22. **Kinkade CW, Castillo-Martin M, Puzio-Kuter A, Yan J, Foster TH, Gao H, Sun Y, Ouyang X, Gerald WL, Cordon-Cardo C, Abate-Shen C**. 2008

Targeting AKT/mTOR and ERK MAPK signaling inhibits hormone-refractory prostate cancer in a preclinical mouse model. J Clin Invest 118:3051-64.

Fig. 1

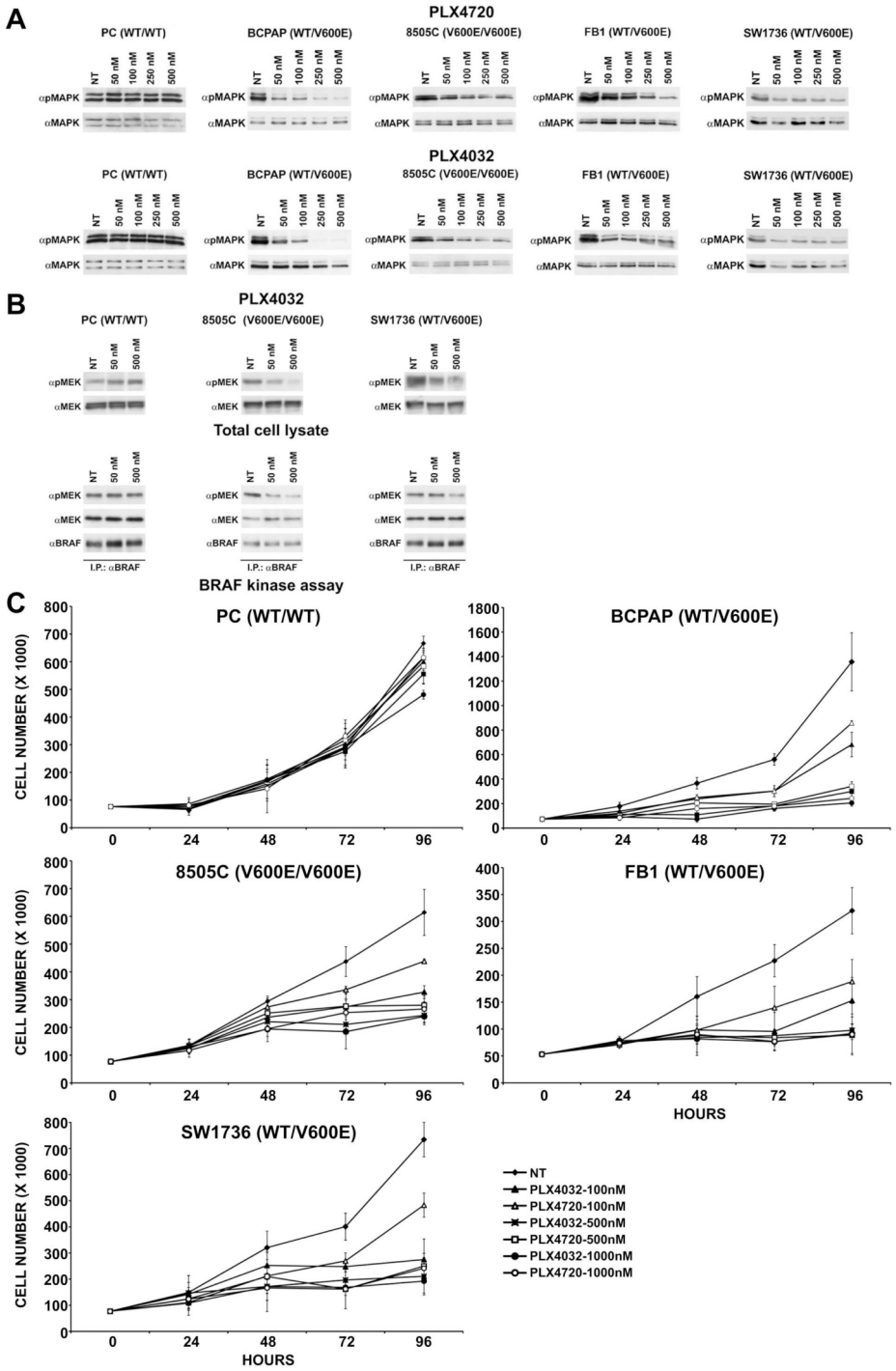
A
PLX4720
PC (WT/WT)
BCPAP (WT/V600E)
8505C (V600E/V600E)
FB1 (WT/V600E)
SW1736 (WT/V600E)
NT
50 nM
100 nM
250 nM
500 nM
αpMAPK
αMAPK
PLX4032
B
PLX4032
αpMEK
αMEK
Total cell lysate
αBRAF
I.P.: αBRAF
BRAF kinase assay
C
CELL NUMBER (X 1000)
HOURS
NT
PLX4032-100nM
PLX4720-100nM
PLX4032-500nM
PLX4720-500nM
PLX4032-1000nM
PLX4720-1000nM

Fig. 2

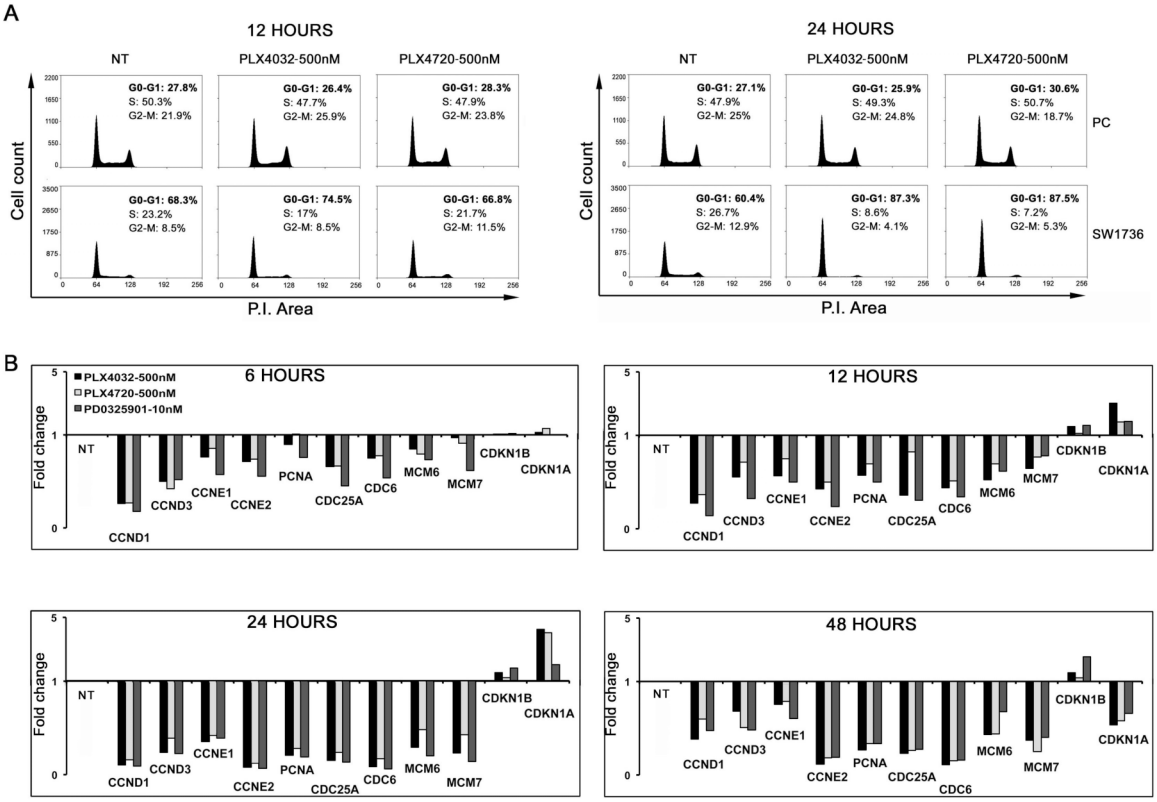
A
12 HOURS
24 HOURS
NT
PLX4032-500nM
PLX4720-500nM
Cell count
P.I. Area
PC
SW1736
G0-G1: 27.8%
S: 50.3%
G2-M: 21.9%
G0-G1: 26.4%
S: 47.7%
G2-M: 25.9%
G0-G1: 28.3%
S: 47.9%
G2-M: 23.8%
G0-G1: 68.3%
S: 23.2%
G2-M: 8.5%
G0-G1: 74.5%
S: 17%
G2-M: 8.5%
G0-G1: 66.8%
S: 21.7%
G2-M: 11.5%
G0-G1: 27.1%
S: 47.9%
G2-M: 25%
G0-G1: 25.9%
S: 49.3%
G2-M: 24.8%
G0-G1: 30.6%
S: 50.7%
G2-M: 18.7%
G0-G1: 60.4%
S: 26.7%
G2-M: 12.9%
G0-G1: 87.3%
S: 8.6%
G2-M: 4.1%
G0-G1: 87.5%
S: 7.2%
G2-M: 5.3%
B
6 HOURS
12 HOURS
24 HOURS
48 HOURS
PLX4032-500nM
PLX4720-500nM
PD0325901-10nM
Fold change
NT
CCND1
CCND3
CCNE1
CCNE2
PCNA
CDC25A
CDC6
MCM6
MCM7
CDKN1B
CDKN1A

Fig. S1

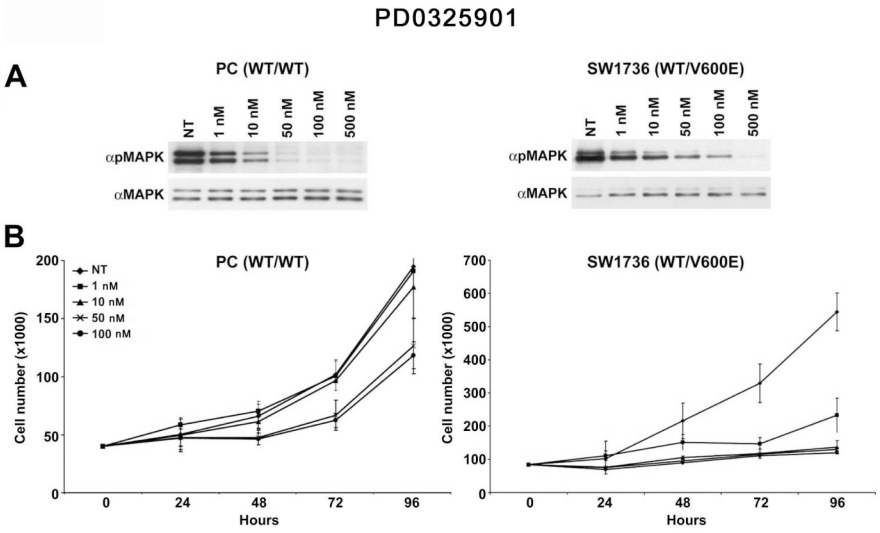
PD0325901
A
PC (WT/WT)
SW1736 (WT/V600E)
NT
1 nM
10 nM
50 nM
100 nM
500 nM
αpMAPK
αMAPK
B
PC (WT/WT)
SW1736 (WT/V600E)
NT
1 nM
10 nM
50 nM
100 nM
Cell number (x1000)
Hours
0
24
48
72
96

Attached manuscript #IV

Donata Vitagliano, Valentina De Falco, **Anna Tamburrino**, Sabrina Coluzzi, Giancarlo Troncone, Fortunato Ciardiello, Giampaolo Tortora, Samuel A Wells Jr, Anderson J. Ryan, Francesca Carlomagno, Massimo Santoro.

The tyrosine kinase inhibitor ZD6474 blocks the growth and tumorigenicity of RET mutation-positive medullary thyroid carcinoma cells.

Manuscript submitted

The tyrosine kinase inhibitor ZD6474 blocks the growth and tumorigenicity of RET mutation-positive medullary thyroid carcinoma cells

Donata Vitagliano, Valentina De Falco, Anna Tamburrino, Sabrina Coluzzi, Giancarlo Troncone, Fortunato Ciardiello, Giampaolo Tortora, Samuel A Wells Jr, Anderson J. Ryan, Francesca Carlomagno, Massimo Santoro.

Istituto di Endocrinologia ed Oncologia Sperimentale del CNR, c/o Dipartimento di Biologia e Patologia Cellulare e Molecolare, Università di Napoli Federico II, Napoli, Italy (DV, FC, SC, MS). Dipartimento di Scienze Biomorfologiche e Funzionali, Università di Napoli Federico II, Napoli, Italy (GTr). Division of Medical Oncology, Dipartimento di Medicina e Chirurgia Sperimentale e Clinica "F Magrassi and A Lanzara", Seconda Università di Napoli, Napoli, Italy (FC). Dipartimento di Endocrinologia e Oncologia Molecolare e Clinica, Università di Napoli Federico II, Napoli, Italy (GTo). Department of Surgery, Duke University School of Medicine, Durham, NC, USA (SAWJr). Cancer Discovery, Astra Zeneca Mereside, Alderley Park, Macclesfield, Cheshire, SK10 4TG, UK (AJR).

Short Title: ZD6474 effects on MTC cells

Keywords: thyroid, tyrosine kinase inhibitor, RET, multiple endocrine neoplasia, vandetanib

Corresponding author: Massimo Santoro, Dipartimento di Biologia e Patologia Cellulare e Molecolare, Universià di Napoli Federico II, via S. Pansini 5, 80131 Naples, Italy

Tel: +39 081 7463056; Fax: +39 081 7463037; e-mail: masantor@unina.it

Abstract

Purpose. Oncogenic conversion of the RET kinase is a frequent feature of medullary thyroid carcinoma (MTC), a tumor that is unresponsive to systemic therapies. We have assessed the effects of ZD6474 (ZACTIMA™, vandetanib), which is an ATP-competitive inhibitor of RET, EGFR and VEGFR, in human MTC cell lines carrying RET mutations. *Experimental Design.* We evaluated the effects of ZD6474 in the TT and MZ-CRC-1 MTC cell lines, which carry the cysteine 634 to tryptophan (C634W) and the methionine 918 to threonine (M918T) RET mutations, respectively. The RET mutation-negative 6-23C6 and MTC-M MTC cell lines served as controls. *Results.* ZD6474 arrested *in vitro* growth and inhibited RET, Shc and p44/p42 MAPK phosphorylation in RET mutation-positive cells. It also significantly reduced the size of TT tumor xenografts in nude mice. The mean tumor size in mice treated with 50 mg/kg/day ZD6474 for 17 days was 26 mm^3 versus 560 mm^3 in control mice ($P < 0.0001$). The effects of ZD6474 on the growth of 6-23C6 xenografts did not reach statistical significance. Inhibition of tumor growth paralleled phospho-RET suppression. *Conclusions.* ZD6474 is a powerful inhibitor of the RET signaling pathway and a potential therapeutic tool in RET-positive MTC. Phospho-Shc and phospho-MAPK could serve as surrogate markers to monitor the effect of ZD6474 treatment in MTC patients.

Introduction

RET (REarranged during Transfection) is a single-pass transmembrane tyrosine kinase receptor (1). Oncogenic conversion of RET is involved in the pathogenesis of papillary (PTC) and medullary (MTC) thyroid carcinoma (2). MTC arises from neural crest-derived thyroid C cells and it accounts for about 3% of all thyroid cancers (3). It is sporadic in about 75% of cases; in the remaining cases it is inherited as a component of the autosomal dominant multiple endocrine neoplasia type 2 (MEN 2) syndrome. There are three MEN 2 subtypes [MEN 2A, MEN 2B and familial MTC (FMTC)] and distinct germline activating mutations of RET confer predisposition to MEN 2 subtypes (4, 5). Moreover, RET point mutations, particularly M918T, V804L/M and E768D, at the somatic level, are found in 30–50% of sporadic MTC cases (2, 4, 5). MTC-associated mutations activate the RET kinase and convert RET into a dominantly transforming oncogene (2). The finding that activating mutations of RET are present in the germline of familial MTC demonstrates that RET triggers MTC in these patients; likely, RET exerts a similar function in sporadic MTC cases associated with somatic mutations in RET. In this scenario, RET appears to be a promising target for molecular therapy of MTC. Accordingly, expression of a dominant negative RET kinase mutant impaired growth of MTC cells (6).

While adjuvant radioiodine treatment is very effective in the vast majority of thyroid cancers arising from follicular cells, there is no systemic treatment for MTC. MTC does not respond to standard chemotherapy or radiotherapy. In fact, high-dose doxorubicin (used as single agent or associated with cisplatin) results in a response rate less than 20% (7). Total thyroidectomy, if performed early, is curative in a high percentage of MTC patients (7) and early preventive surgery in RET mutation carriers has significantly improved the prognosis of

familial MTC (8). However, MTC patients are often incurable because the cancer has already metastasized to regional lymph nodes or distant sites at the time of diagnosis (7, 9, 10).

Small molecule tyrosine kinase inhibitors are used to disrupt tyrosine kinase signaling in cancer (11, 12). Five of the clinically approved kinase-targeted oncology agents are small molecules and the other three are monoclonal antibodies (12). The efficacy of imatinib in BCR-ABL-positive chronic myelogenous leukemia (CML) and in c-KIT-positive gastro-intestinal stromal tumors (GIST) and of the epidermal growth factor receptor (EGFR) inhibitors gefitinib and erlotinib in non small cell lung carcinomas (NSCLC), carrying specific EGFR mutations or EGFR amplification, illustrates the power of small molecule tyrosine kinase inhibitors (12). These examples also show that mutations causing gain-of-function of the kinase and dependence of the cancer cell on the increased signaling by the mutant kinase are the best parameters available to identify candidates for treatment with these compounds (13).

Small ATP-competitive inhibitors of various chemical classes have been reported to inhibit RET (14–23). ZD6474 (ZACTIMA™, vandetanib) [N-(4-bromo-2-fluorophenyl)-6-methoxy-7-[(1-methylpiperidin-4-yl)methoxy]quinazolin-4-amine] is an anilinoquinazoline compound with a molecular weight of 475 Da. It is a potent RET inhibitor, blocking RET kinase with an inhibitory concentration 50 (IC_{50}) of 100 nM (15). ZD6474 was effective against a *Drosophila* model of RET-mediated tumorigenesis (24). Besides RET inhibition, the compound has anti-angiogenic activity because it also targets vascular endothelial growth factor receptor type 2 (VEGFR-2 also named KDR), a receptor for VEGF-A and related VEGF family members, (IC_{50} = 40 nM) and VEGFR-3 (Flt-4), a receptor for VEGF-C and VEGF-D, (IC_{50} = 110 nM). It also inhibits the epidermal growth factor receptor (EGFR) (IC_{50} = 500 nM) (25–27). ZD6474 is orally available and phase I clinical evaluation has shown that

it is well-tolerated and that it has a pharmacokinetic profile appropriate for once-daily oral dosing. ZD6474 at doses of 100–300 mg in single-agent and combination regimens is undergoing phase II and III evaluation in a range of solid tumors (27); in particular, the compound is now undergoing clinical trials in patients with familial MTC associated with germline RET mutations (http://clinicaltrials.gov).

The aim of this study was to assess efficacy of ZD6474 in human MTC cells sustaining oncogenic mutations in RET.

Materials and Methods

Compounds. ZD6474 and gefitinib (iressa, ZD1839) were provided by AstraZeneca Pharmaceuticals (Macclesfield, UK). Stock solutions (50 mM) were made in 100% DMSO and diluted with culture media before use. Culture media containing an equivalent DMSO concentration served as vehicle controls.

Cell Cultures. TT, 6-23C6 and MTC-M cells were from American Type Culture Collection (Manassas, VA). MZ-CRC-1 cells were kindly provided by Robert F. Gagel. TT cells were derived from the primary tumor of an apparently sporadic MTC (28) and harbor the cysteine 634 to tryptophan (C634W) exon 11 RET mutation (29) as well as a tandem duplication of the mutated RET allele (30). MZ-CRC-1 were derived from a malignant pleural effusion from a patient with a metastatic MTC (31). The 6-23C6 cell line was established from transplantable rat MTC carried in the WAG/Rij strain (33). The MTC-M cell line was derived from a transplantable MTC in the BALB/c mouse strain (34). TT cells were grown in RPMI 1640 supplemented with 16% fetal calf serum. MZ-CRC-1 cells were grown in Dulbecco's

modified Eagle's medium (DMEM) supplemented with 10% fetal calf serum. 6-23C6 cells were cultured in RPMI 1640 supplemented with 15% horse serum; MTC-M cells were cultured in RPMI 1640 supplemented with 10% horse serum and 5% fetal calf serum. All media were supplemented with 2 mM L-glutamine and 100 units/ml penicillin-streptomycin (GIBCO, Paisley, PA).

Immunoblotting Analysis. Protein lysates containing comparable amounts of proteins, estimated by a modified Bradford assay (Bio-Rad, Munich, Germany), were subjected to direct western blot. Immune complexes were detected with the enhanced chemiluminescence kit (Amersham Pharmacia Biotech, Little Chalfort, UK). Signal intensity was analyzed at the Phosphorimager (Typhoon 8600, Amersham Pharmacia Biotech) interfaced with the ImageQuant software. Anti-phospho-Shc (#Y317), which recognizes Shc proteins when phosphorylated at Y317, was from Upstate Biotechnology Inc. (Lake Placid, NY). Anti-Shc (H-108) was from Santa Cruz Biotechnology (Santa Cruz, CA). Anti-MAPK (#9101) and anti-phospho-MAPK (#9102), specific for p44/42MAPK (ERK1/2) phosphorylated at Thr202/Tyr204, were from Cell Signaling (Beverly, MA). Anti-cyclin D1 (A-12) was from Santa Cruz Biotechnology. Monoclonal anti-α-tubulin was from Sigma Chemical Co., and anti-p27Kip1 was from BD Transduction Laboratories (San Jose, CA). Anti-phosphotyrosine (4G10) was from Upstate Biotechnology Inc. Anti-RET is a polyclonal antibody raised against the tyrosine kinase protein fragment of human RET. Anti-pY905 and anti-pY1062 are phospho-specific affinity-purified polyclonal antibodies that recognize RET proteins phosphorylated at Y905 and Y1062, respectively (16). Secondary antibodies coupled to horseradish peroxidase were from Amersham Pharmacia Biotech.

Growth Curves and Cell Cycle Analysis. Compounds or vehicle were added to the cell culture medium and changed every two days. Cells were counted every day. For flow cytometry (FACS) analysis, cells were grown to subconfluence in 100-mm dishes, and then treated with vehicle or 200 nM ZD6474 for 48 hours. After harvesting, cells were fixed in ice-cold 70% ethanol in phosphate-buffered saline. Propidium iodide (25 μg/ml) was added and samples were analyzed with a FACScalibur flow cytometer (Becton Dickinson, San Jose, CA) interfaced with a Hewlett Packard computer (Palo Alto, CA). DNA synthesis was measured by the 5'-bromo-3'-deoxyuridine (BrdU) Labeling and Detection kit from Boehringer Mannheim. Cells were seeded on glass coverslips and treated or not with the compounds for 24 hours. Then, cells were incubated for 1 hour with BrdU (final concentration of 10 μM), fixed with paraformaldehyde (4%), and permeabilized with Triton X-100 (0.2%). Coverslips were incubated with anti-BrdU mouse monoclonal antibody and with a secondary Texas red-conjugated antibody (Jackson ImmunoResearch Laboratories, Philadelphia, PA). All coverslips were counterstained in PBS containing Hoechst 33258 (final concentration, 1 mM; Sigma Chemical Co.), rinsed in PBS, and mounted in Moviol on glass slides. The fluorescent signal was visualized with an epifluorescent microscope (Axiovert 2, Zeiss; equipped with a 100 lens) interfaced with the image analyzer software KS300 (Zeiss).

To determine cell viability, TT and MZ-CRC-1 cells (500,000/dish) were treated or not with ZD6474 at 500 nM or 2 μM for 5 days. Each day, cells in suspension were harvested. The cell suspension was mixed with 0.4% trypan blue (1:1) (Sigma) and the mixture was incubated for 3 min at room temperature. Unstained (viable) and stained (non viable) cells were counted separately.

Tumorigenicity in Nude Mice. Animals were housed in barrier facilities on a 12-hour light:dark cycle at the Dipartimento di Biologia e Patologia Cellulare e Molecolare (University of Naples "Federico II", Naples, Italy), and had free access to food and water. This study was conducted in accordance with Italian regulations for experimentation on animals. All manipulations were performed while animals were under isoflurane gas anesthesia. TT cells ($1x10^7$/mouse) or 6-23C6 cells ($1 x10^6$/mouse) were inoculated subcutaneously into the right dorsal portion of 4-week-old male BALB/c nu/nu mice (Jackson Laboratories, Bar Harbor, ME). When established tumors developed, ZD6474 (50 mg/kg/day dissolved in PBS containing 0.5% v/v Tween 80) or vehicle alone was administered by oral gavage for five consecutive days/week. Tumor diameters were measured with calipers at regular intervals. Tumor volumes (V) were calculated with the rotational ellipsoid formula: $V=AxB^2/2$ (A=axial diameter; B= rotational diameter). Tumors were excised and divided in two parts. Half the tissue was snap-frozen in liquid nitrogen and used for protein extraction. The other half was fixed overnight in neutral buffered formalin and processed for histological examination or immunohistochemistry. Briefly, 5 μM sections were deparaffinized, alcohol-rehydrated, subjected to heat-induced antigen retrieval and incubated overnight with anti-CD31 antibodies (PECAM-1 [M-20] SC-1506 goat polyclonal; Santa Cruz Biotechnology). Finally, the slides were incubated with biotinylated anti-IgG and with premixed avidin-biotin complex (Vectostain ABC kits, Vector Laboratories, Burlingame, CA). The immune reaction was revealed with 0.06 mmol/L diaminobenzidine (DAB-DAKO, Carpinteria, CA) and 2 mmol/L hydrogen peroxide. As a negative control, tissue slides were incubated with pre-immune serum.

Statistical Analysis. We used the two-tailed unpaired Student's *t* test and the JMP software program (version 5.1.1, SAS Institute, Inc, Austin, TX) for statistical analyses. Differences were significant at $P < 0.05$.

Results

RET sequence analysis of MTC cells. TT cells harbor the C634W RET mutation (29). The sequence of RET cDNA from MZ-CRC-1, 6-23C6, and MTC-M cells was determined by RT-PCR using overlapping primers. Sequences were compared to the human (Accession number NM_020630), mouse (Accession number NC_000072) and rat (Accession number NW_047696) RET sequences available in the GenBank (National Center for Biotechnology Information) using the Basic Alignment Search Tool (BLAST) software. The RET sequences of MTC-M, and 6-23C6 were found to be wild type. Instead, MZ-CRC-1 cells revealed a heterozygous (ATG to ACG) transition in exon 16 resulting in the MEN 2B-associated substitution of threonine 918 for methionine (M918T) (Fig. 1A).

Inhibition of RET Signaling in RET Mutation-Positive MTC Cells by ZD6474. Cells were treated with increasing concentrations of ZD6474 for 24 hours and RET phosphorylation levels were measured by immunoblotting with phospho-specific antibodies that recognize RET only when phosphorylated at tyrosine 905 (Y905) or 1062 (Y1062). Y905 maps in the activation loop of the RET kinase while Y1062 maps in the carboxyl-terminal tail of the receptor. When phosphorylated Y1062 binds to Shc and other adaptor proteins thereby leading to the activation of various intracellular signaling cascades (34). Treatment with ZD6474 reduced RET/C634W and RET/M918T phosphotyrosine content with an IC_{50} of 50-

250 nM (average 150 nM), whereas the vehicle had no effect (Fig. 1B–C). The two RET kinases were completely blocked when cells were exposed to 1 μM ZD6474. RET expression was barely detectable in 6-23C6 cells and no RET phosphorylation was detected in these cells irrespective of treatment (Fig. 1B).

Due to their constitutive enzymatic activity, oncogenic versions of RET bind to the Shc docking protein that, in turn, mediates Grb2/Sos recruitment and phosphorylation of p44/p42MAPK (mitogen-activated protein kinase) (34). We asked whether this pathway was active in MTC cells and responsive to ZD6474. We treated MTC cells with increasing concentrations of ZD6474 and analyzed Shc and p44/p42MAPK phosphorylation by immunoblotting with phospho-specific antibodies. The results of one experiment representative of three independent determinations are reported in Fig. 2. In TT and MZ-CRC-1 cells, ZD6474 inhibited phosphorylation of both Shc and p44/42MAPK with an IC_{50} of 50–250 nM. No Shc phosphorylation was seen in 6-23C6 cells. However, these cells had significant levels of MAPK phosphorylation that were not affected by ZD6474 (up to 1 μM) (Fig. 2).

Cytostatic effects of ZD6474 in RET mutation-positive MTC cells. We measured ZD6474 effects on the growth of MTC cells. After 5 days of treatment, TT cells treated with vehicle numbered 1,300 x 10^3 and those treated with 250 nM of ZD6474 numbered 800 x 10^3 [difference = 500 x 10^3, 95% confidence interval (CI) = 310–690 x 10^3, $P < 0.0015$)] (Fig. 3A). MZ-CRC-1 cells treated (6 days) with vehicle or with 250 nM of ZD6474 numbered 1,144 x 10^3 and 712 x 10^3, respectively (difference = 432 x 10^3, 95% CI = 253-611, $P <$ 0.001) (Fig. 3B). One μM of the drug virtually arrested proliferation of both cell lines. In TT cells, 1 μM ZD6474 exerted a modest degree of cytotoxicity only at late (4–5 days) time-

points (Fig. 3A). This was confirmed by trypan blue exclusion assay of detached TT cells (data not shown).

The growth-inhibitory effects of ZD6474 in MTC cell lines was correlated with the expression of RET-activating mutations. Indeed, at concentrations equal or below 1 μM, ZD6474 did not affect RET mutation-negative 6-23C6 and MTC-M cell lines (Fig. 4). Only 5 μM ZD6474 (~50-fold the IC_{50} for the RET kinase) exerted a modest but statistically significant cytostatic effect also on these cells (at 7 days, $P = 0.0014$ in 6-23C6; $P < 0.0001$ in MTC-M).

In addition to RET, ZD6474 also inhibits EGFR (IC_{50} =500 nM), and VEFGR-2 and -3 (IC_{50} = 40 nM and 110 nM, respectively) (27). To evaluate whether EGFR inhibition is involved in the ZD6474-mediated inhibition of MTC cell growth, we used gefitinib, a highly selective EGFR inhibitor (*in vitro* IC_{50} = 27nM) (35). Gefitinib does not inhibit RET (15). Treatment with gefitinib, at a concentration of 5 μM, did not significantly affect TT cell proliferation: after 6 days of treatment, TT cells treated with vehicle numbered 1,950 x 10^3 and those treated with 5 μM gefitinib numbered 1,800 x 10^3 (difference = 150 x 10^3, $P <$ 0.081). Thus, EGFR block did not result in inhibition of TT cell growth.

We used flow cytometry and bromodeoxyuridine (BrdU) incorporation assays to characterize ZD6474-mediated growth inhibition. Cell cycle profiles showed a marked accumulation in G1 phase of TT and MZ-CRC-1, but not of control 6-23C6 cells, after treatment for 24 h with 250 nM of ZD6474 (Fig. 5). This was accompanied by a reduced accumulation of cells in the S and M phases. Besides its cytostatic effect, short-term treatment with a low concentration of ZD6474 did not result in major pro-apoptotic effects. Importantly, ZD6474 greatly reduced DNA synthesis, measured by BrdU incorporation in TT and MZ-CRC-1 cells, with an IC_{50} of 50–250 nM. One μM of ZD6474 virtually abrogated DNA

synthesis in both cell lines (Fig. 6A). Parallel to cell cycle G1 arrest, treatment with ZD6474 for 24 h resulted in marked up-regulation of the cyclin-dependent kinase inhibitor p27Kip1 and down-regulation of the cyclin D1 (Fig. 6B). This is consistent with recent evidences of RET-mediated control of p27Kip1 and cyclin D1 gene expression (36).

Inhibition of TT-Induced Tumor Formation in Nude Mice by ZD6474. Nude mice were injected with $1x10^7$ TT cells. About 30 days later, when tumors measured ~200 mm^3, the animals (7 for each group) were randomly assigned to receive *per os* ZD6474 (50 mg/kg/day) or vehicle 5 days/week for 17 days. Tumor growth was monitored every 3–4 days with calipers. Treatment with ZD6474 greatly reduced the tumor burden (Fig. 7A). After 17 days of treatment, the mean size of tumors in mice treated with vehicle or ZD6474 was 560 mm^3 (95% CI = 406-715 mm^3) and 26 mm^3 (95% CI = 3-55 mm^3), respectively (difference = 35 mm^3, 95% CI =382-687 mm^3, $P < 0.0001$). We next divided the vehicle-treated animals (average tumor size: 560 mm^3) into two groups: one continued to receive vehicle for an additional three weeks, and the other group received ZD6474 for three weeks. ZD6474 exerted significant effects also on these large tumors. As shown in Fig. 7A, the mean difference between vehicle-treated and ZD6474-treated tumors was 460 mm^3 (95% CI = 200-719 mm^3; $P < 0.006$).

We examined RET phosphorylation in proteins extracted from TT tumors treated or not with ZD6474. As shown in Fig. 7A, tumor-growth inhibition was associated with a remarkable reduction of *in vivo* RET phosphorylation levels on tyrosine 1062. Thus, *in vivo*, ZD6474 targeted the RET protein.

By directly targeting VEGFRs in the tumor endothelium (27), ZD6474 might prevent the development of tumor neovascularization. We evaluated this possibility by counting the

number of blood vessels using light microscopy and immunoperoxidase staining with anti-factor VIII antibody, and found that ZD6474 reduced the number of vessels (from 7±3.5 to 2±1 per microscopic field; not shown). Therefore, it appears that the *in-vivo* anti-tumor effects of ZD6474 may be a consequence of inhibiting both RET, and also neoangiogenesis.

Finally, we tested ZD6474 effects in tumor xenografts induced by RET-negative 6-23C6 cells. When tumors measured ~100 mm^3, we randomly assigned animals (7 for each group) to receive *per os* ZD6474 (50 mg/kg/day) or vehicle 5 days/week for 15 days (Fig. 7B). At the end of treatment, the mean size of tumors in mice treated with vehicle or ZD6474 was 1553 mm^3 and 1092 mm^3, respectively ($P = 0.33$). Therefore, ZD6474 had effects clearly less intense in RET mutation negative xenografts, suggesting that RET inhibition was a factor in the ZD6474-mediated inhibition of MTC xenograft growth.

Discussion

We have established an *in vitro* model system to determine the efficacy of RET inhibition by ZD6474 in MTC cells. ZD6474 was equally active in cells harboring a MEN 2A-type (TT) or a MEN 2B-type (MZ-CRC-1) mutation. The compound was active in these RET mutation-positive MTC cells at doses very close to its *in vitro* IC_{50} for the RET kinase. The effects were probably RET-dependent because they were much more modest in cells without the RET mutation. It is still possible that inhibition of targets other than RET contribute to the *in vitro* ZD6474 activity on MTC cells. RT-PCR experiments revealed the expression of at least two other ZD6474 targets, e.g. EGFR and VEGFR-2, in both TT and MZ-CRC-1 cells (data not shown). Moreover, EGFR was reported to be expressed in MTC samples although it is not known whether it may carry mutations (37-39). However, our data with the EGFR selective

inhibitor gefitinib indicate that EGFR inhibition, at least alone, does not have a major effect on MTC cells.

ZD6474 treatment reduced the tumor burden in nude mice xenografted with TT cells. RET inhibition was crucial for this activity. In fact, RET phosphorylation was decreased in treated tumors. Moreover, the effects were more modest in tumors induced by the RET mutation-negative 6-23C6 cells. Also in this case it is feasible that inhibition of ZD6474 targets other than RET, and in particular pro-angiogenic receptors, contributed to these anti-tumor effects. Accordingly, MTC cells have been demonstrated to overexpress VEGF-A (rather than VEGF-C) that might function on tumor endothelial cells (40, 41). The simultaneous attack to neoplastic and endothelial cells could indeed be an advantage of this compound.

ZD6474 has recently entered a phase II clinical study in MTC patients with germline RET mutations and will soon be tested also in sporadic MTC patients (http://clinicaltrials.gov). Surrogate markers of target inhibition can serve to evaluate the efficacy of a compound in a clinical setting. This is well illustrated by the use of phosphorylation of CRKL, a substrate of BCR-ABL, to assess CML patients response to imatinib (42). Our data suggest that phospho-Shc and phospho-MAPK could be proposed as biomarkers to monitor the efficacy of RET targeting in MTC patients treated with ZD6474.

In conclusion, ZD6474 might be a promising anti-cancer agent for MTC patients, particularly those carrying RET mutations. ZD6474 exerted mainly cytostatic effect in MTC cells and cytotoxic effects were limited to high doses and long-term treatments. Combinations of ZD6474 and conventional cytotoxic agents could be exploited in order to increase the therapeutic index and reduce the risk of resistance formation (43-45).

Acknowledgments

We thank Robert F. Gagel for MZ-CRC-1 cells. We thank Elvira Crescenzi and Francesco Merolla for the FACS analysis and Salvatore Sequino and Antonio Baiano for animal care. We thank Jean A. Gilder for text editing. This study was supported by the Associazione Italiana per la Ricerca sul Cancro (AIRC), the Italian Ministero per l'Istruzione, Università e Ricerca Scientifica (MIUR), the Italian Ministero della Salute. This study was also supported by a grant from AstraZeneca. Anderson J. Ryan is an AstraZeneca employee.

Figure legends

Figure 1. Inhibition of RET phosphorylation by ZD6474 in MTC cells. **A**) Schematic representation of RET/C634W and RET/M918T alleles expressed by TT and MZ-CRC-1 cells, respectively. EC: extracellular domain; IC: intracellular (kinase) domain; TM: transmembrane domain. **B–C**) The cell lines were treated with different concentrations of ZD6474 for 24 hours; 100 μg of total cell lysates were subjected to immunoblotting with antibodies specific for phosphorylated RET/Y905 or RET/Y1062. Equal gel loading was determined by using an anti-tubulin antibody (not shown). The signal was analyzed at the Phosphorimager to estimate the concentration of compound causing 50% inhibition (IC_{50}). Data are representative of 3 independent experiments.

Figure 2. Inhibition of RET-mediated signaling by ZD6474. TT, 6-23C6 and MZ-CRC-1 cells were treated with vehicle or increasing concentrations of ZD6474. Cell lysates (50 μg) were immunoblotted with phospho-specific Shc or p44/42 MAPK antibodies. Anti-MAPK and anti-SHC were used for normalization. Data are representative of 3 independent experiments.

Figure 3. Effects of ZD6474 on MTC cell proliferation. TT (**A**), and MZ-CRC-1 (**B**) cells were incubated with vehicle or the indicated concentrations of ZD6474 and counted at different time points. Each point represents the mean value for 3 dishes and error bars represent 95% confidence intervals. Statistical significance was determined with the two-tailed unpaired Student's *t* test.

Figure 4. Effects of ZD6474 on MTC RET-negative cell proliferation. 6-23C6 (**A**) and MTC-M (**B**) cell lines were incubated with vehicle or the indicated concentrations of ZD6474 and counted at different time points. Each point represents the mean value for 3 dishes and **error bars** represent 95% confidence intervals. Statistical significance was determined with the two-tailed unpaired Student's *t* test.

Figure 5. Cell cycle effects exerted by ZD6474 on TT and MZ-CRC-1 cells. Cell lines were treated or not for 24 hours with 250 nM ZD6474 and subjected to flow cytometry. The percentage of cells in the sub-G1 (apoptotic), G_O/G_1, S, and G_2/M compartments is indicated in the insets. Data are representative of 3 independent experiments.

Figure 6. DNA synthesis inhibition by ZD6474 on TT and MZ-CRC-1 cells. (**A**) MTC cells were pretreated with the indicated concentrations of ZD6474 for 24 hours. Bromodeoxyuridine (BrdU) was added for 1 h, and cells were processed for immunofluorescence: anti-BrdU, monitored by a Texas red-conjugated secondary antibody, was used to detect the fraction of cells in S phase. Cell nuclei were counterstained with Hoechst. The average results +/- SD of three independent experiments in which at least 500 cells were counted are shown. (**B**) The indicated cell lines were treated with ZD6474 for 24 h and expression levels of cell cycle regulatory proteins were determined by immunoblot. Anti-tubulin was used for normalization.

Figure 7. The anti-tumorigenic effects of ZD6474 in TT cells xenografts. (**A**) TT cells ($1x10^7$/mouse) were inoculated subcutaneously into the right dorsal portion of BALB/c nude mice. When tumors measured ~200 mm^3, animals were randomly assigned to two

groups (7 mice/group) to receive ZD6474 (50 mg/kg/day, black circles) or vehicle (black squares) 5 days/week by oral gavage. After 17 days of treatment, vehicle-treated animals were randomly assigned to continue vehicle treatment (white squares) or to start receiving ZD6474 (50 mg/kg/day, white circles) for additional three weeks. Tumor diameters were measured with calipers and tumor volumes were calculated. Error bars represent 95% confidence intervals. *P* values for the comparisons (at the different time points) between compound and vehicle are reported. Statistical significance was determined with the two-tailed unpaired Student's *t* test. Proteins (100 μg) extracted from representative tumors (day 38) from untreated or treated animals were immunoblotted with the indicated antibodies. (**B)** 6-23C6 cells ($1x10^6$) were injected in the right dorsal of nude mice. When the tumors size was ~100 mm^3, animals were randomly assigned to receive ZD6474 (50 mg/kg/day, white circles) or vehicle alone (black circles) for two weeks. Tumor volumes were calculated; error bars represent 95% confidence intervals.

References

1. Airaksinen MS, Saarma M. The GDNF family: signalling, biological functions and therapeutic value. Nat Rev Neurosci 2002;3:383-94.
2. Santoro M, Carlomagno F. Drug insight: small-molecule inhibitors of protein kinases in the treatment of thyroid cancer. Nature Clin Practice End & Metab 2006;2:42-52.
3. Matias-Guiu X et al. (2004) Medullary thyroid carcinoma. In World Health Organization Classification of Tumours. Pathology and Genetics. Tumours of Endocrine Organs, 86–91 (Eds DeLellis RA et al.). Geneva: WHO Press.
4. Marx SJ. Molecular genetics of multiple endocrine neoplasia types 1 and 2. Nat Rev Cancer 2005;5:367-75.
5. Kouvaraki MA, Shapiro SE, Perrier ND, et al. RET proto-oncogene: a review and update of genotype-phenotype correlations in hereditary medullary thyroid cancer and associated endocrine tumors. Thyroid 2005;15:531-44.
6. Drosten M, Hilken G, Bockmann Met al. Role of MEN2A-derived RET in maintenance and proliferation of medullary thyroid carcinoma. J Natl Cancer Inst 2004;96:1231-9.
7. Leboulleux S, Baudin E, Travagli JP, Schlumberger M. Medullary thyroid carcinoma. Clin Endocrinol (Oxf) 2004;61:299-310.
8. Skinner MA, Moley JA, Dilley WG, Owzar K, Debenedetti MK, Wells SA Jr. Prophylactic thyroidectomy in multiple endocrine neoplasia type 2A. N Engl J Med 2005;353:1105-13.
9. Cote GJ, Gagel RF. Lessons learned from the management of a rare genetic cancer. N Engl J Med 2003;349:1566-8.
10. Wells SA, Nevins JR. Evolving strategies for targeted cancer therapy--past, present, and future. J Natl Cancer Inst 2004;96:980-1.

11. Baselga J. Targeting tyrosine kinases in cancer: the second wave. Science 2006;312:1175-8.
12. Sebolt-Leopold JS, English JM. Mechanisms of drug inhibition of signalling molecules. Nature 2006; 441:457-62.
13. Pao W, Miller VA. Epidermal growth factor receptor mutations, small-molecule kinase inhibitors, and non-small-cell lung cancer: current knowledge and future directions. J Clin Oncol 2005;23: 2556–68.
14. Carlomagno F, Vitagliano D, Guida T, et al. The kinase inhibitor PP1 blocks tumorigenesis induced by RET oncogenes. Cancer Res 2002;62:1077-82.
15. Carlomagno F, Vitagliano D, Guida T, et al. ZD6474, an orally available inhibitor of KDR tyrosine kinase activity, efficiently blocks oncogenic RET kinases. Cancer Res 2002;62:7284-90.
16. Carlomagno F, Vitagliano D, Guida T, et al. Efficient inhibition of RET/papillary thyroid carcinoma oncogenic kinases by 4-amino-5-(4-chloro-phenyl)-7-(t-butyl)pyrazolo[3,4-d]pyrimidine (PP2). J Clin Endocrinol Metab 2003;88:1897-902.
17. Cuccuru G, Lanzi C, Cassinelli G, et al. Cellular effects and antitumor activity of RET inhibitor RPI-1 on MEN2A-associated medullary thyroid carcinoma. J Natl Cancer Inst 2004;96:1006-14.
18. Strock CJ, Park JI, Rosen M, et al. CEP-701 and CEP-751 inhibit constitutively activated RET tyrosine kinase activity and block medullary thyroid carcinoma cell growth. Cancer Res 2003;63:5559-63.
19. Strock CJ, Park JI, Rosen DM, et al. Activity of irinotecan and the tyrosine kinase inhibitor CEP-751 in medullary thyroid cancer. J Clin Endocrinol Metab 2006;91:79-84.

20. Ouyang B, Knauf JA, Smith EP, et al. Inhibitors of Raf kinase activity block growth of thyroid cancer cells with RET/PTC or BRAF mutations in vitro and in vivo. Clin Cancer Res 2006;12:1785-93.
21. Carlomagno F, Anaganti S, Guida T, et al. BAY 43-9006 inhibition of oncogenic RET mutants. J Natl Cancer Inst 2006;98:326-34.
22. Kim DW, Jo YS, Jung HS, et al. An orally administered multitarget tyrosine kinase inhibitor, SU11248, is a novel potent inhibitor of thyroid oncogenic RET/papillary thyroid cancer kinases. J Clin Endocrinol Metab 2006;91:4070-6.
23. Mologni L, Sala E, Cazzaniga S, et al. Inhibition of RET tyrosine kinase by SU5416. J Mol Endocrinol 2006;37:199-212.
24. Vidal M, Wells S, Ryan A, Cagan R. ZD6474 suppresses oncogenic RET isoforms in a Drosophila model for type 2 multiple endocrine neoplasia syndromes and papillary thyroid carcinoma. Cancer Res 2005;65:3538-41.
25. Wedge SR, Ogilvie DJ, Dukes M, et al. ZD6474 inhibits vascular endothelial growth factor signaling, angiogenesis, and tumor growth following oral administration. Cancer Res 2002;62:4645-55.
26. Ciardiello F, Caputo R, Damiano V, et al. Antitumor effects of ZD6474, a small molecule vascular endothelial growth factor receptor tyrosine kinase inhibitor, with additional activity against epidermal growth factor receptor tyrosine kinase. Clin Cancer Res 2003;9:1546-56.
27. Ryan AJ and Wedge SR. ZD6474-a novel inhibitor of VEGFR and EGFR tyrosine kinase activity. Br J Cancer 2005;92:S6–S13

28. Leong SS, Zeigel R, Chu TM, Baylin S and Mirand EA. A new cell line for study of human medullary thyroid carcinoma. In: M. Andreoli et al (eds), Advances in Thyroid Naoplasia, pp 95-108. Field Educational Italia, Rome 1981.
29. Carlomagno F, Salvatore D, Santoro M, et al. Point mutation of the RET proto-oncogene in the TT human medullary thyroid carcinoma cell line. Biochem Biophys Res Commun 1995;207:1022-8.
30. Huang SC, Torres-Cruz J, Pack SD, et al. Amplification and overexpression of mutant RET in multiple endocrine neoplasia type 2-associated medullary thyroid carcinoma. J Clin Endocrinol Metab 2003;88:459-63.
31. Cooley LD, Elder FF, Knuth A, Gagel RF. Cytogenetic characterization of three human and three rat medullary thyroid carcinoma cell lines. Cancer Genet Cytogenet 1995;80:138-49.
32. Zeytinoglu FN, DeLellis RA, Gagel RF, Wolfe HJ, Tashjian AH Jr. Establishment of a calcitonin-producing rat medullary thyroid carcinoma cell line. I. Morphological studies of the tumor and cells in culture. Endocrinology 1980;107:509-15.
33. Tischler AS, Lee YC, Costopoulos D, et al. Establishment of a continuous somatostatin-producing line of medullary thyroid carcinoma cells from BALB/c mice. J Endocrinol 1986;110:309-13.
34. Asai N, Murakami H, Iwashita T, Takahashi M. A mutation at tyrosine 1062 in MEN2A-Ret and MEN2B-Ret impairs their transforming activity and association with shc adaptor proteins. J Biol Chem 1996;271:17644-9.
35. Von Pawel J. Gefitinib (Iressa, ZD1839): a novel targeted approach for the treatment of solid tumors. Bull Cancer 2004;91:E70-6.

36. Joshi PP, Kulkarni MV, Yu BK, et al. Simultaneous downregulation of CDK inhibitors p18(Ink4c) and p27(Kip1) is required for MEN2A-RET-mediated mitogenesis. Oncogene 2006; Sep 4.
37. Wang W, Johansson HE, Bergholm UI, Westermark KM, Grimelius LE. Expression of c-Myc, TGF-alpha and EGF-receptor in sporadic medullary thyroid carcinoma. Acta Oncol 1997;36:407-11.
38. Nilsson O, Wangberg B, Kolby L, Schultz GS, Ahlman H. Expression of transforming growth factor alpha and its receptor in human neuroendocrine tumours. Int J Cancer 1995;60:645-51.
39. van der Laan BF, Freeman JL, Asa SL. Expression of growth factors and growth factor receptors in normal and tumorous human thyroid tissues. Thyroid 1995;5:67-73.
40. Hung CJ, Ginzinger DG, Zarnegar R, et al. Expression of vascular endothelial growth factor-C in benign and malignant thyroid tumors. J Clin Endocrinol Metab 2003;88:3694-9.
41. de la Torre NG, Buley I, Wass JA, Turner HE. Angiogenesis and lymphangiogenesis in thyroid proliferative lesions: relationship to type and tumour behaviour. Endocr Relat Cancer 2006;13:931-44.
42. Kantarjian H, Giles F, Wunderle L, et al. Nilotinib in imatinib-resistant CML and Philadelphia chromosome-positive ALL. N Engl J Med 2006;354:2542-51.
43. Tuccillo C, Romano M, Troiani T, et al. Antitumor activity of ZD6474, a vascular endothelial growth factor-2 and epidermal growth factor receptor small molecule tyrosine kinase inhibitor, in combination with SC-236, a cyclooxygenase-2 inhibitor. Clin Cancer Res 2005;11:1268-76.

44. Damiano V, Melisi D, Bianco C, et al. Cooperative antitumor effect of multitargeted kinase inhibitor ZD6474 and ionizing radiation in glioblastoma. Clin Cancer Res 2005;11:5639-44.

45. Carlomagno F, Guida T, Anaganti S, et al. Disease associated mutations at valine 804 in the RET receptor tyrosine kinase confer resistance to selective kinase inhibitors. Oncogene 2004;23:6056-63.

Fig. 1

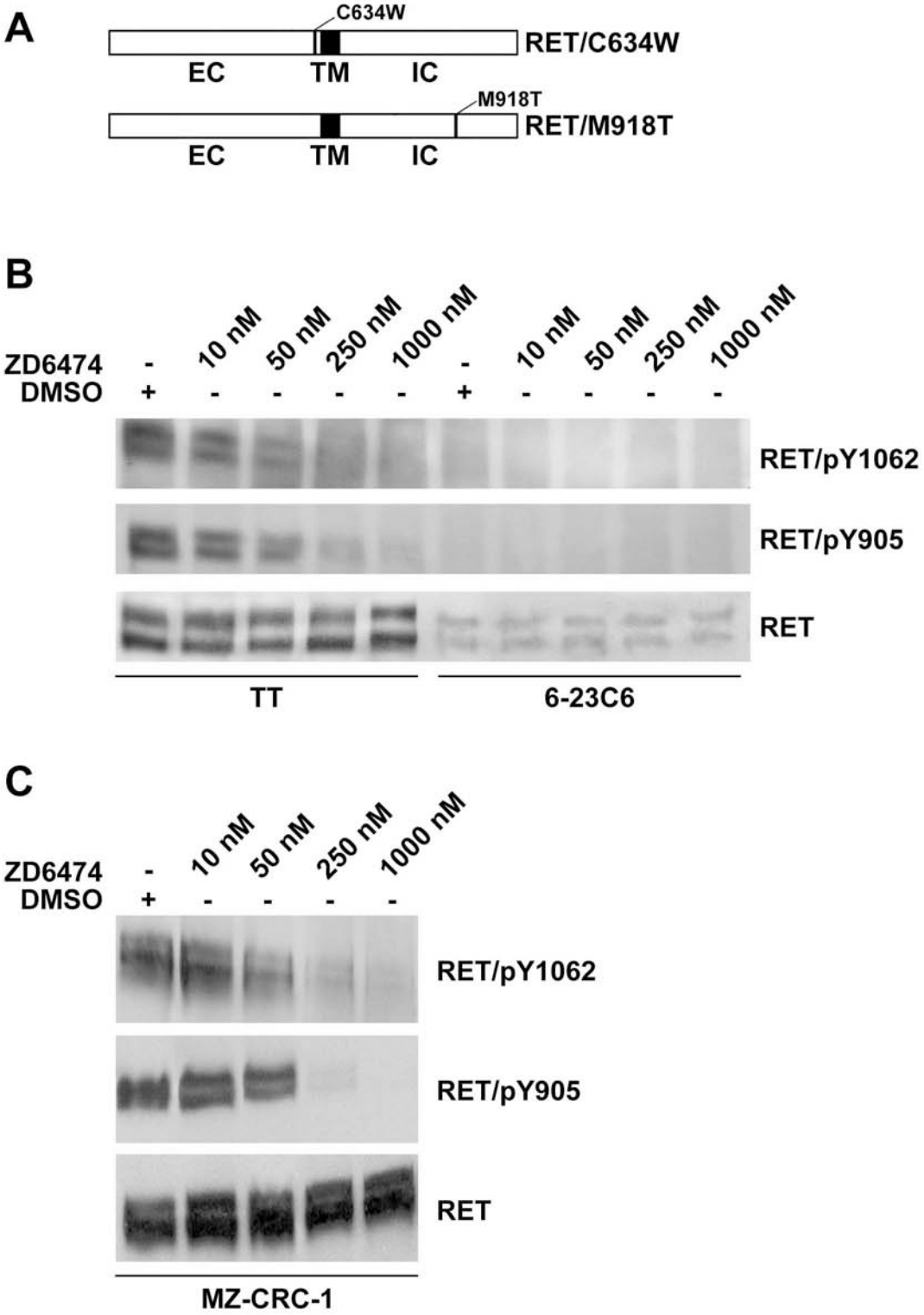
A
C634W
RET/C634W
EC
TM
IC
M918T
RET/M918T
EC
TM
IC
B
ZD6474
DMSO
-
+
10 nM
50 nM
250 nM
1000 nM
-
10 nM
50 nM
250 nM
1000 nM
RET/pY1062
RET/pY905
RET
TT
6-23C6
C
ZD6474
DMSO
-
+
10 nM
50 nM
250 nM
1000 nM
RET/pY1062
RET/pY905
RET
MZ-CRC-1

Fig. 2

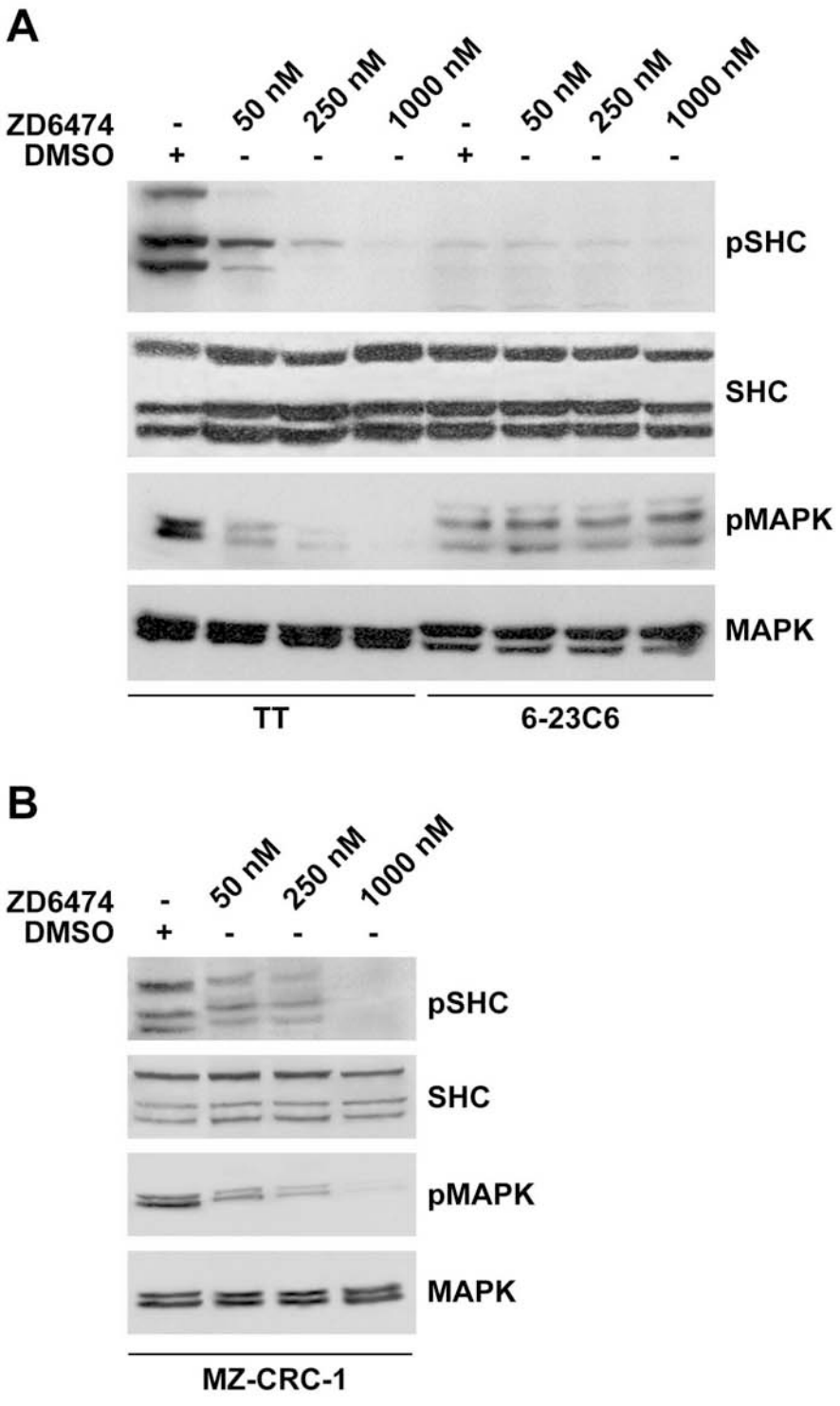
A
ZD6474
DMSO
-
+
50 nM
250 nM
1000 nM
-
-
-
-
50 nM
250 nM
1000 nM
+
-
-
-
pSHC
SHC
pMAPK
MAPK
TT
6-23C6
B
ZD6474
DMSO
-
+
50 nM
250 nM
1000 nM
-
-
-
pSHC
SHC
pMAPK
MAPK
MZ-CRC-1

Fig. 3

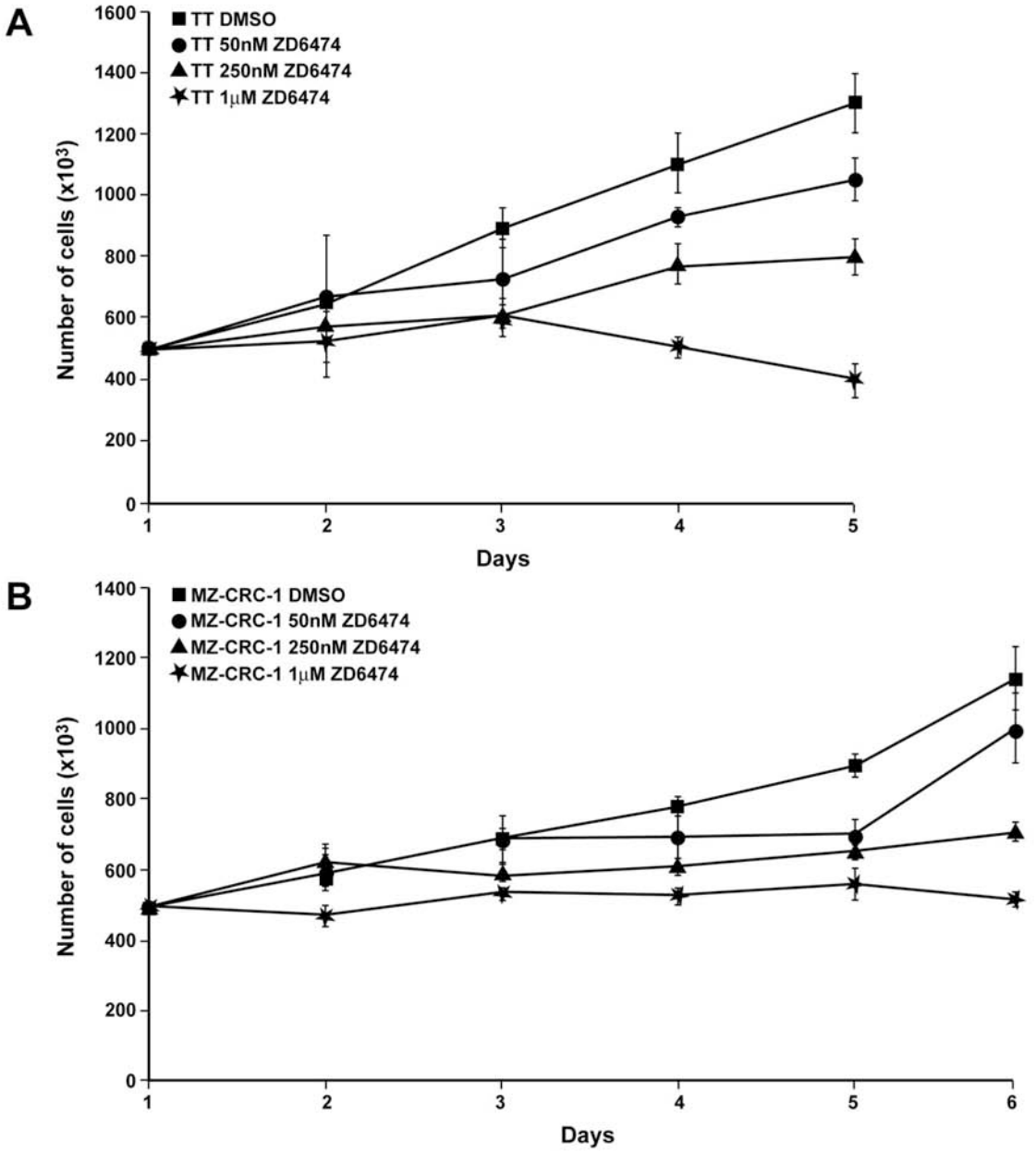
A
TT DMSO
TT 50nM ZD6474
TT 250nM ZD6474
TT 1μM ZD6474
Number of cells (x10³)
Days
B
MZ-CRC-1 DMSO
MZ-CRC-1 50nM ZD6474
MZ-CRC-1 250nM ZD6474
MZ-CRC-1 1μM ZD6474
Number of cells (x10³)
Days

Fig. 4

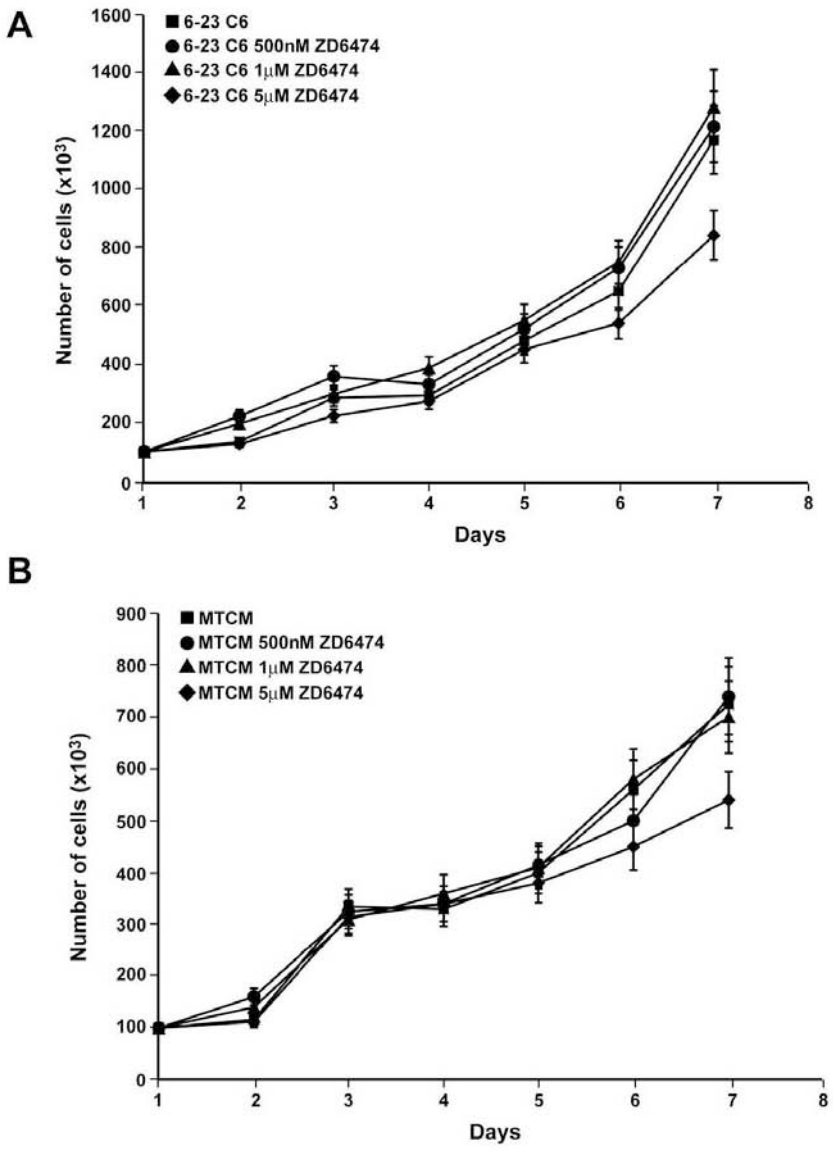
A
6-23 C6
6-23 C6 500nM ZD6474
6-23 C6 1μM ZD6474
6-23 C6 5μM ZD6474
Number of cells (x10³)
Days
B
MTCM
MTCM 500nM ZD6474
MTCM 1μM ZD6474
MTCM 5μM ZD6474
Number of cells (x10³)
Days

Fig. 5

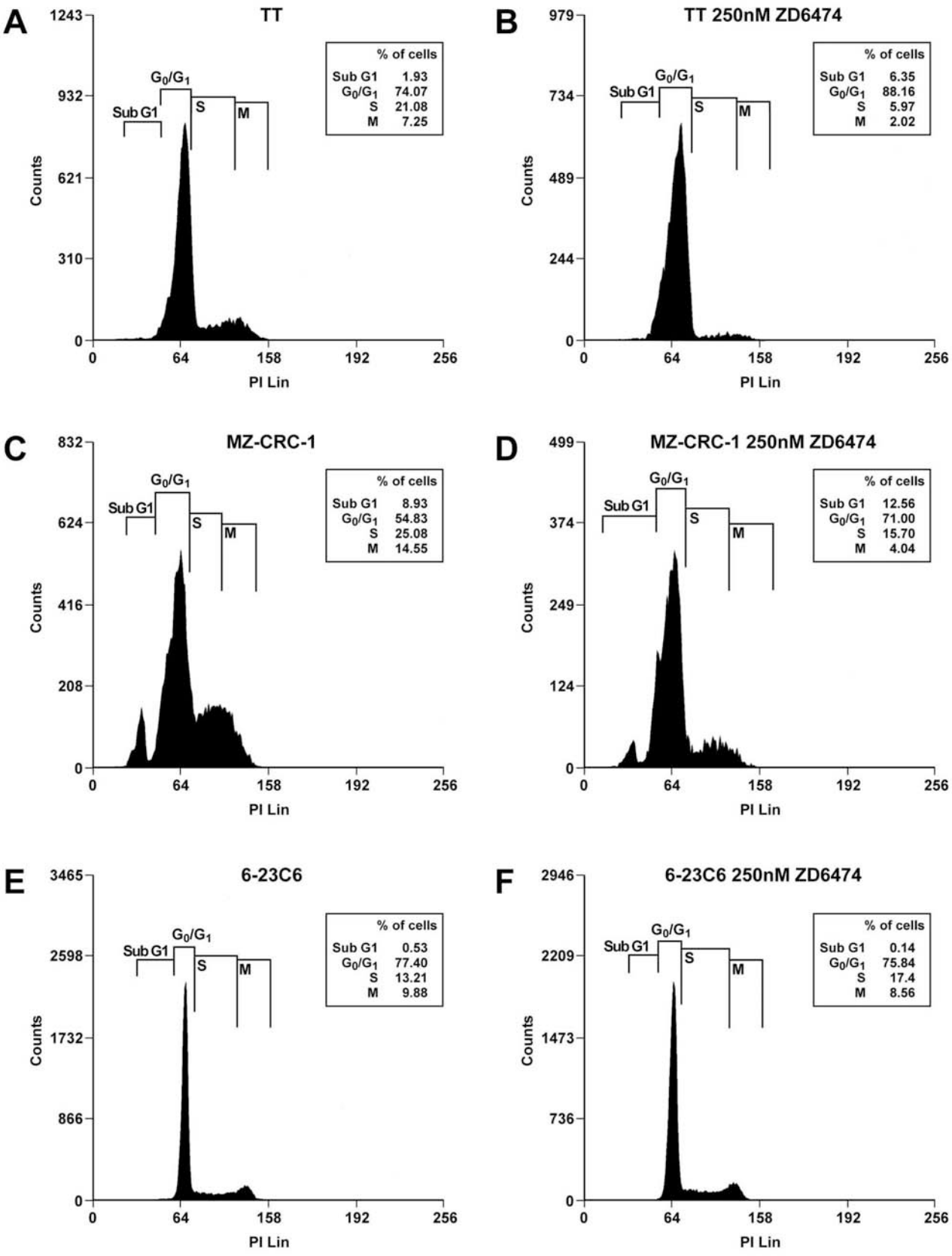
A
TT
% of cells
Sub G1 1.93
G0/G1 74.07
S 21.08
M 7.25
B
TT 250nM ZD6474
% of cells
Sub G1 6.35
G0/G1 88.16
S 5.97
M 2.02
C
MZ-CRC-1
% of cells
Sub G1 8.93
G0/G1 54.83
S 25.08
M 14.55
D
MZ-CRC-1 250nM ZD6474
% of cells
Sub G1 12.56
G0/G1 71.00
S 15.70
M 4.04
E
6-23C6
% of cells
Sub G1 0.53
G0/G1 77.40
S 13.21
M 9.88
F
6-23C6 250nM ZD6474
% of cells
Sub G1 0.14
G0/G1 75.84
S 17.4
M 8.56
Counts
PI Lin
0
64
158
192
256

Fig. 6

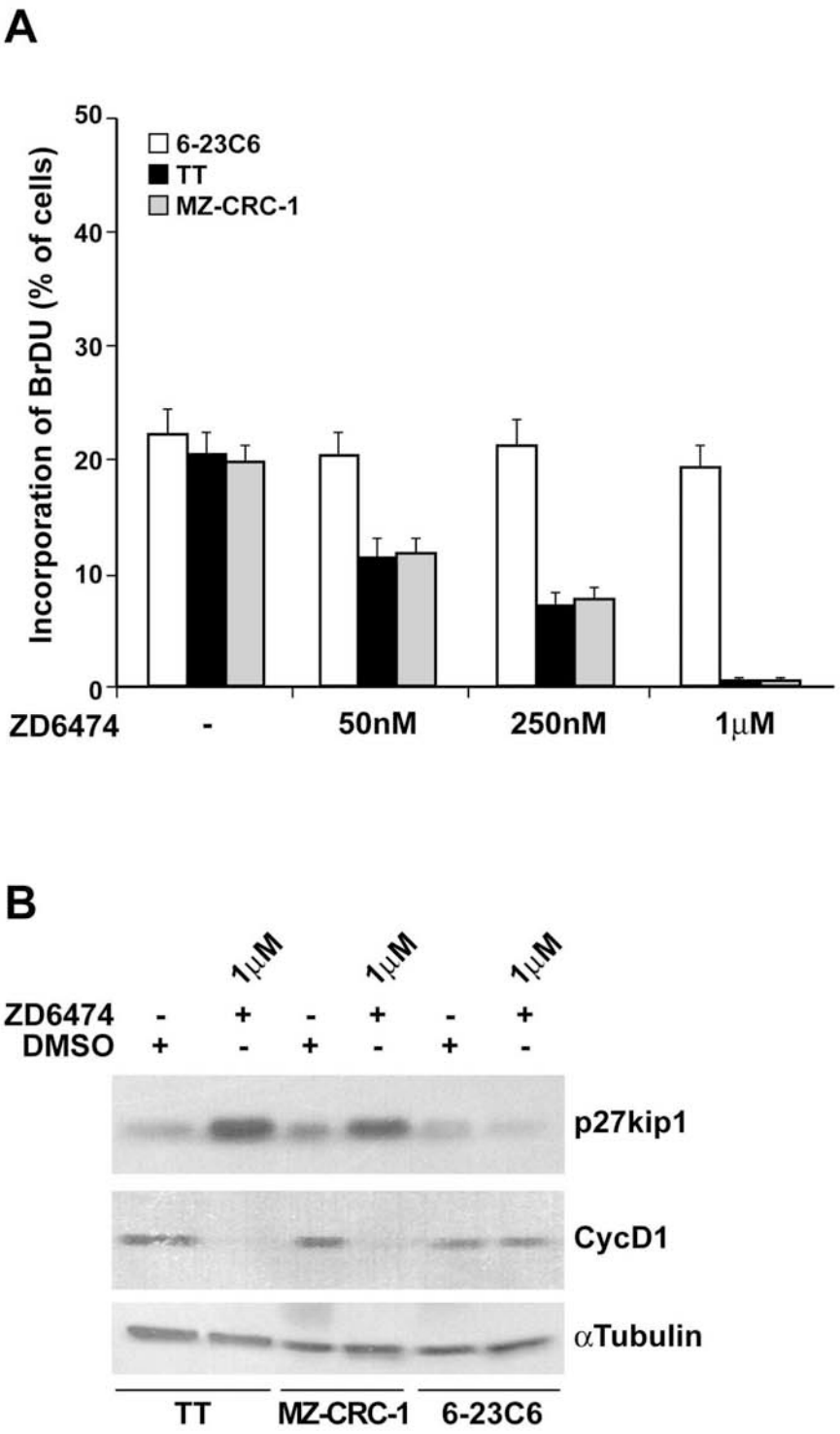
A
Incorporation of BrDU (% of cells)
50
40
30
20
10
0
6-23C6
TT
MZ-CRC-1
ZD6474
-
50nM
250nM
1μM
B
1μM
1μM
1μM
ZD6474 - + - + - +
DMSO + - + - + -
p27kip1
CycD1
αTubulin
TT
MZ-CRC-1
6-23C6

Fig. 7

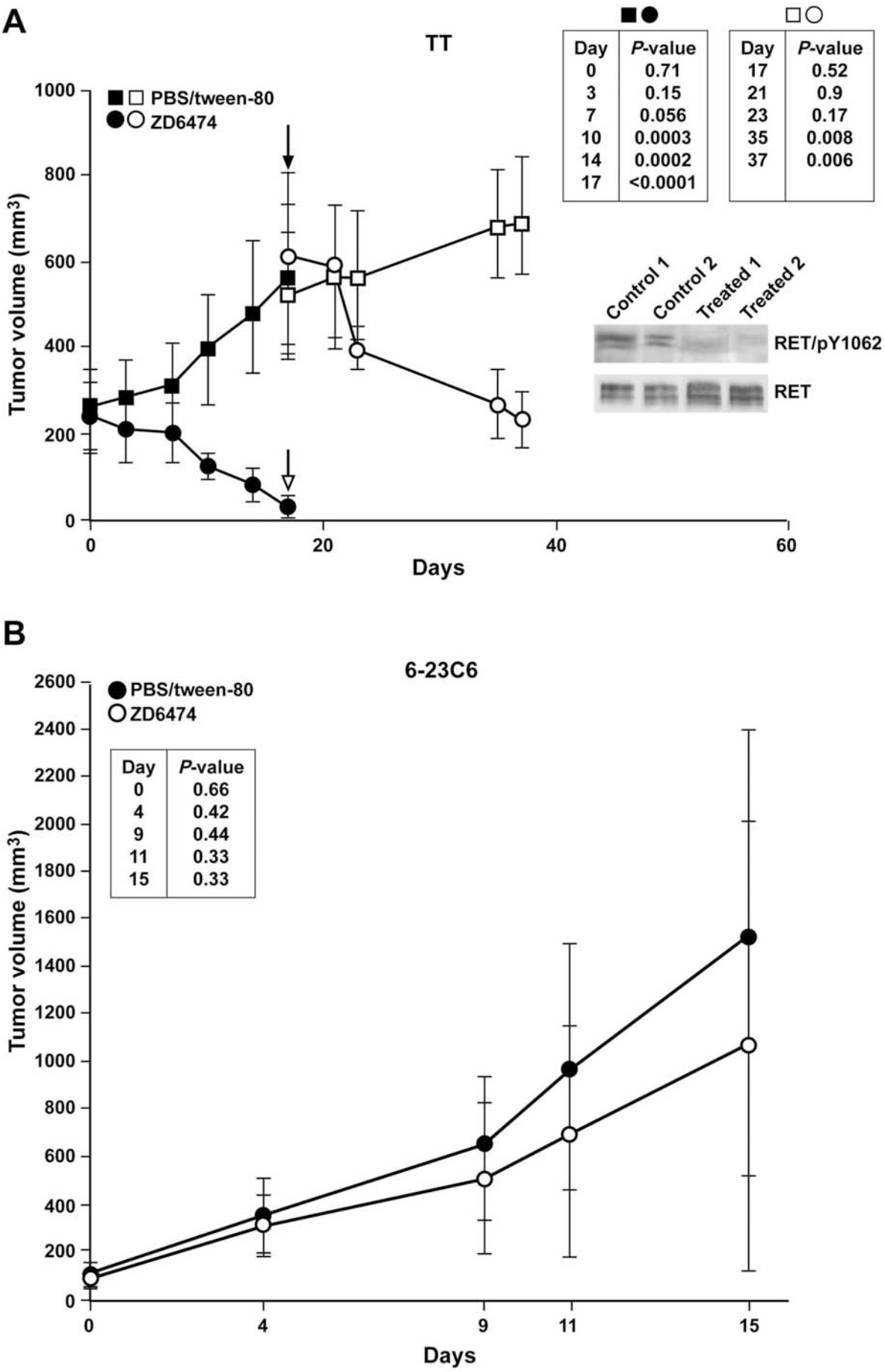
A
TT
PBS/tween-80
ZD6474
Tumor volume (mm3)
Days
0
200
400
600
800
1000
0
20
40
60
■●
Day P-value
0 0.71
3 0.15
7 0.056
10 0.0003
14 0.0002
17 <0.0001
□○
Day P-value
17 0.52
21 0.9
23 0.17
35 0.008
37 0.006
Control 1
Control 2
Treated 1
Treated 2
RET/pY1062
RET
B
6-23C6
PBS/tween-80
ZD6474
Tumor volume (mm3)
Days
0
200
400
600
800
1000
1200
1400
1600
1800
2000
2200
2400
2600
0
4
9
11
15
Day P-value
0 0.66
4 0.42
9 0.44
11 0.33
15 0.33